Universidade de Aveiro Departamento de Engenharia Mecânica
2020

Paulo Miguel Azevedo Amorim

Experimental monitoring of pollutants emissions from road vehicles

Monitorização experimental de emissões de poluentes de veículos rodoviários

Universidade de Aveiro Departamento de Engenharia Mecânica
2020

Paulo Miguel Azevedo Amorim

Experimental monitoring of pollutants emissions from road vehicles

Monitorização experimental de emissões de poluentes de veículos rodoviários

Dissertação apresentada à Universidade de Aveiro para cumprimento dos requisitos necessários à obtenção do grau de Mestre em Engenharia Mecânica, realizada sob orientação científica da Professora Doutora Margarida Isabel Cabrita Marques Coelho, Professora Auxiliar Com Agregação do Departamento de Engenharia Mecânica da Universidade de Aveiro e coorientação do Doutor Paulo Jorge Teixeira Fernandes, Investigador Doutorado (Nível 1) do Departamento de Engenharia Mecânica da Universidade de Aveiro.

Este trabalho teve o apoio financeiro dos projetos UIDB/00481/2020 e UIDP/00481/2020 - FCT - Fundação para Ciência e para Tecnologia; e CENTRO-01-0145-FEDER-022083 - Programa Operacional Regional do Centro (Centro2020), no âmbito do Acordo de Parceria Portugal 2020, através do Fundo Europeu de Desenvolvimento Regional, e ainda dos projetos de investigação MobiWise (P2020 SAICTPAC/0011/2015) e DICA-VE (POCI-01-0145-FEDER-029463).

o júri / the jury

presidente / president

Prof. Doutor Fernando José Neto da Silva
Professor Auxiliar da Universidade de Aveiro

Doutora Célia dos Anjos Alves
Investigadora Principal com Habilitação ou agregação em Regime Laboral da *Universidade de Aveiro (Arguente)*

Doutor Paulo Jorge Teixeira Fernandes
Investigador Doutorado (Nível 1) da Universidade de Aveiro (co-orientador)

agradecimentos / acknowledgements

Em primeiro lugar, estou eternamente agradecido aos meus pais por todo o esforço que fizeram e por todo o apoio que me deram ao longo desta etapa da minha vida, tornando possível o cumprimento de um dos maiores objetivos da minha vida. Deixo também uma palavra especial de apreço para a minha família e namorada pelo apoio e interesse que mostraram pelo trabalho que eu estava a desenvolver ao longo destes meses. Aproveito para dedicar a realização desta dissertação a todos eles. Gostaria também de agradecer à Professora Doutora Margarida Coelho e ao Doutor Paulo Fernandes pela excelente orientação dada, mostrando-se sempre disponíveis e prontos a ajudar naquilo que eu precisasse de forma a que o trabalho desenvolvido ficasse sempre o mais completo e bem feito possível. Deixo também uma palavra de agradecimento à restante Equipa de Mobilidade e Transportes da Universidade de Aveiro, em especial ao Investigador Auxiliar Behnam Bahmankhak pelo seu auxílio prestado no decorrer das campanhas de recolha de dados experimentais. Este trabalho teve o apoio financeiro dos projetos UIDB/00481/2020 e UIDP/00481/2020 - FCT - Fundação para Ciência e Tecnologia; e CENTRO-01-0145-FEDER-022083 - Programa Operacional Regional do Centro (Centro2020), no âmbito do Acordo de Parceria Portugal 2020, através do Fundo Europeu de Desenvolvimento Regional, e ainda dos projetos de investigação MobiWise (P2020 SAICTPAC/0011/2015) e DICA-VE (POCI-01-0145-FEDER-029463).

key-words

Driving Style; Emission Rates; Emission Monitoring; Portable Emissions Measurement System; Real Driving Emissions; Vehicular Jerk; Vehicle Specific Power

abstract

It is well-known the inconstancy that is verified on the obtained laboratory-test values, which present emission rates that are below the ones that are verified on the field. In order to achieve more reliable values the use of the Portable Measurement Emissions System (PEMS) is becoming more popular among researchers who work on this area. The main objective of this masters dissertation was to conduct an experimental monitoring of tailpipe pollutant emissions from different vehicles, with different types of fuels and routes. It was accomplished by the development of an empirical method which embraced vehicle data collection regarding its operating conditions and its consequent emissions. The two main purposes of the development of this method were to be able to, firstly, observe what were the impacts that different driving style parameters, such as the acceleration, vehicular jerk or RPM, along with the Vehicle Specific Power (VSP) and the characteristics of the route, had on the emission rates of the CO_2, NO_x and PM; and, secondly, to be able to analyze the relationship between the VSP and the obtained on-road emission rates by developing predictive based-modal approach. Two vehicles were submitted to the tests, being one of them ran by gasoline and the other by diesel, along four different routes, being two of them performed on highways, one on a partly urban/rural road and one along urban roads. Testing vehicles were equipped with a PEMS, a Global Positioning System (GPS) and an On-Board Diagnostic (OBD) scan device that were used to collect data about exhaust emissions, location and engine parameters, respectively. For both vehicles and in the intercity routes, the variance of the acceleration and the vehicular jerk was significantly high at low and moderate speeds, namely from 0-20 km/h and from 60-90 km/h, compared to the remaining ones. It was concluded that the NO_x Euro 6 limit was surpassed in about 44 times and in 66% by the diesel and the gasoline vehicle, respectively. Results showed that both cars were below the PM limits defined for their corresponding emission standards. Regarding the VSP-based prediction model approach and in the case of the diesel vehicle, high determination coefficients were obtained for the CO_2 and for the NO_x ($R^2 > 0.9$) and a moderate coefficient was obtained for the PM ($R^2 > 0.6$). VSP model showed as effective in predicting emissions in the gasoline vehicle, regardless of the pollutant ($R^2 > 0.83$). Regarding the validation of the VSP-based prediction model and for the diesel vehicle, the average VSP predicted values for the CO_2, NO_x and PM were 8 and 28% higher and 46% lower than the ones measured on the field, respectively. In the case of the gasoline vehicle and for the same pollutants, these values were 7, 20 and 33% superior to the field ones, respectively. The implementation of an effective method such as the VSP-based one is useful to estimate emissions in diesel or gasoline vehicles for all types of driving cycles and it could be incorporated on national inventories in order to calculate traffic emissions, for instance.

palavras-chave

Estilo de Condução; Taxas de Emissão; Monitorização de Emissões; Sistema Portátil de Medição de Emissões; Emissões Reais de Condução; Jerk Veicular; Potência Específica do Veículo

resumo

É bem conhecida a inconstância verificada nos valores obtidos em testes de laboratório, que apresentam taxas de emissão que estão abaixo daquelas que são verificadas na recolha de valores de emissões no terreno. De forma a obter valores mais confiáveis a utilização de Sistemas Portáteis de Medição de Emissões (PEMS) está-se a tornar mais popular entre os investigadores que operam nesta área. O principal objetivo desta dissertação de mestrado foi efetuar uma monitorização experimental das emissões de poluentes provenientes de veículos com diferentes combustíveis ao longo de diferentes tipos de vias. Este objetivo foi cumprido através do desenvolvimento de um método empírico que consistiu na recolha de dados no que diz respeito às condições de operação e às emissões dos gases de escape dos veículos. Os dois principais objetivos do desenvolvimento deste método foram, em primeiro lugar, observar os impactos que diferentes parâmetros ao nível da condução tais como a aceleração, a primeira derivada da aceleração (jerk), RPM, Potência Específica do Veículo (VSP) e o tipo de via tinham no nível das taxas de emissões de CO_2, NO_x e PM; e, em segundo lugar, ter a capacidade de analisar a relação entre o VSP e as taxas de emissão obtidas através do desenvolvimento de modelos preditivos. Dois veículos foram submetidos aos testes, operando um deles a gasolina e o outro a gasóleo, ao longo de quatro rotas distintas, sendo duas delas em auto-estrada, uma em zonas parcialmente urbanas/rurais e uma ao longo de vias urbanas. Os veículos de teste foram equipados com um PEMS, um Sistema Global de Posicionamento (GPS) e um Sistema de Diagnóstico a Bordo (OBD) que foram usados para recolher dados acerca das emissões libertadas através do tubo de escape dos veículos, da localização e dos parâmetros relativos ao motor do veículo, respectivamente. Para ambos os veículos e nas rotas inter rurais, a variância da aceleração e do jerk do veículo foi significativamente alta em velocidades baixas e moderadas, nomeadamente dos 0-20 km/h e dos 60-90 km/h, comparativamente às velocidades restantes. Foi concluído que o limite Euro 6 de NO_x foi ultrapassado em cerca de 44 vezes e em 66% para o veículo a diesel e a gasolina, respetivamente. Os resultados indicaram que ambos os veículos se mantiveram abaixo dos limites de emissão de PM definidos. No que diz respeito à aproximação utilizando o modelo de previsão baseado no VSP e para o caso do veículo a gasóleo, foram obtidos coeficientes de determinação elevados para o CO_2 e NO_x ($R^2 > 0.9$) e um coeficiente moderado para as PM ($R^2 > 0.6$). O modelo VSP provou ser igualmente eficaz na previsão das emissões do veículo a gasolina, independentemente do poluente ($R^2 > 0.83$). No que diz respeito à validação do modelo VSP e no caso do veículo a diesel, os valores de previsão para o CO_2, NO_x e PM foram 8 e 28% superiores e 46% inferiores aos valores medidos no terreno. No caso do veículo a gasolina e para os mesmos poluentes, os valores foram 7, 20 e 33% superiores aos medidos, respectivamente. A implementação de um método VSP efetivo poderá ser útil no que ao cálculo de emissões para todos os tipos de ciclos de condução diz respeito, podendo ser, por exemplo, incorporado em inventários nacionais.

Contents

List of Tables

Intentionally blank page.

List of Figures

Intentionally blank page.

List of Abbreviations, Acronyms and Chemical Symbols

ρ_{CO_2}	CO_2 Density (in kg/l)
ρ_{fuel}	Fuel Density (in kg/l)
ρ_{NO_x}	NO_x Density (in kg/l)
a	Vehicle Acceleration (in m/s^2)
A/F	Air Fuel Ratio
ADT	Average Daily Traffic
CF	Conformity Factor
CO	Carbon Monoxide
CO_2	Carbon Dioxide
d	Distance (in m)
DPF	Diesel Particulate Filter
DPV	Diesel Passenger Vehicle
ECU	Electronic Control Unit
EFR	Exhaust Flow Rate
EU	European Union
$EUDC$	Extra Urban Driving Cycle
FC	Fuel Consumption
FFR	Fuel Flow Rate (in l/s)
GHG	Greenhouse gas
GPS	Global Positioning System
GPV	Gasoline Passenger Vehicle
H	Humidity (in %)

h Altitude (in m)

HC Hydrocarbon

HEV Hybrid Electrical Vehicle

HP Horsepower

IAT Intake Air Temperature

$L/100km$ Liters per 100 kilometers

m_{air} Mass Air Flow Rate (in g/s)

m_{CO_2} CO_2 Mass Flow Rate (in g/s)

m_{ex} Exhaust Mass Flow Rate (in g/s)

m_{fuel} Mass Fuel Flow Rate (in g/s)

m_{NO_x} NO_x Mass Flow Rate (in g/s)

MAF Mass Air Flow Rate (in g/s)

MAP Manifold Absolute Pressure

MPA Mean Positive Acceleration

$NEDC$ New European Driving Cycle

NO Nitrogen Monoxide

NO_2 Nitrogen Dioxide

NO_x Nitrogen Oxide

OBD On Board Diagnostic

PCC Pearson Correlation Coefficient

$PEMS$ Portable Emission Measurement System

PM Particulate Matter

$PM10$ Coarse Particulate Matter

$PM2.5$ Fine Particulate Matter

PN Particulate Number

r Road Grade (in %)

R^2 Coefficient of Determination

RDE Real Driving Emissions Cycle

RPA Relative Positive Acceleration

RPM Revolutions per Minute

SCR Selective Catalytic Reduction System

T Temperature

THC Total Hydrocarbons

UDC Urban Driving Cycle

US United States

USA United States of America

v Vehicle Speed (in km/h)

V_{ex} Exhaust Volumetric Flow Rate (in m^3/s)

v_{jerk} Vehicular Jerk (in m/s^3)

$va_{\text{pos\_}}$[95] 95th Percentile of the Product of Speed and Positive Acceleration greater than 0.1 m/s^2 (in m^2/s^3)

VOC Volatile Organic Compound

VSP Vehicle Specific Power

$WLTC$ Worldwide Harmonized Light Vehicles Test Cycle

$WLTP$ Worldwide Harmonized Light Vehicles Test Procedure

X_{CO_2} CO_2 Volume Fraction (in %)

Intentionally blank page.

Chapter 1

Introduction

1.1 Background

1.1.1 The Emissions Matter

Air pollution can be defined as the presence of toxic chemicals or compounds in the atmosphere which are usually not naturally present at levels that lower the quality of the air and that cause adverse changes to the quality of life, harming human health, damaging culture heritage like buildings, monuments and materials and destroying the environment (such as the damaging of the ozone layer or causing global warming) [EEA 2016]. Road transport brings many benefits to humanity such as the fast and easier movement of persons, goods or aliments, it provides economic growth and it even creates new jobs. On the other hand, even though that there were many technological improvements made during the past decades, this sector is still one of the biggest contributors to Europe's emissions of greenhouse gases and air pollutants. Favorable progress has been obtained during the last decades in what concerns to limiting exhaust emissions from road transport, by the merge of policies and measures, such as improved transport planning, public transport use incentives, the creation of legislation that establishes air quality limits or even setting technological standards for vehicle emissions and fuel quality [EEA 2016]. However, reasons such as the global growth in passenger and shipment requirement along with the under performance of some vehicles standards under real life driving conditions, have implied that emissions diminution has not been as large as originally intended. Almost one tenth of Europe's greenhouse gas emissions (GHG) came from the road transport sector in 2016, being approximately 60% of these emissions derived from passenger transport vehicles (such as passenger cars, motorcycles and buses), as depicted in Fig. 1.1 [Roser 2016]. The European Environmental Agency (EEA) estimates that the road transport sector contributes to about 23% of the European Union (EU) total emissions of Carbon Dioxides (CO_2), 30% of the Nitrogen Oxides (NO_x) emissions and around 12% of the primary PM2.5 emissions (which are fine inhalable particles, that have diameters that are usually 2.5 micrometers or smaller [EPA 2020]) [EEA 2016].

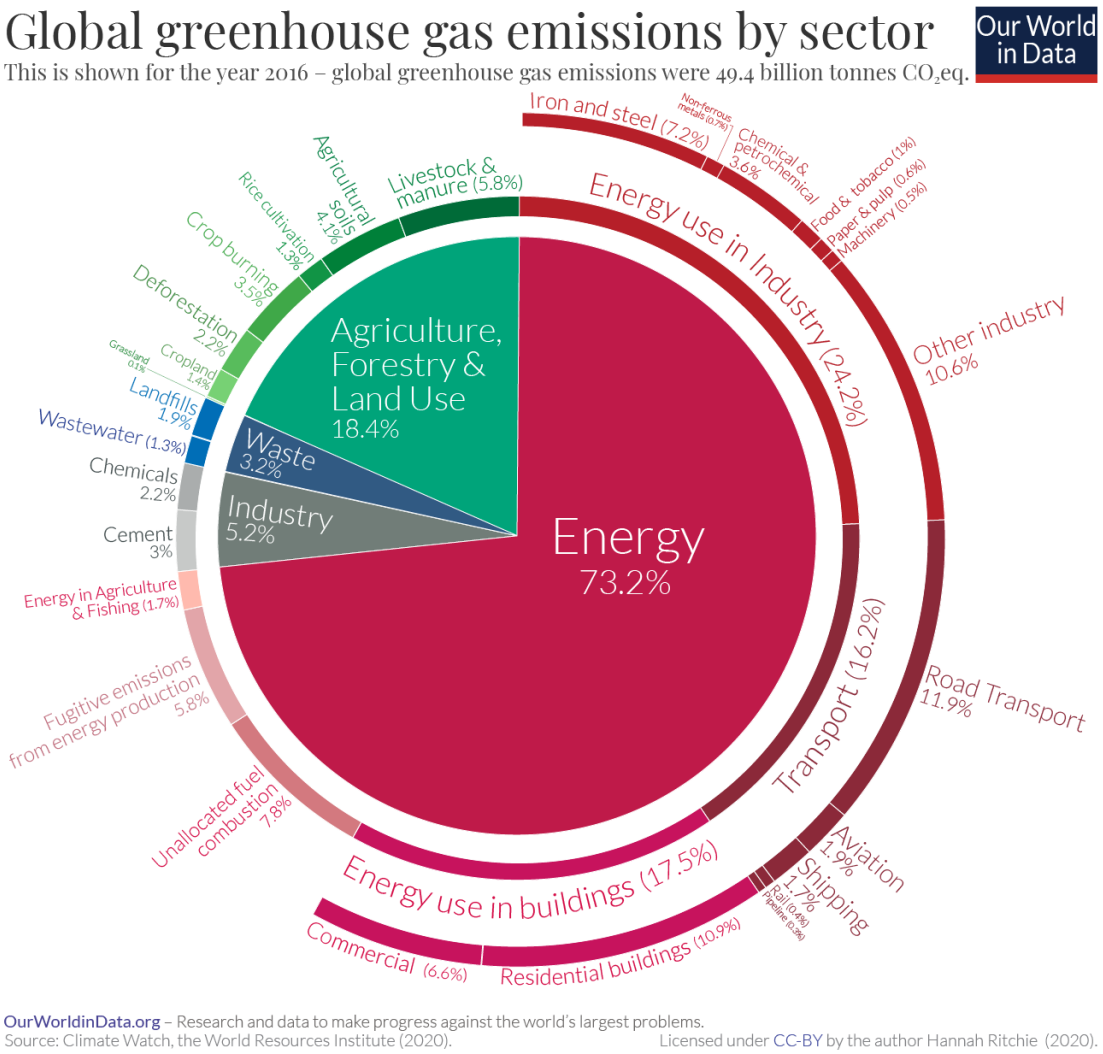

Figure 1.1: Global Greenhouse Gas Emissions by Sector [Roser 2016]

1.1.2 The "Dieselgate" Scandal

In 2015, a controversial scandal, designated as "Dieselgate", has been made public and it consisted in what concerned to the reliability in terms of the accuracy of the emissions measurements that car makers claimed that their vehicles emitted. This scandal has revealed harsh shortcomings in car manufacturers struggle to minimize the impacts of driving on local air quality and on global climate change, like the greenhouse effect. It has been proved the use by the Volkswagen Group of a "defeat device", which was only activated during the official tests, that identifies when a diesel car is being subjected to an official emissions test and optimises engine performance to minimise air pollutant emissions in order to match rigorous emissions regulations. Vehicles that were manufactured by other brands (such as Renault, Citroen and Volvo) have also been revealed to surpass emissions in real world driving conditions. Nevertheless, there has been no proof that the "defeat device" was used outside the Volkswagen Group. When the device was turned off the differences in the NO_x emissions increased up to 40 times [Brand 2016].

1.1.3 The Paris Agreement

Implemented in 2016 by the United Nations Framework Convention on Climate Change aiming to strengthen the global response to the threat of climate change, in the context of sustainable development and effort to eradicate poverty, the Paris Agreement has been created with three main objectives to accomplish [EU 2016]:

1) Holding the increase in the global average temperature to well below 2°C above pre-industrial levels and pursuing efforts to limit the temperature increase to 1.5°C above pre-industrial levels, recognizing that this would significantly reduce the risks and impacts of climate change;

2) Increasing the ability to adapt to the adverse impacts of climate change and foster climate resilience and low greenhouse gas emissions development, in a manner that does not threaten food production;

3) Making finance flows consistent with a pathway towards low greenhouse gas emissions and climate-resilient development.

In order to control and to achieve the objectives that were set by the Paris Agreement, as depicted in Fig. 1.2, each one of the new models of passengers vehicles sold in the European Union must undergo a standardised, off-the-road emissions test to determine the GHGs along with other adverse pollutants such as NO_x.

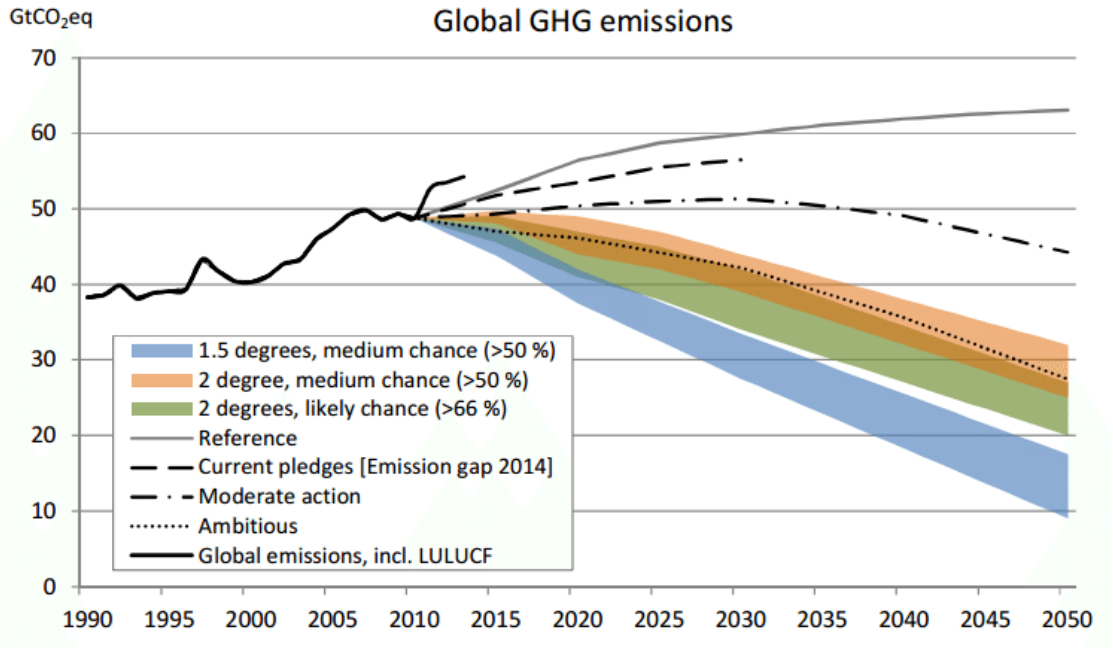

Figure 1.2: Four mitigation scenarios for global Greenhouse Gases (GHG) emissions compared to emission reduction pathways for 2 degree target [Lindroos and Ekholm 2015]

1.1.4 European Emission Standards

The European Emission Standards were created by the EU in 1992 in order to control the levels of pollution that the transport sector emits. Different restrictions were applied to light-duty cars and to heavy-duty vehicles. These restrictions vary from Euro 1 (implemented in 1992) to Euro 6 (implemented in 2014). Over the years the emissions limit has been more restricted and limited in order to try to reduce as maximum as possible the greenhouse effect caused by the transport sector. Emissions of NO_x, Total Hydrocarbons (THC), Carbon Monoxide (CO) and Particulate Matter (PM) are the pollutants that are controlled by these norms. Concerning the CO_2, emission reduction targets have been introduced by the EU. For passenger cars produced between 2015 and 2019, the objective was of 130 grams of CO_2 per kilometre (which corresponds to a fuel consumption of approximately 5.6 Litres per 100 km of petrol (L/100km) or 4.9 L/100km of diesel); and, for vehicles produced between 2020 and 2021, the target was of 95 grams of CO_2 per kilometre (which corresponds to a fuel consumption of approximately 4.1 of petrol L/100km or 3.6 L/100km of diesel) [EU 2020]. The limit values for passenger vehicles are listed in Table 1.1 [European Parliament and Council of the European Union 2007, The European Commission 2016].

Table 1.1: European Emission Standards for passenger cars (g/km)

Stage	Date	CO	HC	HC+NO_x	NO_x	PM	PN [#/km]
Gasoline (or petrol)							
Euro 1	07/1992	2.72	-	0.97	-	-	-
Euro 2	01/1996	2.2	-	0.5	-	-	-
Euro 3	01/2000	2.3	0.2	-	0.15	-	-
Euro 4	01/2005	1.0	0.1	-	0.08	-	-
Euro 5a	09/2009	1.0	0.1	-	0.06	0.005	-
Euro 5b	09/2011	1.0	0.1	-	0.06	0.0045	-
Euro 6b	09/2014	1.0	0.1	-	0.06	0.0045	6.0×10^6
Euro 6c	09/2015	1.0	0.1	-	0.06	0.0045	6.0×10^6
Euro 6d-Temp	09/2017	1.0	0.1	-	0.06	0.0045	6.0×10^6
Euro 6d	01/2020	1.0	0.1	-	0.06	0.0045	6.0×10^6
Diesel							
Euro 1	07/1992	2.72	-	0.97	-	0.14	-
Euro 2	01/1996	1.0	-	0.7	-	0.08	-
Euro 3	01/2000	0.64	-	0.56	0.5	0.05	-
Euro 4	01/2005	0.5	-	0.3	0.25	0.025	-
Euro 5a	09/2009	0.5	-	0.23	0.18	0.005	-
Euro 5b	09/2011	0.5	-	0.23	0.18	0.0045	6.0×10^6
Euro 6b	09/2014	0.5	-	0.17	0.08	0.0045	6.0×10^6
Euro 6c	09/2015	0.5	-	0.17	0.08	0.0045	6.0×10^6
Euro 6d-Temp	09/2017	0.5	-	0.17	0.08	0.0045	6.0×10^6
Euro 6d	01/2020	0.5	-	0.17	0.08	0.0045	6.0×10^6

1.1.5 Types of Vehicle Emissions

The vehicle emissions origins can be categorised into three different groups, as stated in Fig. 1.3, which are the following [EEA 2016]:

1) Abrasion Emissions: produced from the mechanical abrasion and corrosion of vehicle components. PM emissions and emissions of some heavy metals are the major ones that are present. Vehicles tyres, brakes, clutch, the road surface wear or even the corrosion of the bodywork and the chassis can contribute to these kind of emissions. A study performed on Switzerland indicated that for the PM_{10} concentration (coarse PM), in the case of an urban road, it can result from brake-disc abrasion (21%), from resuspension dust (38%) or from exhaust emissions (41%), while the concentration of the same kind of particles along a highway consisted majorly due to resuspension dust (56%) and exhaust emissions (41%) [Penkala *et al.* 2018];

2) Evaporative Emissions: they are the consequence of vapours that escape from the vehicle's fuel system. The major elements that compose this kind of emissions are the Volatile Organic Compounds (VOCs). Petrol fuel vapour is composed by a diversity of various Hydrocarbons (HCs) that can be emitted at any time that fuel is present in the tank, no matter if the vehicle is stopped and even with its engine shut off.

3) Exhaust emissions: these are the kind of emissions that are collected in this master dissertation. They consist in the pollutants released from the combustion of several petroleum compounds like petrol, diesel or natural gas that are mixtures of diverse hydrocarbons. Since no combustion process is ideal, car engines release several distinct gases through their tailpipe besides water and CO_2. The type of fuel being used influences on the amount of each pollutant that is emitted, whether the vehicle is thrust by petrol, diesel or if it is hybrid. The technology present on the engine and the year that the vehicle was constructed also has a major influence on the amount of exhaust emissions that the car releases.

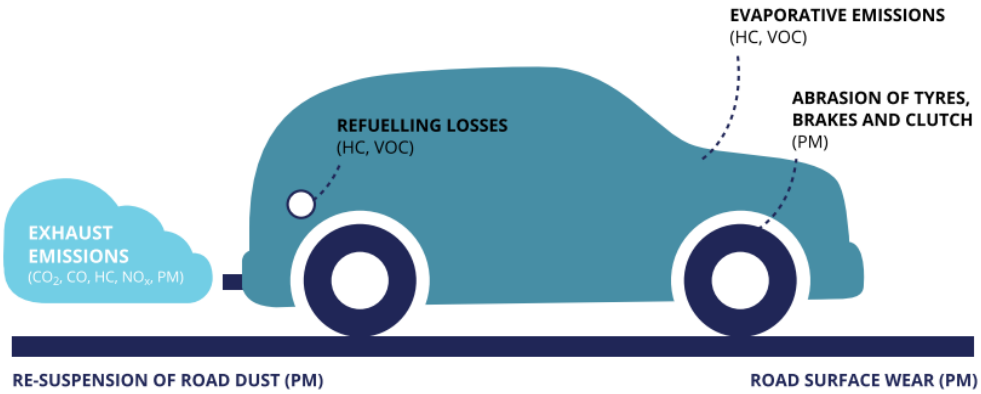

Figure 1.3: The different types of emissions from vehicles [EEA 2016]

1.1.6 Emission Test Cycles History

Throughout the years the type of test cycles that are involved in what concerns to emission testing suffered several changes and adaptations. In the beginning, the original EU test cycle (also known as the UDC 15 + EUDC) was performed under laboratory

conditions included urban, extra-urban segments and was performed from a hot start. After this, the year 2000 brought the New European Driving Cycle (NEDC), that was similar to the previous test cycle but with one major modification that consisted in the elimination of the 40 seconds engine warm-up period before the beginning of the emission control procedures [Mock *et al.* 2014]. In 2017, The Worldwide Harmonized Light Vehicles Test Procedure (WLTP) and the matching Test Cycle (WLTC) were introduced as the main test cycle. This type of emission control protocol is way more effective and provides information to the costumer about vehicle emissions that are much more approximated to the real ones than the ones that were provided by the previous cycles. In comparison with the NEDC, the WLTC is based on a more dynamic type of driving, applying higher speeds during the test, 4 different driving phases (2 rural and 2 urban routes) and it is performed during a longer distance. But, since the WLTC is a test that is made under laboratory conditions, it is still not enough to approximate the theoretical emissions with the real ones. That is why the Real Driving Cycle (RDE) was created along with the WLTC. The RDE is not meant to replace the WLTC, but to complement it. It is performed under real on-road conditions. A car, provided with the equipment that is needed to be able to perform this kind of tests, is driven around rural, urban, and motorway roads, including the grade presence in it and recording, with the assistance of a device called Portable Emissions Measurement System (PEMS), the emissions that were released into the atmosphere from pollutants such as NO_x, CO_2 or the PM. Other pollutants that are also measured by the PEMS such as the HC or the CO will not be on focus on this dissertation.

1.1.7 Technological Development in the European Vehicle Manufacturing Industry

In order to keep up with the stricter European standards in terms of emissions limits along the course of the years, new strategies and developments had to be implemented by the European vehicles manufacturers. Some of those improvements are innovations such as:

- **The manufacturing of hybrid vehicles,** which are more efficient than conventional vehicles and are able to reduce CO_2 emissions and fuel consumption by 35% [German 2015]. These kind of vehicles have an internal combustion engine and one or more electric motor(s) that make this reduction possible. The electrical motors provide instant torque for better response and low-speed acceleration of the car. Along with systems that are able to capture and reuse energy that is usually lost to the brakes (in a process that is known as regenerative braking); preserve their performance while using a smaller but more efficient engine; shutting off the engine at very low load conditions, allowing to conserve fuel and to cut tailpipe emissions to zero; replace the traditional alternator with more efficient motor/generator systems with the purpose of generating electrical power; substitute less-efficient mechanical water and oil pumps with electrical pumps.
- **The manufacturing of electric vehicles,** that exclusively have an electrical motor instead of the classic internal combustion engine. These kind of motors have an efficiency that may exceed 80% and their batteries are also in the same range. A typical electric vehicle requires about 0.15 kWh/km to operate, instead of the

approximated 0.6 kWh/km that a conventional petrol vehicle needs [Ntziachristos and Dilara 2012]. However, this type of vehicle production also has its limitations. It is known that electrical vehicles do not use petrol as the conventional vehicles do, nevertheless, there is a possibility that these kind of automobiles depend on other limited resources because of their battery construction constitution. These batteries are composed by minerals like lithium, cobalt and nickel, that have been considered as critical minerals for national security and the economy by the United States (U.S.) Department of the Interior. It has been estimated that worldwide demand for cobalt for battery production could consume about 14% of current cobalt reserves by 2050 [Gaines and Richa 2019]. Another limitation is related with the end of life of batteries and with its recycling after it is stopped being used. Normally a battery can last around 10 years before it is disabled. Recycling this batteries is what should be done but there are some limitations associated to this process. There are several methods for recycling these batteries in use but none of them is ideal for all battery types and volumes. For example the "Pyrometallurgical recycling" (smelting) method recovers valuable transition metals but leaves both of the lithium and the aluminium in the slag, which makes them difficult to recover. Furthermore, a large capital is expended for an economical industrial-scale smelting plant, mainly because of the gas treatment that in needed in order to prevent the release of fluorine compounds and harmful organics [Gaines and Richa 2019]. So, as proved, electrical vehicles are a good alternative to conventional vehicles but they also have their limitations;

- **The introduction of "eco-innovations" into EU vehicle legislation,** which allow a vehicle manufacturer to apply for the approval of new technologies developed in order to reduce CO_2 emissions in savings that could be higher than 1 gram of CO_2 per kilometer [EEA 2016]. Some examples of this kind of innovations are the use of ambient energy sources (photovoltaic panels in the roofs of vehicles); efficient lighting systems (LED lighting); improved electrical components (high efficient alternators); engine compartment encapsulation (which is an extra insulation component to maintain the heat in the engine compartment that decreases the waste of energy); energy storage systems (the utilization of the potential energy of the roads in order to recharge vehicles batteries).

- **The improvement of engine efficiency strategies,** because of the fact that only about 25% of the energy included in fuel is used to move vehicles and with the implementation of the right strategies and a bigger engine efficiency there could be a reduction of about 30% in terms of CO_2 emissions [Leach *et al.* 2020]. Techniques such as the use of Direct Fuel Injection (which is the direct injection of petrol into the cylinder, allowing that the timing and quantity of fuel is precisely controlled resulting in higher compression rations and more efficient fuel intake, delivering a superior performance while consuming less fuel); the implementation of valves with variable timing and lift (which allow that the valve opening and closing times and its lift is varied to the optimum settings for different engine speeds); the deactivation of some of the engine's cylinders when they are not necessary, especially at low speeds; the implementation of turbochargers and superchargers into the engines (these are fans that compress air into the cylinders, allowing that a bigger quantity of compressed air and fuel to be injected into them, generating

extra power from each combustion and admitting that car manufacturers use minor engines without the loss of any performance); the utilization of start-stop systems (a feature that shuts down the engine whenever the car comes to a complete stop and that restarts it whenever the driver engages the clutch, preventing the waste of fuel and the pollutants emission whenever the vehicle is stopped).

- **The implementation of efficient exhaust technologies,** since the development of engine technologies itself was good but not enough in order to meet the emission goals imposed, so the introduction of innovations in what concerns to the exhaust systems was necessary to complement them. This exhaust system technologies consist mainly in the use of different types of catalytic converters, traps and filters. A catalytic converter is an instrument that uses a catalyst to convert the main prejudicial air pollutants that are present in vehicle exhaust emissions into inoffensive compounds. It activates certain oxidation and reduction reactions that convert CO, HCs and NO_x into CO_2, water and nitrogen and it is typical constituted by one or more honeycomb bricks, possessing a characteristic cross-section of small squares or alternatively triangles [EEA 2016]. One example of this technology is the Selective Catalytic Reduction System (SCR), which is an equipment that reduces NO_x emissions by injecting a liquid reducing agent (usually urea) through a special catalyst into the exhaust stream of a diesel engine, as depicted in Fig. 1.4. This liquid starts a chemical reaction that converts NO_x into nitrogen, water and CO_2 that are consequently expelled through the vehicle exhaust. This is one of the most effective equipment that exists proven to reduce diesel NO_x in order to comply with the emission standards goals; other type of device are the Diesel Particulate Filters (DPFs) which are used to reduce the Particulate Matter (PM) emissions. These devices operate with the use of wall-flow filters, which are made of a honeycomb structure, that retain the PM particles in its walls contained in the exhaust gases that are being expelled. Traps are specially used when engine operating conditions are not ideal for conventional catalysts to achieve their total capacity. They control emissions of particular pollutants (NO_x or HCs), storing them but realising them when the conditions are appropriated for it to react with the catalytic components.

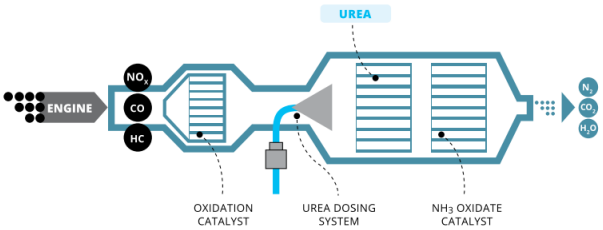

Figure 1.4: Selective Catalytic Reduction System example [EEA 2016]

Although of the above cited implemented measures, the CO_2 emissions targets are still not being accomplished by the manufacturers and the divergence between the field emission measurements and the laboratory ones is noticeable, as depicted in Fig. 1.5. Since 2019, each manufacturer has to pay a penalty of 95€ for each g/km of CO_2 target exceedance for each registered car.

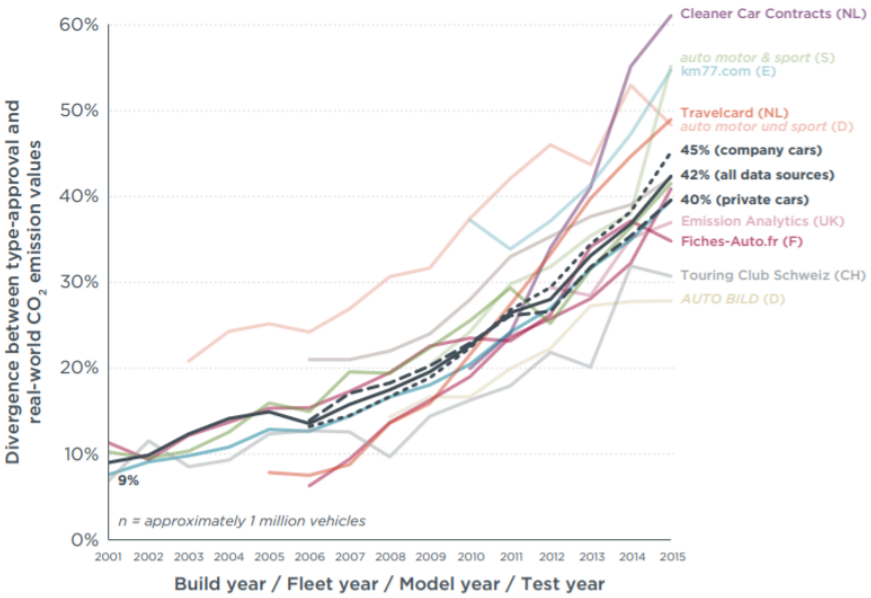

Figure 1.5: Divergence between the field emission and the laboratory CO_2 measurements [Tietge *et al.* 2017]

Despite of the increase along the recent years in the number of sales of electric and hybrid vehicles, the ones that continue to dominate the European market are the gasoline and diesel ones, as stated in Fig. 1.6. However, comparing what was registered in July 2019 to the values registered in July 2020 it can be stated that the sales of electric and hybrid vehicles were more than double, which means that sales of electric vehicles and hybrid cars rose to their highest ever share in Europe, grabbing 18% of the total European passenger car markets, along with the 52% of the gasoline and the 28% of the diesel vehicles [Driven 2020].

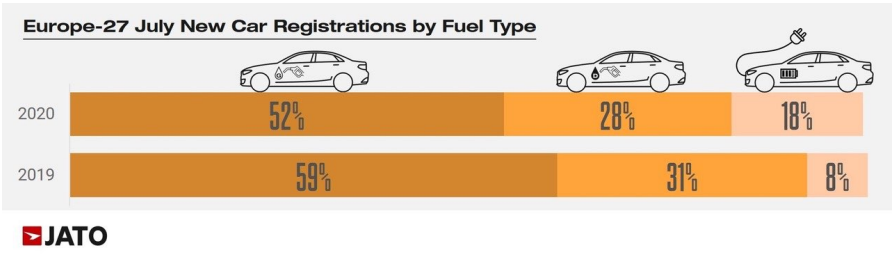

Figure 1.6: Sales by Vehicle Type [Driven 2020]

1.2 Objectives

The main objective of this master dissertation will be to perform the experimental monitoring of pollutants emissions from different road vehicles that use different types of fuels on different kind of routes. An empirical method embracing vehicle data collection

regarding its operating conditions and its consequent emissions will be developed. The specific objectives are as follows:

- To identify the impacts of acceleration, vehicular jerk, engine parameters, vehicle specific power (VSP) and route characteristics on the emission rates of the CO_2, NO_x and PM;
- To develop a predictive emission model based on the VSP methodology in gasoline and diesel passenger cars.

The routes that were selected for the tests include two highways (A1 and A29), partly urban/rural roads (N109) and urban itineraries that have different road grades and traffic conditions that are situated in the Aveiro region, Portugal. Two vehicles were used during the tests, being one of them ran by gasoline and the other one by diesel. All the data that are gathered after the on-road tests being performed, are treated and analysed with the objective of extracting information such as the speed profiles, accelerations, road grade, vehicular jerk, the vehicle specific power (VSP), the emission factors associated to each kind of car, the amount of different pollutants that are sent to the atmosphere by the different vehicles that were tested and the fuel consumption that each car consumes. Driving style was characterised by metrics for both validating PEMS trips according to the European Union commission regulation and for investigating the effect of these parameters on emission rates [European Parliament and Council of the European Union 2007]. By analysing this data, the comparison between on-road and laboratory tests cycles and the association of the difference VSP modes with emission factors associated with real driving conditions has been performed. A VSP-based approach predictive model was also applied in order to observe the concordance between the VSP and the field CO_2, NO_x and PM emissions.

1.3 Structure

The purpose of the Chapter 1 (Introduction), was firstly to provide a background to the reader in order for him to acquire knowledge about the motivations that led to the execution of this document. Afterwards, the objectives to accomplish during this work were set in function of the motivations that led to its performing.

In what concerns to the Chapter 2 (Literature Review), it consisted in the research about the already existing laboratory testing procedures and in the study about the diverse areas which compose the Real Driving Emission testing, such as the driving style characterization parameters, the influence of different road grades, the comparison between the on-road and the laboratory obtained emissions and the reliability of the VSP-based approach methodology.

With the purpose of adapting the concepts and technical aspects described in the Literature Review, an appropriated methodology which fulfilled the objectives of this work was adopted (Chapter 3). Firstly, a well defined structure of the work plan was described (3.1), then, the delineated experimental design in terms of selected vehicles and test routes was represented (3.2), being the specifications of the utilised test instruments and its installation characterised right next (3.3). Afterwards, a description about the on field collected data measurements was also stated (3.4), along with the approach that was carried out in order to grant the quality of the collected data (3.5). Finally, the

way in that the collected data were analysed in terms of the validation of the PEMS trips, driving style parameters, estimation of the road grade, vehicular jerk calculation, emission rates and the VSP methodology was also described (3.6).

After applying the above mentioned procedures to the collected data, the obtained results and respective analysis was performed (Chapter 4). The validated test trips (4.1), the driving style parameters (4.2), the obtained on-road emissions compared to the Euro 6 imposed limits (4.3), its hotspot emission locations (4.4) and the relationship between the VSP-based predictive model and the obtained emission rates (4.5) was also in analysis, as well as the reliability of the proposed model (4.6). In the sequence of the Chapter 4, the Chapter 5 (Conclusion) was written with the purpose of performing a brainstorm about the previously analysed data and to suggest future work developments.

Intentionally blank page.

Chapter 2

Literature Review

2.1 Laboratory Testing Procedures

2.1.1 NEDC

The NEDC (New European Driving Cycle) is a version of the former UDC (Urban Driving Cycle) + EUDC (Extra Urban Driving Cycle). These cycles were originally developed when vehicles were lighter and less powerful than those available today. Before the test, the car was authorised to soak for about 6 hours at a test temperature of 20-30°C and allowed to idle for 40 seconds before starting the emission sample collection. After the year 2000, this idling period has been removed, which means that engine started at 0 seconds and the emissions sample collection also started at the same time. This change generated the modified cold-start procedure that is called the New European Driving Cycle (NEDC), whose Driving Cycle is depicted in Fig. 2.1. The overall distance of the whole test is about 11.03 km for about 1180 seconds with a medium speed of 33.6 km/h [Mock *et al.* 2014].

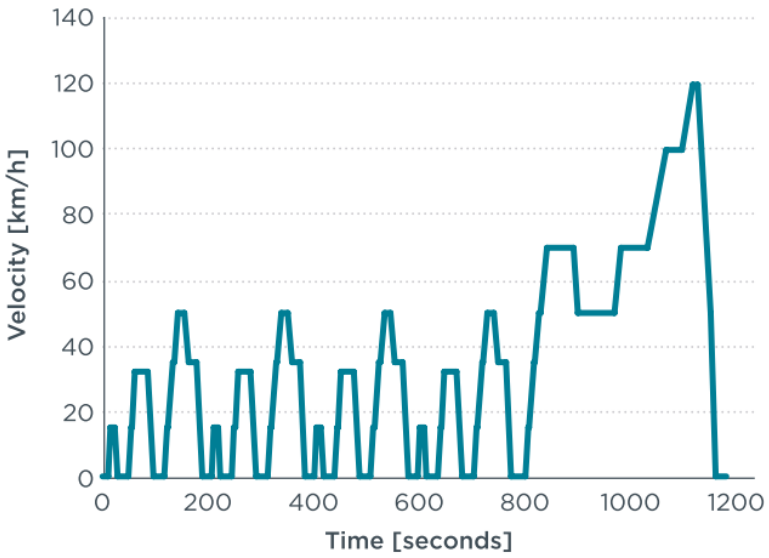

Figure 2.1: NEDC Driving Cycle [Mock *et al.* 2014]

However, a gap between real world and test cycle emissions exists and it is mainly

due to three main factors [Kadijk 2012], [Transport and Environment 2015]:

1) An outdated test procedure that does not reflect real-world driving conditions;

2) Flexibilities in the current procedures that allow manufacturers to optimise the testing, and thereby achieve lower fuel consumption and CO_2 emissions;

3) Several in-use factors which are driving dependent (for example different driving styles that vary from driver to driver and that change emissions rates) or independent (for example windy conditions, fog, rain or other meteorological conditions that also have influence on the emissions rate).

There are two major categories in which manufacturers can exploit some facilities that are divided into: the ones that concern to the initial coast-down test and the ones that concern the collection of CO_2 emissions and fuel economy data [Kadijk 2012].

The coast-down test consists in driving a vehicle up to a determined speed and decelerating it in its neutral gear until it comes to a complete stop. The travelled distance and the car's speed are continually recorded throughout the all test. This test has the purpose of establishing the proper resistance levels that are going to be used on the dynamometer for each vehicle model during the type approval test.

The main flexibilities that concern the coast-down test consist in the selection of low-rolling resistance tyres, low width wheels and tyres that optimise rolling and aerodynamic resistance; the overinflation of tyres in comparison to normal use, culminating in a lower rolling resistance; adjustments to vehicle brakes with the purpose of eradicating parasitic drag, which are losses that come from unintentional braking; the optimisation of vehicles temperature during the testing in order to obtain lower rolling resistance; the use of tyres with minimum tread depth; the optimisation of road surface in which the vehicle is tested to a surface that is as smooth as possible in order to reduce rolling resistance. A study conducted in the Netherlands concluded that using all flexibilities related to road based measurement of the coast down times could lead to a 4.5% reduction in CO_2 emissions, along with other reductions in PM and NO_x emissions throughout the NEDC testing [Kadijk 2012].

For the NEDC type approval test and for the collection of CO_2 emissions and fuel economy data the major allowed flexibilities that manufacturers may take advantage of are strategies such as reducing the vehicle testing mass by specifying items as dealer-fitted optional extras, turning into lower resistances in the chassis dynamometer; the optimisation of the overall vehicle configuration for testing, for instance by choosing low-rolling resistance tyres and an excessive tyre pressure in order to reduce the area of contact between the tyre and the ground, consequently reducing the friction associated to it, specifying that this is the standard vehicle setting; the calibration of the instrumentation equipment used to perform the test being made towards one end of the allowable range, such as the temperature, atmospheric pressure and humidity of the test cell, accuracy of the gas analysers, etc.; raising the temperature in the test cell before and during the test that reduces friction in the engine and vehicle components in order to improve efficiency and to reduce CO_2 emissions; the choice of using a "cookbook" method that consists in standard "table values" that can be used to simulate the road load during the type approval test for vehicles that have relatively high aerodynamic or rolling resistance and under perform in the coast-down test; if a vehicle cannot reach a speed of 15 km/h while on first gear, the use of higher gears in allowed. This reduces fuel consumption as higher gears permit that the engine operates more cleanly while functioning on lower rotations per minute.

Other factors such as the ones that are going to be mentioned are also responsible for the divergences between laboratory measurements and real-world emissions [EEA 2016]:

- **The use of on-board electrical equipment** that is switched off during the type approval test (such as window defrosters, air-conditioning, entertaining systems, heated seats), increasing the fuel consumption and not being taking into account to the data that are collected;
- **The state of the car** and some additional passengers or cargo that has been added, which makes the car heavier and which makes it consequently to consume more fuel that leads to an increase in emissions; the addition of accessories for carrying cargo in the roof of the car that enhance wind drag or even lower than recommended tyre pressure that intensifies rolling resistance;
- **The different driving behaviour of each person and weather conditions** such as a person that is more nervous while driving, producing rapid accelerations and braking that will consequently increase fuel consumption; weather conditions and road surface conditions such as unexpected bumps or obstacles that are present in the road can also alter fuel economy.

In this study made by the EEA in 2016, a software named of AVL Cruise was used to determine the impact that adding some of these conditions could have in the fuel consumption and CO_2 emissions. A typical mid-sized petrol car was used that had an official fuel consumption of 7.6 L/100 km, is estimated by the software to have a fuel consumption of 8.8 L/100 km, 16% higher than reported. Some additional parameters can be estimated using this vehicle simulation software such as turning the air-conditioning unit on; the additional cargo of four persons and luggage; the inflation of 30% in average speed, rapid acceleration and braking; adding a roof rack that increased the aerodynamic drag coefficient and the frontal area in contact with the wind.

After inputting all of these parameters in the AVL Cruise Software, it was concluded that real-world fuel consumption for this car might be as high as 12.6 L/100 km, which represents an increase of 65% compared to the measurements of the NEDC type approval test [EEA 2016].

2.1.2 WLTP

The World-Harmonized Light-duty Vehicle Test Procedure (WLTP), was started to be developed in 2008 and applied from 2017 on [EEA 2016]. Its Driving Cycle is depicted in Fig. 2.2. While the term WLTP indicates the complete framework of the test procedure, testing conditions and the test cycle, the term WLTC (World-Harmonized Light-duty Vehicle Test Cycle) is used to specifically identify the test cycle only. The purpose of this cycle was to bring some fundamental regulatory modifications compared to the previous NEDC approach in order to achieve values that are more representative of real-world emissions and that will have a direct impact on CO_2 emissions.

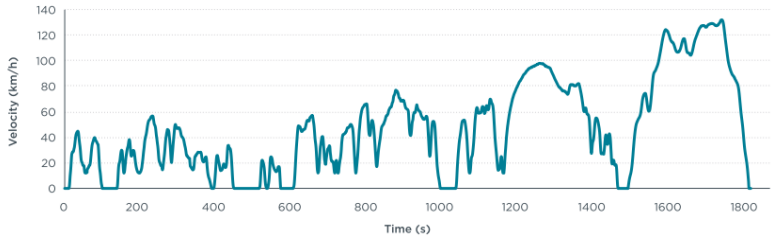

Figure 2.2: WLTP Driving Cycle (WLTC) [Mock *et al.* 2014]

Some of the main differences that can be noticed caused by the introduction of this renewed cycle are, as follows [Mock *et al.* 2014]:

- **The influence in the emissions released during the cold start,** when a vehicle is driven while its engine is cold, the CO_2 emissions increase due to higher mechanical friction and higher fluid viscosity. This cold start is almost independent of the driving pattern so whoever is driving the vehicle will almost always obtain higher emissions than usual while the engine operates at inferior temperatures. So, the WLTC has a longer duration and distance compared to the NEDC (1800 seconds versus 1180 seconds and 23 km versus 11 km), which means that the added cold start contribution to the total emission result is only about half of the added cold start contribution in the NEDC;

- **In terms of vehicle load,** the WLTC attains superior speeds compared to the NEDC (131.3 km/h versus 120 km/h), hits stronger acceleration forces and the vehicle stays less time at a constant speed, accelerating and decelerating much more time and consequently obtaining higher vehicle loads;

- **Engine speed also has a direct impact on CO_2 emissions,** because the higher the engine speed is the higher the friction and the pumping losses that aggravate the CO_2 emissions are. Vehicles that have manual transmissions have to follow strict specifications that determine at which point in a time a certain gear position has to be selected in the NEDC. This is not the same in the WLTP, since in this Cycle the gear shift points are adjusted to the unique characteristics that each vehicle possesses. This means that the shifting points in the WLTP will be at lower engine speeds than in the NEDC, reducing engine speeds for manual transmission vehicles and resulting in proportionally lower CO_2 emissions for these vehicles in the WLTC;

2.2 Real Driving Emission Testing

In this section, studies including the use of the PEMS were divided into five subsections, namely the Driving Style (2.2.1), the Vehicular Jerk (2.2.2), the Road Grade (2.2.3), the Real World versus Standard Laboratory Emissions Limits (2.2.4), the VSP-based Predictive Models (2.2.5) and the Concluding Remarks (2.2.6).

2.2.1 Driving Style

As expected, the way that a vehicle is driven makes a huge difference in several parameters, such as car and engine wear, tyres management and in fuel consumption. So, vehicle emissions rates are not an exception and are also related to the driving style of whoever is driving the automobile.

By changing driving styles, accelerating and decelerating with different frequencies and intensities, through the use of several different vehicles and observing internal and external variables, such as the acceleration based parameters like Relative Positive Acceleration (RPA), Mean Positive Acceleration (MPA) or the 95^{th} percentile of the product of speed and positive acceleration greater than 0.1 m/s^2 ($va_{pos\_}[95]$), it was concluded that the emissions of HC and CO suffered minor changes compared to the ones that CO_2 and NO_x suffered [Gallus *et al.* 2017, Tzirakis *et al.* 2007]. On the other hand, CO_2 and NO_x emissions measured by the PEMS showed a strong correlation with the selected driving parameters and it was proved that larger driving parameters led to a significant increase of these 2 pollutants compared to normal trips. While compared to average driving, CO_2 emissions increased by 20-40% and the NO_x emissions grew in about 50-255% [Gallus *et al.* 2017]. Concerning the fuel consumption, it was concluded that its increase due to aggressive driving compared to defensive driving, varied from 78-137% for petrol vehicles and from 116-128% for diesel vehicles [Tzirakis *et al.* 2007]. The impact of the driving style on THC and CO emissions was also evaluated with the use of three distinct types of driving cycles, namely a "cautious", a "normal" and a "dynamic" type of driving, being the first cycle the most calm one and the last one the most aggressive one [Satlawa *et al.* 2020]. It was concluded that for the "dynamic" type of cycle the THC emissions oscillated between 2-6 mg/s, being much lower for the other 2 types of cycles, never exceeding a value of 1.5 mg/s. Also, concerning the CO emissions, on the "dynamic" cycle, they ranged between 250-2000 mg/s, oppositely from what it was verified in the case of the other two types of cycles, where they did not exceed 6.5 mg/s [Satlawa *et al.* 2020].

2.2.2 Road Grade

It is well known that when a road is steeper any vehicle will be submitted to an extra effort that will bring some consequences along with it. It was concluded that flat roads can save up to 10-20% of fuel compared to the hilly ones [Boriboonsomsin and Barth 2009, Hu and Frey 2017].

In terms of pollutants emissions, it was concluded that the step from 0-5% road grade led to a CO_2 increase of 65-81% and to a NO_x raise of 85-115% [Gallus *et al.* 2017]. Other investigations concluded that CO_2 emissions increased due to uphill in about 85% and 60% that NO_x emissions grew in about 33% and 40%, respectively [Cnr *et al.* 2018, Hu and Frey 2017]. It was also deduced that the reduction caused in CO_2 and in NO_x emissions by downhill descents is of about 45% and 60% [Cnr *et al.* 2018].

It was also stated that high altitude shows a great influence on vehicle emissions because of lower pressure and shortage of oxygen concentrations [Wang *et al.* 2018]. Research results show that CO emissions increased with the elevated altitude. At the altitude of 2990m, the CO emissions increased by 209% in comparison with that of near sea level in whole test cycle. Both PM and NO_x emissions also rose with altitude while NO_x emissions at 2990m showed a decreasing tendency [Wang *et al.* 2018].

2.2.3 Vehicular Jerk

Vehicular jerk can be defined as the change of rate of acceleration profiles with respect to time [Fernandes *et al.* 2020, Feng *et al.* 2017, Bagdadi 2013, Khattak *et al.* 2019, Wali *et al.* 2019], being considered the first derivative of acceleration/deceleration, which is a strong indicator of driving volatility and of the driving style of each person.

Although there have not been produced many articles about this parameter, specially related to the monitoring of vehicle emissions testing, jerk has been used for decades. It started to be useful to determine the smoothness or abruptness of a certain movement in several domains such as the trajectory planning of the human arm [Viviani 1995] and industrial robots [Macfarlane and Croft 2003]. After being adapted to the vehicle's domain, vehicular jerk has been proved to be related to a driver's physiological feeling of ride comfort and transmission shift [Huang and Wang 2018]. Jerk was even used to detect drivers' stress levels, by the use of a driving simulator study [Othman *et al.* 2008] that discovered that the larger the jerk was when the driver was commencing to accelerate or decelerate to stop, the higher the self-stated stress levels were. An innovative method, named of critical jerk, was developed for detecting jerks in safety critical events, based on the characteristics of the braking caused by the driver in critical situations [Bagdadi and Várhelyi 2012, Bagdadi 2013]. The peak-to-peak jerk measure of jerks was used, consisting in analysing the difference between the maximum positive jerk and the maximum negative jerk during a brake manoeuvre, allowing to distinguish between the manoeuvres performed in situations where the driver had less than 1.5s to react and in situations that the driver had more than 1.5s to react. So, with this type of analysis, it was concluded that the proposed method of critical jerk was able to distinguish between critical and potentially critical situations as well as detecting traffic conflicts and also distinguish between traffic conflicts estimated to be more serious and conflicts with lower severity.

It was concluded that compared to deceleration/acceleration, vehicular jerk can better characterize the volatility in microscopic instantaneous driving decisions prior to involvement in safety critical events, such as crashes [Wali *et al.* 2019]. It was also found out that a one-unit increase in intentional volatility is associated with positive vehicular jerk in the longitudinal direction which increases the chance of crash or near crash outcome by 15 and 12%, respectively.

Vehicular jerk also contains useful information that can be potentially used to identify aggressive drivers. There are singular characteristics of vehicle jerk in drivers' gas and brake pedal operations [Feng *et al.* 2017]. When the gas pedal is pressed, the jerk is positively correlated to the speed the driver was pressing the gas pedal. So, this discovery can have potentially advantages such as warning the surrounding drivers or vehicles using the connected vehicle technologies that an aggressive driver is driving in their proximity. This parameter is also affected by roundabouts, since vehicles experience fast gear changes and sometimes a more aggressive driving and hard braking manoeuvres when they are circulating in them [Fernandes *et al.* 2020].

2.2.4 Real World versus Standard Laboratory Emissions Limits

In terms of emissions disparities between the ones measured in real world tests and on standard laboratory cycles, there are several researches that approached if the quantities of NO_x, CO_2 and Fuel Consumption matched what was previous stated on laboratory

procedures or not.

NO_x emissions seem to be the most affected by this change of methodology. It was found out that NO_x average emissions of an Euro 6 car are considerably lower than the ones from the Euro 4-5 cars. Although CO and THC emissions of both diesel and gasoline vehicles stay within the Euro 3-5 emission limits and the NO_x emissions of gasoline vehicles are also matching these limits, average NO_x emissions of all tested diesel vehicles substantially exceed the Euro 3-6 emission standards by about $260\% \pm 130\%$ [Weiss *et al.* 2011, Weiss *et al.* 2012]. In a slightly different approach,a filter to the real driving emissions tests that were performed in order to match on-road events to NEDC conditions was applied, in terms of vehicle speed, acceleration, road grade and ambient temperature. Despite the application of this filter, filtered NO_x emissions exceeded by 206% those measured on the NEDC. For the unfiltered NO_x emissions and as expected, these measurements surpassed the registered NEDC NO_x emissions by 266% [Degraeuwe and Weiss 2016].

The use of conformity factors was applied in 2017. The conformity factor (CF) consists in the ratio between the on-road measured NO_x emissions for a vehicle and the laboratory testing limit for NO_x emissions. Euro 5 and Euro 6 vehicles were submitted to tests. In the paper it was stated that for Euro 5 diesel vehicles, CFs ranged from just over 1, which naturally means that those cars almost complied legal limits under real-world conditions, to 11, which means that real-world registered emissions surpassed in about 11 times the legal limit. The average CF for Euro 5 vehicles was of about 4.1. Additionally, for Euro 6 diesel cars, the registered CFs varied from 1 to 12, meaning that the range was slightly wider and the average CF for all cars tested from this category was of about 4.5 which means that the emissions from every vehicle were above the standard laboratory imposed limits [Baldino *et al.* 2017].

In the United States of America (USA), it was stated that the standard driving cycles and certification emission rates are not representative of real-world measured DPVs emission rates, being this real-world emission rates on average 43% higher than the certification levels [Frey *et al.* 2017]. Two types of hybrid electrical vehicles (HEVs) were also studied and both failed the Euro 6 limit of PN emissions by a margin of 34 and 99.3%, being 82% of the emissions of PN of one of the vehicles emitted during the urban driving stage of the entire route [Yang *et al.* 2019]. More recently and to corroborate the studies that were previously performed, the NO_x emissions of four diesel vehicles were measured and it was also stated that these were on average 3-4 times higher than standard emissions limits [Fernandes *et al.* 2019a].

In terms of CO_2 emissions, the circumstances are not as critical as in the NO_x emissions case but they are still not in concordance with the imposed standard limits. An exceeding in both gasoline and diesel vehicles CO_2 emissions of $21\% \pm 9\%$ and of $8\% \pm 13\%$ from the NEDC emission standards in two distinct papers was noticed [Weiss *et al.* 2011, Weiss *et al.* 2012]. Two other papers also took similar conclusions, concluding that CO_2 emissions were about 30% and 105% higher than the standard emissions limits, respectively [Baldino *et al.* 2017, Fernandes *et al.* 2019a].

2.2.5 VSP-based predictive models

The Vehicle Specific Power (VSP) is a parameter which accounts for power demand, rolling resistance, road grade and aerodynamic drag, that is estimated considering

second-by-second speed, acceleration and road grade [Jimenez-palacios 1999]. Therefore, this method was shown to have a direct relationship in CO_2, NO_x and PM emission rates, as well in the fuel consumption values for both gasoline and diesel type of vehicles [Frey *et al.* 2008, Coelho *et al.* 2009].

A distinct approach was used by Frey et al. (2008), which had the purpose of employing the VSP methodology in order to predict pollutant emission rates in different routes, analysing several parameters that influenced these emission rates such as the road grade or the hour of the day when the trip was being performed [Frey *et al.* 2008]. According to the developed research, it was concluded that emission rates were increased in about 20% in the presence of positive road grades present on the routes and that emissions could rise in approximately 19% when the road traffic was superior. Three main reasons for the increase in vehicle emissions were stated by this article, which consisted in the speed, acceleration and the road grade.

In a slightly different perspective, it is also possible to apply the VSP methodology to more peculiar situations. In 2009, Choi and Frey, used the VSP-based approach in order to estimate emission factors on small highway segments on speeds that were superior to 105 km/h [Choi and Frey 2009]. It was concluded that emission factors are easily affected to increase in speeds from 105 km/h to 126 km/h, specially in the case of the CO. However, it was also verified that increases in the emission rates of the CO_2, NO_x and HC were superior when there was an increase of low speeds compared to the increase in high speeds.

2.2.6 Concluding Remarks

As analysed before, several studies referred the effects of different driving styles and road grade on emissions. Others stated the differences between real driving emissions and laboratory emissions, as well as the obtained results through the use of VSP-based predictive models. However, the inclusion of the vehicular jerk parameter is almost null. On this master dissertation, and like in some of the previously cited articles, the variables of the driving style and of the road grade will also be on study related to the influence that they have on vehicle emissions, as well as the comparison between these obtained emissions with the standard limits applied by the European Union and if they comply with them or not. The implementation of a VSP-based predictive model of the emission rates for both vehicles will be also performed. An attentive analysis of the relation between speed, acceleration and vehicular jerk will be done. The critical hotspots of vehicle emission rates and of the parameters which have direct influence on its variations, like steep slopes or aggressive driving, will also be performed.

To complete this chapter, the major observations for each one of the most relevant analysed articles to account for was made, as depicted in Table 2.1.

Table 2.1: Literature review on the analysis of vehicle emissions

Analysed Articles				
Subchapter	Reference	Fleet	Description	Limitations
2.2.1; 2.2.2	[Gallus *et al.* 2017]	2 Diesel Passenger Vehicles (DPVS) (Euro 5-6)	Aggressive driving increased CO2 by 20-40% and NO_x by 50-255%; CO and HC were not affected by it; The step from 0-5% road grade led to a CO_2 increase of 65-81% and NO_x of 85-115%	Did not use the parameter of the vehicular jerk
2.2.1	[Tzirakis *et al.* 2007]	10 Gasoline Passenger Vehicles (GPVS); 2 DPVs	Fuel Consumption increased by 79-137% in GPVs and by 116-128% in DPVs due to aggressive driving	Did not use the parameter of the vehicular jerk
2.2.1	[Satlawa *et al.* 2020]	1 DPVs (Euro 6)	THC emissions for the "dynamic" type of cycle the oscillated between 2-6 mg/s, being much lower for the other 2 types of cycles ("cautious" and "normal"), never exceeding a value of 1.5 mg/s; CO emissions, on the "dynamic" cycle, ranged between 250-2000 mg/s, oppositely from what it was verified in the calmer two types of cycles, where they did not exceed 6.5 mg/s	Did not use the parameter of the vehicular jerk
2.2.2	[Boriboonsomsin and Barth 2009]	1 GPV	Flat roads can save up to 15-20% of fuel compared to hilly roads	Did not use the parameter of the vehicular jerk

Continuation of Table 2.1				
Subchapter	Reference	Fleet	Description	Limitations
2.2.2	[Cnr *et al.* 2018]	1 GPV (Euro 5)	CO_2 and NO_x emissions increase due to uphill of 85 and 33%, respectively; Reductions in emissions caused by the downhill are 45 and 60% on CO_2 and NO_x, respectively	Did not use the parameter of the vehicular jerk
2.2.2	[Frey *et al.* 2017]	3 GPVs	Average fuel consumption, CO and NOx emissions increased 10%, 60% and 40%, respectively, for the high-altitude mountainous routes compared to the low altitude piedmont ones	Did not use the parameter of the vehicular jerk
2.2.2	[Wang *et al.* 2018]	1 DPV	At the altitude of 2990m, the CO emissions increased by 209% in comparison with that of near sea level in whole test cycle; Both PM and NO_x emissions also rose with altitude while NO_x emissions at 2990m showed a decreasing tendency	Did not use the parameter of the vehicular jerk
2.2.3	[Bagdadi and Várhelyi 2012]	1 GPV	The proposed method (critical jerk) seems to be capable of distinguish between critical and potentially critical situations as well as to distinguish between traffic conflicts estimated to be more serious and conflicts with lower severity	Did not use the parameter of the vehicular jerk

Continuation of Table 2.1				
Subchapter	Reference	Fleet	Description	Limitations
2.2.3	[Bagdadi 2013]	100 car naturalistic driving study data set	The proposed method (critical jerk) performs statistically significantly higher success rates compared to the longitudinal acceleration method for detecting near-crashes (1.6 times higher detection rate, that means 86% versus 54%)	Further research and development are needed to incorporate both longitudinal and lateral manoeuvres in the method, which is a necessity for the analysis of evasive manoeuvres other than braking
2.2.3	[Feng *et al.* 2017]	16 Automatic GPVs	When the gas pedal was pressed, the jerk is positively correlated to the speed the driver was pressing the gas pedal; The frequency of using large negative jerk seems to have better performance in identifying aggressive drivers	Did not use the parameter of the vehicular jerk
2.2.3	[Fernandes *et al.* 2020]	1 DPV (Euro 6)	Single-lane roundabouts generate lower travel time (13-15%) and CO_2 emissions per unit distance (5-20%) compared to multi-lane and compact two-lane	Only one vehicle type (DPV) was used during the experiment

Continuation of Table 2.1

Subchapter	Reference	Fleet	Description	Limitations
2.2.4	[Weiss *et al.* 2011]	12 DPVs and GPVs (Euro 3 to 5); 2 Transporters; 1 Minivan	Average NO_x emissions of diesel vehicles (0.93 g/km), including Euro 5 diesel vehicles (0.62 g/km), substantially exceed respective Euro 3-5 emission limits; NO_x emissions of gasoline vehicles as well as CO and THC emissions of both diesel and gasoline vehicles stay within Euro 3-5 emission limits; Both gasoline and diesel vehicles exceed the CO_2 emissions as specified on the laboratory testing by on average 21%	Future PEMS applications may particularly focus on polluting driving modes such as cold start at very low temperatures and driving at very high speed as it occurs on the German Autobahn
2.2.4	[Weiss *et al.* 2012]	7 DPVs (1 Euro 6; 6 Euro 4-5)	NO_x average emissions of the Euro 6 car are considerably lower than the ones from the Euro 4-5 cars; All tested cars exceed the NEDC emission standards by 260%; CO_2 emissions deviated by 8% from the NEDC emission standards	Did not use the parameter of the vehicular jerk
2.2.4	[Degraeuwe and Weiss 2016]	7 DPVs (Euro 4-6)	A filter in order to match on-road driving events to NEDC conditions was applied; On-road NO_2 (filtered) emissions exceeded by 206% those measured on the NEDC; On-road NO_x (unfiltered) measurements exceeded the NEDC emissions by 266%	Did not use the parameter of the vehicular jerk

Continuation of Table 2.1				
Subchapter	Reference	Fleet	Description	Limitations
2.2.4	[Baldino *et al.* 2017]	541 DPVs (Euro 5-6)	Conformity factors obtained during on-road NO_x emissions measurements were about 1 to 11 times higher, depending on the vehicle, compared to the standard laboratory emissions limits; CO_2 emissions were about 30% higher than the average CO_2 gap for Euro 5 and 6 diesel vehicles built between 2011 and 2015	Did not use the parameter of the vehicular jerk
2.2.4	[Frey *et al.* 2017]	122 GPVs	Certification levels emission standards are on average 70% lower than the applicable standards; Real-world emission rates are on average 43% higher than certification levels	Did not use the parameter of the vehicular jerk
2.2.4	[Yang *et al.* 2019]	2 HEVs (1 port fuel injection; 1 gasoline direct injection)	Both HEVs tested failed the Euro-6 limit of PN emissions by exceedances of 34 and 99.3%; 82% of the PN emissions from the PFI-HEV were emitted during the urban driving stage	Did not use the parameter of the vehicular jerk
2.2.4	[Fernandes *et al.* 2019a]	4 DPVs	Measured CO_2 emissions were inflated up to 105% compared to the regulated ones; Measured NO_x emissions were 3-4 times higher on average than standard emission	Did not use the parameter of the vehicular jerk

Continuation of Table 2.1

Subchapter	Reference	Fleet	Description	Limitations
2.2.5	[Choi and Frey 2009]	-	Emission factors were easily affected to increase in speeds from 105 km/h to 126 km/h, specially in the case of the CO; Increases in the emission rates of the CO_2, NO_x and HC were superior when there was an increase of low speeds compared to the increase in high speeds	Did not use the parameter of the vehicular jerk
2.2.5	[Frey *et al.* 2008]	-	Emission rates were increased in about 20% in the presence of positive road grades present on the routes and emissions rose in approximately 19% when the road traffic was superior	Did not use the parameter of the vehicular jerk

End of Table

Chapter 3

Methodology

The practical component of this master dissertation was performed following the Real Driving Emission Protocol procedures, complying with all the demands that are present in the RDE regulation [European Parliament 2017]. Only hot stabilised emissions were evaluated and the test fleet was composed by one GPV and by one DPV (both Euro 6c) that were driven through four different types of routes: one partly urban/rural, two highways and one urban. The exhaust emissions were analysed by the use of the PEMS device, the OBD, and by the use of GPS receivers.

The methodology stage can be divided into 6 distinct phases that will be fully described further ahead in this chapter, namely the structure of the work that was done (Section 3.1), the experimental design (Section 3.2), instruments and test conditions (Section 3.3), field measurements (Section 3.4), quality assurance (Section 3.5), and data analysis (Section 3.6).

3.1 Structure

The initial work plan that was developed in order to guide the elaboration of this document consisted in 5 major tasks that can be described as follows:

- **1) -** To perform a literature review consulting the previously available technical information about on-road experimental monitoring of pollutant emissions and fuel consumption of passenger vehicles;
- **2) -** To establish an experimental plan which included the choice of the selected test vehicles, test routes, time and days of the monitoring, and the resources (human and equipment) that were going to be required to perform the practical tests;
- **3) -** To perform an experimental monitoring of pollutant emissions for vehicles with different propulsion systems (GPV and DPV) on different types of routes (urban, rural and highway) and different driving styles using a Portable Emission Measurement System (PEMS);
- **4) -** To compare and to perform a detailed analysis of the data collected about the analysed vehicles monitored emissions;
- **5) -** To write the master dissertation.

The timings to accomplish and the respective tasks between the months in that the work was performed are listed on Table 3.1.

Table 3.1: Timings that were accomplished between the designated tasks and the respective months of the year 2020

Task ID	**02/20**	**03/20**	**04/20**	**05/20**	**06/20**	**07/20**	**08/20**	**09/20**	**10/20**	**11/20**
1	✓	✓	✓	✓	✓	✓				
2	✓									
3	✓									
4			✓	✓	✓	✓	✓			
5			✓	✓	✓	✓	✓	✓	✓	✓

To sum up the steps that were taken throughout the development of this master dissertation, a flowchart is shown in Fig 3.1:

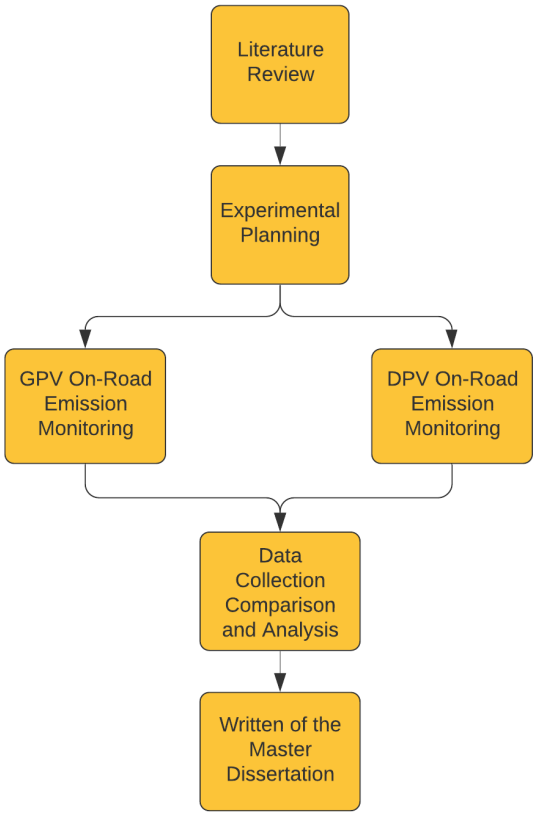

Figure 3.1: Fluxogram describing the different stages of the dissertation

3.2 Experimental design

The on-road experimental tests were performed using 1 DPV (Fiat Tipo 5) that was equipped with the SCR system and 1 GPV (Renault Clio 1.0 Tce Intens), which are represented in Fig 3.2 and that were selected due to the fact that they represent a typical European fleet [Inc 2020]. These cars differed in the type of fuel usage and engine size, between other aspects, as listed in Table 3.2, were tested along four different routes located in the region of Aveiro, Portugal. These routes included one partly urban/rural trajectory (R1) and two different highways (R2,R3), that were travelled between point A and B (in both ways) as listed in Fig 3.3, and one urban trajectory inside the city of Aveiro (R4), that was also travelled between point C and D (in both ways), as described in Fig 3.4.

(a) (b)

Figure 3.2: Test vehicles: a) Fiat Tipo 5 (V1) [Fiat 2019]; b) Renault Clio 1.0 Tce Intens (V2) [Renault 2019]

The test routes were previously selected because they included a vast range of European on-road driving conditions [European Parliament 2017] such as speed range, acceleration-deceleration profiles, traffic conditions or altitude profiles, as listed in Table 3.3. It is important to note that the highway that is present in the R2 (A29) is a highway that has electronic tolls, on the contrary to the one that the highway present in the R3 has (A1), which are manual tolls, meaning that two stops had to be performed, namely when entering and leaving the highway.

It was not possible to precise the average number of vehicles per day that circulate in all segments that compose R4 but it is known that along the segment which is located in the avenue which goes from the University of Aveiro until the Hospital of Aveiro, the average daily traffic (ADT) is of about 10205 vehicles [Fernandes *et al.* 2019b]. It also could be verified that during the rush hour (from 5:30 PM to 7:30 PM) road traffic substantially increased. Fact that was proven in 2019, by an article that reported that the traffic in R1 varied between 831 and 2035 vehicles per hour in this rural route [Fernandes *et al.* 2019c]. For the routes R2 and R3, it is stated that the ADT for each one of these two highways is roughly 23100 and 39800 vehicles, respectively [IMT 2020]. The region of Aveiro is mostly constituted by flat areas, even though, some of the routes present elevation variations in some areas, specially in R2 and R3, on the contrary of R1 and R4, as depicted in Fig 3.5. It was stated that the R1 and that the R4 present a positive gain in inclination in about 36% of all segments which compose each route, oppositely

Table 3.2: Specifications of the tested vehicles

Specification	**Fiat Tipo 5 (V1)**	**Renault Clio 1.0 Intens (V2)**
Fuel Type	Diesel	Gasoline
Year	2019	2019
Weight (Kg)	1695	1603
Mileage (km)	5600	2500
European Emission Standard	Euro 6c	Euro 6c
Engine Displacement (cm^3)	1248	999
Engine Cylinders	4	3
Horsepower (hp)	95	100
Transmission Type	6-Speed Manual	5-Speed Manual
Maximum Speed (km/h)	181	187
0-100 (km/h) acceleration (s)	12.5	11.8
Combined Fuel Consumption (l/100) (WLTP)	4.5	5.2
Combined CO_2 emissions (g/km) (WLTP)	119	118

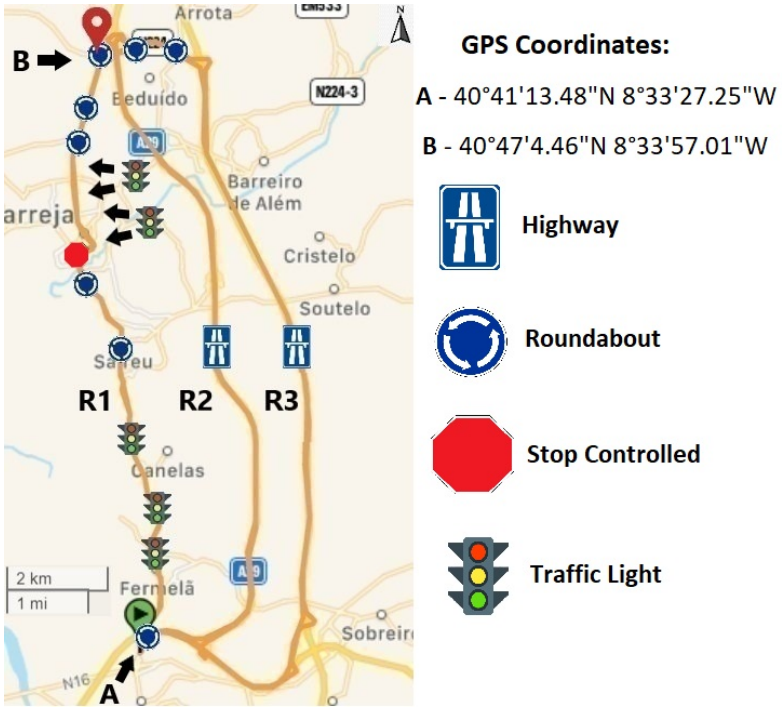

Figure 3.3: R1, R2 and R3 Aerial View. Background Map Source [Open Street Maps and GPS Visualizer]

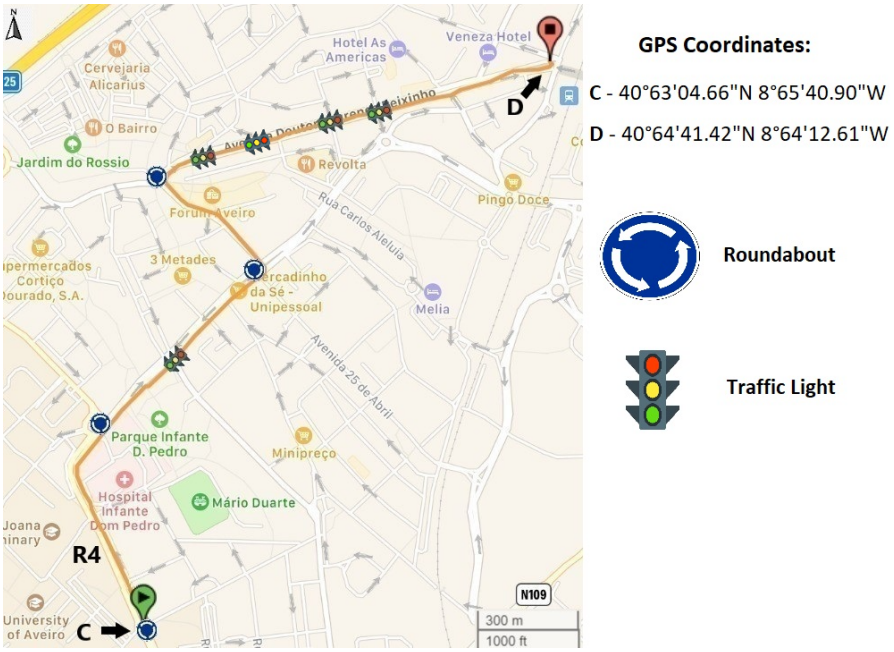

.

Figure 3.4: R4 Aerial View. Background Map Source [Open Street Maps and GPS Visualizer]

Table 3.3: Test routes characteristics

Route ID	Length (km)	Composition (%)	Observations
R1	23.6	77% rural; 23% urban	1 lane; 12 roundabouts; 14 traffic lights; 1 stop-controlled intersection
R2	30.2	75% highway; 25% rural	2 to 3 lanes; Low-traffic volume and high traffic electronic toll highway sections
R3	34.1	61% highway; 39% rural	2 to 3 lanes; Low-traffic volume and high traffic manual toll highway sections
R4	5.2	100% urban	1 to 2 lanes; 4 roundabouts; 5 traffic lights

from the R2 and from the R3 which present 49%. Regarding car speed averages and as normally expected, higher speeds were achieved in the highway routes (R2;R3), instead of the lower speeds recorded in the rural route (R1) and even lower in the urban route (R4) as listed in Fig 3.5. The use of manual tolls in R3 was implemented with the purpose of evaluating the two extra stops on the results.

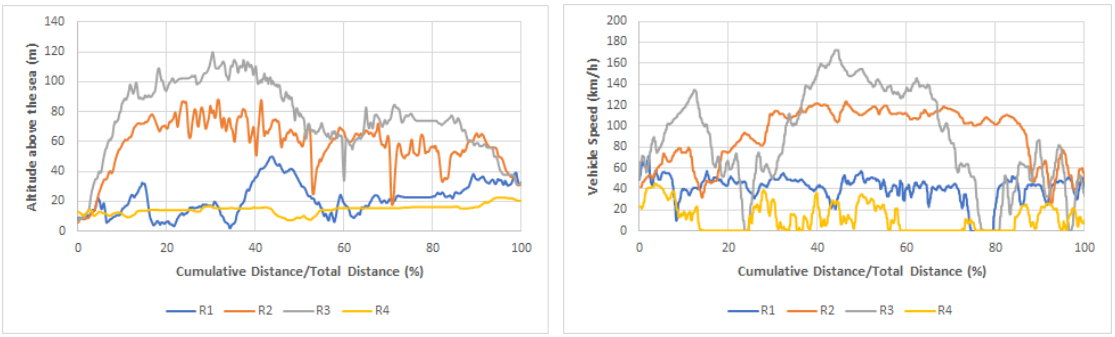

(a) (b)

Figure 3.5: Route characteristics: a) Altitude profiles per route; b) Vehicle speed along the route

3.3 Instruments and test conditions

3.3.1 PEMS Specifications

As mentioned before, the main instrument that was used during the entire testing period was a PEMS, namely the 3DATX ParSYNC integrated PEMS (iPEMS) [3DATX 2020], that was produced by the 3DATX company, as shown in Fig. 3.6. This device weights about 3.7 kg (with batteries included) and it provides unique, hot-swap cartridges that are capable of measuring volume fractions of CO_2, NO, NO_2. To measure the PM, three detection methods are used by the iPEMS. The first one is based on opacity, which is sensitive to PM size fractions in the coarse PM (of about 2.5 μm to over 10 μm), the second one is based on ionization, which is sensitive to fine PM (approximately 0.3 μm to 2.5 μm) and the third one, based on light scattering, is sensitive to ultra-fine PM (0.4-0.5 μm). Each one of these three indicators provides a voltage that is subtracted from a reference value reported for each test [3DATX 2020]. A Sensor Cartridge, used to obtain the real-time PN/PM, and a GasMOD Sensor Cartridge, that can measure NO_x (with a linear range of 0-5000 ppm) and CO_2 (with a range of 0-20% and an absolute accuracy of +-0.3%), are included in the equipment [3DATX 2020]. The measurements principles and sample conditions of the gadget are sum up in Table 3.4 as well has its specifications in Table 3.5. A water trapper that was connected to the iPEMS was also used, in order to remove the humidity out of the pollutants composition, which allowed to obtain more precise measurements. Both devices are represented in Fig 3.6.

.

Figure 3.6: 3DATX iPEMS (white) and the Water Trapper (black) devices

Table 3.4: Measurements Principles and Sample Condition of the 3DATX iPEMS

Measurement Type	**3DATX iPEMS**
CO/HC	Not applicable
NO_x	NO and NO_2 separately - Electrochemical
CO_2	In volume fraction (X_{CO2}) by non-dispersive infrared
Exhaust Flow	None
Gaseous Sample Conditioning	Chiller captures condensed water
PM Measurement	No mass estimation

Table 3.5: Gas Analyzer specifications of the 3DATX iPEMS

Sensor	**Range**	**Sensitivity**	**Resolution**
CO_2	0.00 - 20.00 vol.%	± 70 ppm ± 0.5 vol.%	0.01 vol.%
NO	0 - 5000 ppm	0.05 ± 0.01 μA/ppm	1 - 2 ppm
NO_2	0 - 300 ppm	0.05 ± 0.01 μA/ppm	0.1 ppm
Scattering	N/A	N/A	0.001 mV
Ionization	N/A	N/A	0.001 mV
Opacity	N/A	N/A	0.001 mV

3.3.2 Calibration and Installation Process

The 3DATX iPEMS comes with a computational associated software which allowed to operate all parameters and to adjust them before starting the data collection. The calibration process consisted in connecting the iPEMS to the software, zeroing it, and after to check if its operating temperature is the ideal one (around 35°) and to connect the parSYNC to a cylinder (UN 1956 gas mixture) that emits exhaust gases. In this

case, the gas cylinder was emitting, as stated in the paper label which identified the type of gas cylinder that that was, the gases of NO (300 ppm), NO_2 (100 ppm) and CO_2 (6.0%). The UN 1956 gas mixture is listed on Fig. 3.7. So, the major task here was to, after knowing these values, check if the parSYNC was detecting them correctly and showing matching values on the software or not. When turned on, the PEMS should detect the CO_2 values that were being expelled from the UN 1956 gas cylinder. If it was, the iPEMS was ready to be installed in the vehicles for practical tests, if it was not, the raw values in the software were adjusted for them to match the real ones. In terms of the opacity, ionization and scattering sensors calibration, it was not necessary to perform it because they were already calibrated in the manufacturer installations when the PEMS was produced.

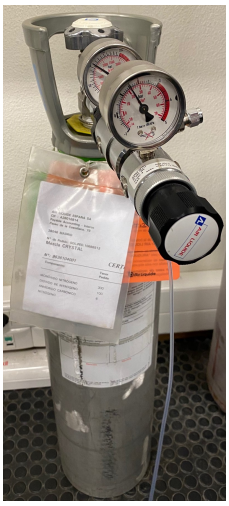

Figure 3.7: UN 1956 gas mixture that was used during the iPEMS calibration

In terms of installation of the devices, the parSYNC was decided to be placed into the trunk of both vehicles, as well as the water trapper that was connected to it. After these devices being placed and properly connected, the next step to take was to connect the sample exhaust tube, already connected to the water trapper that was connected to the iPEMS, to the exhaust pipe, in order to provide to the parSYNC the emissions emitted by the engine. This step is registered in Fig 3.8. One tube that performed the water drain was plugged to the water trapper and another one was plugged to the iPEMS with the purpose of releasing the gases from the exhaust pipe and that went through the water trapper and than through the iPEMS to the atmosphere. The next thing to do was to initialize the software and to zero it, importing the already acquired files that resulted from the calibration process into the system for them to be applied in order to obtain more precise results. The OBD was also plugged in into the car and a wait of about 30 minutes for the engine to warm up and for its emissions to stabilize was carried on, starting the data collection after this process. Cold emissions were not analysed due to the inconstancy that the PEMS presents when registering them.

Figure 3.8: Installation process of the devices before starting the data collection

3.4 Field measurements

Prior to initializing the on-road dynamic tests, the minimum amount of time travel trips was determined for each route. The field measurements occurred in the second half of February 2020, in three different days, taking place during the morning (10 AM to 1 PM) and during the afternoon throughout the evening (4:30 PM to 7:30 PM) under dry and windless weather conditions. However, more data should have been collected on the following months, but, unfortunately and due to the Covid-19 pandemic, the further data collection had to be cancelled. Despite the initial objective being that different drivers should drive the vehicles and for reasons that are unrelated to the group of Mobility and Transportation that was also not possible, so, the same person drove both vehicles despite having different driving styles in diverse trips which had its influence on vehicle emissions.

Each complete PEMS pack of trips duration was of about 120 min of data collection although it could take even more considering that the internal battery is able to power the device for more than 3 hours. In order to record ambient temperature (T) and humidity (H), a temperature/pressure sensor was used. A QSTARZ GPS Travel Recorder, which had an absolute position accuracy of about 3 meters and a tracking sensitivity of 165 decibel miliwatt (dBm), repeatedly registered vehicle position and elevation at a frequency of 1 Hz [Qstarz 2020]. An OBD-II ELM327 was also used in order to measure major engine data, such as speed, fuel flow rate (FFR), mass air flow (MAF), manifold absolute pressure (MAP), revolutions per minute (RPM) and intake air temperature (IAT). Information about variability in measured data and observed ranges of the parameters cited above for all of the test routes and for both test vehicles are listed in Table 3.6.

The start-stop system was disabled before the beginning of the test trips in both vehicles because that the iPEMS requires a continuously energy power source during measurements. About 13,000 s and 10,500 s along with 109 km and 114 km of valid PEMS, OBD and GPS data were collected for the diesel and for the gasoline vehicle, respectively. The overall temperature range for all tests was between 11-17°C and the overall humidity range was of about 57-76%.

Table 3.6: Ambient and real-world data collected for both vehicles tested in R1, R2, R3 and R4, on both directions of travelling

Parameter	**Vehicle ID**	**R1**	**R2**	**R3**	**R4**
Driving Time (minutes)	V1 V2	17 34	18 19	12 23	168 101
Average OBD speed (km/h)	V1 V2	42 42	96 97	86 87	20 16
Average Fuel Consumption (l/100km)	V1 V2	3.4 4.7	5.6 5.4	6.7 7.1	5.3 8.8
Min. to Max. MAF (g/s)	V1 V2	6-55 2-29	7-81 2-49	6-87 1-74	5-23 1-35
Min. to Max. MAP (kPa)	V1 V2	12-28 0-2	12-36 0-3	12-36 0-3	10-29 0-3
Min. to Max. RPM (rpm)	V1 V2	790-2830 830-3675	955-3690 840-3775	800-3985 785-5150	615-3075 670-4065
Min. to Max. IAT (°C)	V1 V2	14-18 16-23	15-17 16-25	14-16 18-29	17-42 17-39
Min. to Max. T (°C)	V1 V2	12 13	13 14	12 13	13-17 14-16
Min. to Max. H (%)	V1 V2	64-67 60-64	60-62 56-58	61-63 55-58	62-76 54-68
Min. to Max. X_{CO_2} (%)	V1 V2	1-9 1-12	1-10 1-13	1-10 1-13	1-11 2-13
Min. to Max. NO (ppm)	V1 V2	55-3163 1-1571	83-6755 0-2122	80-6597 0-2480	22-8530 3-1265
Min. to Max. NO_2 (ppm)	V1 V2	14-165 0-1	14-307 0-1	7-307 0-1	1-328 0-1

3.5 Quality assurance

In order to obtain a better quality assurance and a much more reliable data processing, two major procedures were adopted [Sandhu *et al.* 2013, Delavarrafiee and Frey 2018]:

- **The check of the data screening in order to correct or remove data errors**, namely indicators such as engine RPM, MAF and MAP, which presented

unusual values that remained constant indicating that the data were no longer being updated, as well as negative CO_2, NO, NO_2 and PM values. Consequently, the deviant data values were removed prior to data analysis. It can be estimated that about 0.5% of the total collected data were removed, mainly due to lost of connection between the OBD and its software, not providing second by second data that could not be synchronised with the rest of the data that were being collected;

- **The synchronization of all data streams**, namely the data collected by the PEMS, the OBD and the GPS Tracker. In order to assure proper time alignment, both computational and visualization methods were used, namely the maximization of the Pearson Correlation Coefficient (PCC) between two indicator variables and confirming the result by matching concurrent increases in indicator variables. Before evaluating time alignment, the three data streams used were set to be reported at the same frequency (1 Hz). For each pair of streams to be synchronised, one of them was selected as the "primary" and the other as the "secondary", along with an "indicator variable" selected from each data stream. The indicator that was selected for the PEMS data source was the NO_x concentration and for the OBD data source it was the RPM. Properly synchronised data streams should have a relatively high PCC, so, the selected approach to synchronization was based on selecting the time difference that maximised the PCC between the NO_x and the RPM. After plotting the maximised time difference, a visualization method was used in order to confirm that the increases in the RPM values matched the increases in the NO_x concentration, which meant that both indicator variables were synchronised, and, consequently, both data sources were in the same condition too.

For the diesel vehicle, V1, the pair that was used in order to synchronize PEMS and OBD data was the NO_x concentration (in ppm) versus Engine RPM (in rpm) [Sandhu *et al.* 2013]. Three synchronizations had to be performed due to the reason that all devices had to be shut off between three different sets of performed trips. The obtained PCC peaks for V1 were between 0.55 and 0.65 which meant that the pairs were well synchronised according to Sandhu and Frey [Sandhu *et al.* 2013]. The time alignment that was necessary to adjust for this synchronization to be made was of about -4 to -5 seconds between the raw and the synchronised data. The plots for each one of the 3 performed synchronizations are listed in Fig. 3.9, Fig. 3.10 and Fig. 3.11, respectively.

For the gasoline vehicle, V2, the pair that was used differed from the one used in V1. For this type vehicle propulsion it was advised by Sandhu and Frey (2013) to use the parameter of the CO (in %) versus Engine RPM (in rpm) to synchronize PEMS and OBD data, respectively [Sandhu *et al.* 2013]. However, this parSYNC could not measure the required parameter so a change was made. Instead of the CO (%), the CO_2 (%) was utilised. Only two synchronizations were need to be done for this vehicle, due to the reason that less overall data were collected. The PCC obtained peaks varied between 0.64 and 0.52 which indicated that a proper data alignment was being done, being the adjustment in time of about -5 and -3 seconds for each alignment between raw and synchronised data. Both synchronization plots are exhibited in Fig. 3.12 and in Fig. 3.13, respectively.

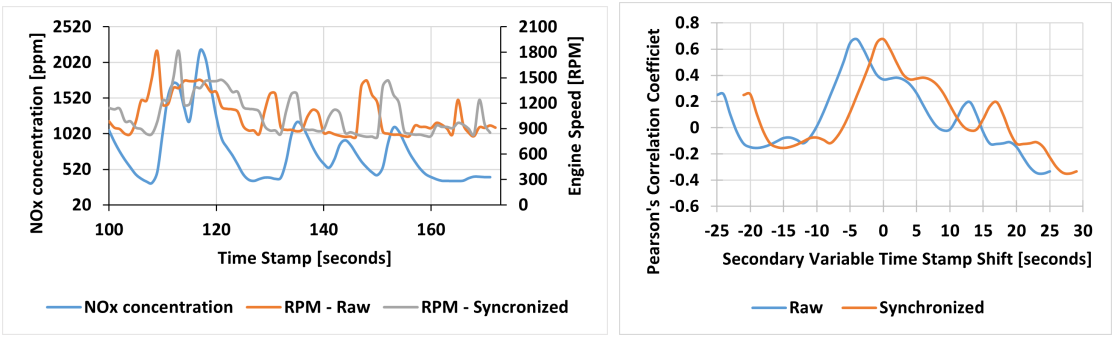

(a) (b)

Figure 3.9: First V1 synchronization of the data streams: a) NO_x concentration versus RPM; b) PCC values according to time

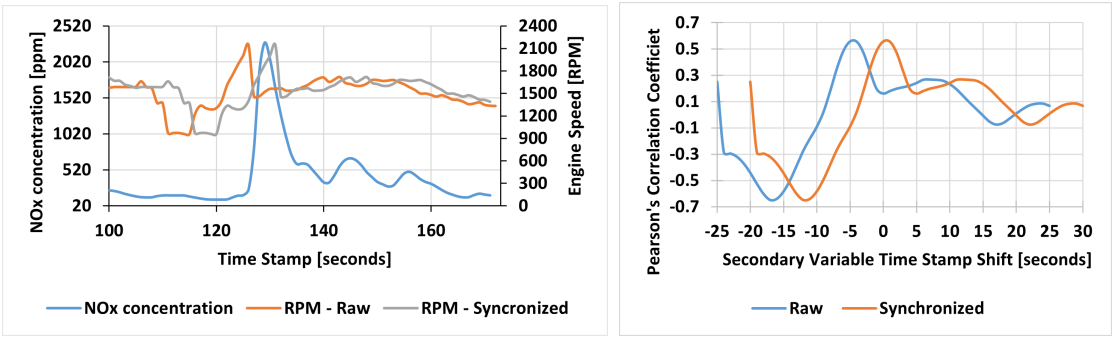

(a) (b)

Figure 3.10: Second V1 synchronization of the data streams: a) NO_x concentration versus RPM; b) PCC values according to time

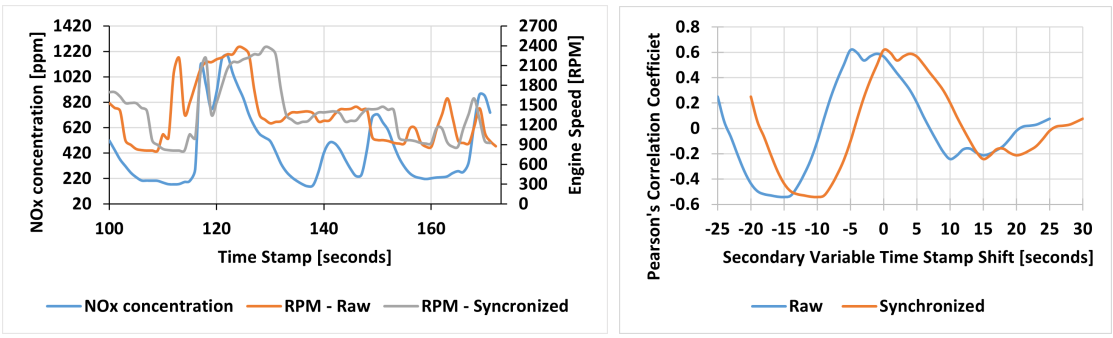

(a) (b)

Figure 3.11: Third V1 synchronization of the data streams: a) NO_x concentration versus RPM; b) PCC values according to time

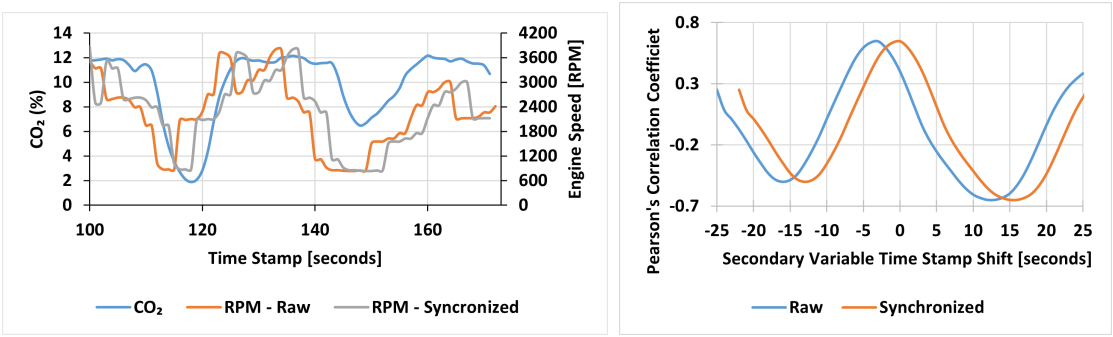

(a) (b)

Figure 3.12: First V2 synchronization of the data streams: a) CO_2 (%) versus RPM; b) PCC values according to time

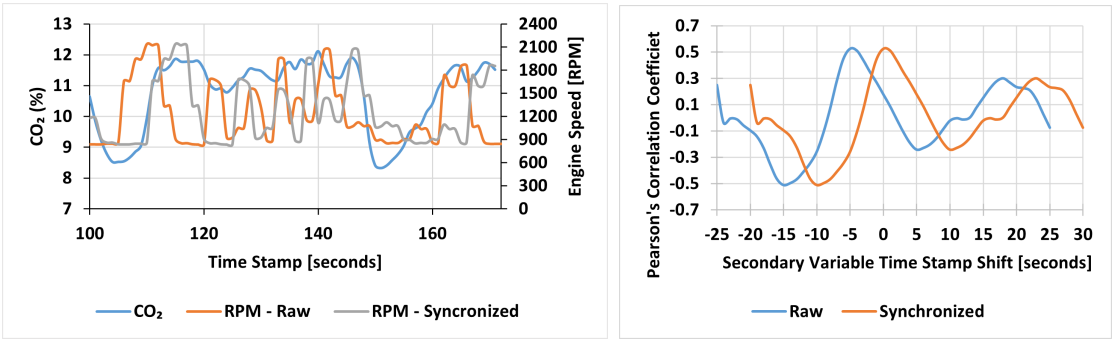

(a) (b)

Figure 3.13: Second V2 synchronization of the data streams: a) CO_2 (%) versus RPM; b) PCC values according to time

3.6 Data analysis

3.6.1 Validation of the trips

In order to characterize the driving profile of the PEMS route trips so that it was possible to validate or to reject all of the performed trips, according to the European Union requirements, several driving parameters were calculated [European Parliament 2017]. As expected, one of these parameters was the acceleration that was calculated through the speed collected from the OBD and that can be expressed by Eq. (3.1) as [European Parliament and Council of the European Union 2007]:

$$a_{\mathrm{i}} = \frac{v_{\mathrm{i+1}} - v_{\mathrm{i-1}}}{2 \times 3.6} \tag{3.1}$$

Where:

a_{i} - Acceleration in the second of travel i in m/s^2;

$v_{\mathrm{i+1;i-1}}$ - Vehicle instantaneous speed in the second of travel *i+1* and *i-1*, respectively in km/h.

There are two metrics to evaluate the maximum and the minimum dynamic boundary conditions that are present in the Commission Regulation (EU) 2017/1151 implemented in June of 2017, being one of them the 95th percentile of the product of vehicle speed and positive acceleration, $va_{pos\_}[95]$, and being the other the Relative Positive Acceleration (RPA), respectively [European Parliament and Council of the European Union 2007]. This means that if the $va_{pos\_}[95]$ is lower than a certain value, then it can be considered that a PEMS trip is a valid one in the RDE procedure. Also, if a PEMS trip presents a RPA above a certain value, then this trip is also valid in the RDE procedure.

As a result of the explained above, only the PEMS trips that fulfilled the mentioned criteria were used for the emissions study. From a total of 42 trips performed using both vehicles, it was determined that 40 of them were valid and that 2 of them were invalid in the RDE procedure requirements, being these 2 trips excluded from the data that were afterwards analysed. The validation of the PEMS trips are presented in the Section 4.1.

The above mentioned parameters, namely the RPA (in m/s^2), the MPA (in m/s^2) and the $va_{pos\_}[95]$ (in m^2/s^3) were determined using the Eqs. (3.2), (3.3) and (3.4), respectively [European Parliament and Council of the European Union 2007]:

$$RPA = \frac{\sum \frac{v_i}{3.6} \times {a_i}^+}{d}; \tag{3.2}$$

$$MPA = mean({a_i}^+); \tag{3.3}$$

$$va_{pos\_}[95] = P95(\frac{v_i}{3.6} \times {a_i}^+) \tag{3.4}$$

Where:

${a_i}^+$ - Positive values for acceleration higher than 0.1 m/s^2 for the second of travel i (m/s^2);

d - Total distance of the route (m);

$P95$ - 95th percentile.

3.6.2 Vehicular Jerk

The vehicular jerk is defined as the change rate of vehicle acceleration with respect to time, being the first derivative of acceleration/deceleration [Fernandes *et al.* 2020, Feng *et al.* 2017, Bagdadi 2013, Khattak *et al.* 2019, Wali *et al.* 2019], as stated in Eq. (3.5). It is a parameter which illustrates driving volatility and that characterizes the driving style of each person. It is also related to how safety the driving that is being performed is. If the jerk values are high this means that the driving is being more aggressive, in terms of acceleration and deceleration [Feng *et al.* 2017], either in the moments when the gas pedal is pressed, when fast gear changes occur or either in hard braking manoeuvres caused by critical situations (traffic conflicts, preventing a sudden crash) that might have happened during the performed trip [Bagdadi 2013]. So, low vehicular jerk values mean that the performed driving is being smooth as ideally pretended [Feng *et al.* 2017].

$$v_{\text{jerk}}(t) = \frac{\mathrm{d}a}{\mathrm{d}t} \tag{3.5}$$

Where:

$v_{\text{jerk}}(t)$ - Vehicular Jerk (in m/s^3) in function of the time (t);

$\frac{da}{dt}$ - First derivative of acceleration in function of the time (t).

3.6.3 Driving Style

The driving style that was adopted by the driver for each one of the routes was characterised by the analysis of the RPA, the maximum acceleration and deceleration and by the vehicular jerk values obtained for both vehicles. RPA is a parameter which measures acceleration values during high power demand, considering that high accelerations that are correlated with high torque do not always require high power [Tutuianu *et al.* 2015], which led to the fact that this parameter was recognised to be a valuable measure of driving behaviour style and of driving performance, as previously stated in studies about the RDE [Gallus *et al.* 2017, Fernandes *et al.* 2019a, Fernandes *et al.* 2020]. The used RPA thresholds values which are in concordance with the WLTC and that differ according to the road type were the following [Gallus *et al.* 2017]: 0.12 m/s^2 for the urban routes and 0.14 m/s^2 for the rural ones. In the case of the maximum acceleration, deceleration and vehicular jerk, the following values were utilised: a maximum acceleration of 2.16 m/s^2 [Choi *et al.* 2017]; a maximum deceleration of 3.4 m/s^2 [Deligianni *et al.* 2017] and a vehicular jerk of 0.9 m/s^3 [Liu 2015]. The analysis of these parameters was performed based on the percentage of time spent above the thresholds for each one of the routes.

3.6.4 Estimation of the road grade

Road grade is the change in elevation divided by the horizontal distance travelled, usually presented in percentage [Boroujeni and Frey 2014]. To estimate the road grade for each route, two major steps were taken, which resided into firstly correcting the instantaneous vehicle altitude data provided by the GPS Tracker and secondly on the estimation of the cumulative positive elevation gain. Furthermore, each instantaneous altitude data provided by the GPS device was reviewed under the conditions stated in Eq. (3.6) [European Parliament and Council of the European Union 2007]:

$$\bar{h} = \begin{cases} h_{\text{i-1}}, \text{if } |h_{\text{i}} - h_{\text{i-1}}| > \frac{v_{\text{i}}}{3.6 \times sin45^\circ} \\ h_{\text{i}}, \qquad \text{otherwise,} \end{cases} \tag{3.6}$$

Where:

$\bar{h}$ - Corrected altitude (m above the sea level);

$h_{\text{i;i-1}}$ - Altitude in the second of travel i and *i-1*, respectively (m above the sea level).

Cumulative altitude gain values (in m) were calculated using these values, as listed in Eq. (3.7) [Gallus *et al.* 2017]:

$$altgain = \sum_{i} \ \triangle \bar{h}_{\text{i}} \text{ for } \triangle \bar{h}_{\text{i}} > 0 \tag{3.7}$$

A segment method with the "Combined Runs" approach proposed by Boroujeni and Frey [Boroujeni and Frey 2014] was applied in order to determine road grade regarding a superior precision along every location of the analysed route. This approach consists in [Boroujeni and Frey 2014]: (a) the estimation of the distance travelled along each route and in each run, adjusting it to a "true" value; (b) dividing the route into segments of 100 meters of length for each run (because of the fact that the length of 100m is the best trade-off between the number of GPS data points per segment, regarding that a small

number decreases the veracity of the estimated road grade and that excessively large segments length can bring too long inappropriate smoothed out grade variations); (c) aligning the average elevation among multiple GPS runs in each segment; (d) combining multiple runs into one dataset; (e) estimating average road grade for each segment.

3.6.5 Emission Rates

The method that is stated in the Regulatory Information 40 CFR 86.144 was applied in order to estimate pollutant mass at each second due to the fact that the parSYNC does not measure the exhaust flow. For the diesel vehicle (V1) the Fuel Flow Rate (FFR) and the Mass Air Flow Rate (MAF) parameters were already given by the OBD, so, in order to estimate the Exhaust Flow Rate the Eq. (3.8) was applied [Leland and Stanard 2018]:

$$\dot{m}_{\text{ex}} = MAF + FFR.\ \rho_{\text{fuel}}, \tag{3.8}$$

Where:
$\dot{m}_{ex}$ - Exhaust Mass Flow Rate (g/s);
MAF - Mass Air Flow Rate (g/s);
FFR - Fuel Flow Rate (l/s);
ρ_{fuel} - Fuel Density (kg/l), being this value equal to 0.78 kg/l and 0.85 kg/l for gasoline and for diesel, respectively [ToolBox 2019].

For the vehicle that operated on gasoline (V2), a way to estimate its Mass Air Flow Rate had to be used. The parameters of the Air Fuel Ratio (A/F) and of the Mass Fuel Flow Rate ($\dot{m}_{fuel}$) were provided by the OBD and could be correlated through the Eq. (3.9) [Grimaldi and Millo 2015]:

$$\dot{m}_{\text{air}} = \frac{A}{F} \times \dot{m}_{\text{fuel}} \tag{3.9}$$

Where:
$\dot{m}_{air}$ - Mass Air Flow Rate (g/s);
A/F = Air Fuel Ratio;
$\dot{m}_{fuel}$ - Mass Fuel Flow Rate (g/s).

For the purpose of this dissertation, it was estimated that the NO_x concentration corresponds to the sum of concentration signals for NO and NO_2 [Sandhu *et al.* 2013]. In order to estimate CO_2 and NO_x mass emission rates, the Eq. (3.10) and Eq. (3.11) were applied, respectively [EEA 2012]:

$$m_{\text{CO}_2} = \dot{V}_{\text{ex}} \rho_{\text{CO}_2} X_{\text{CO}_2} \tag{3.10}$$

$$m_{\text{NO}_x} = \dot{V}_{\text{ex}} \rho_{\text{NO}_x} X_{\text{NO}_x} \frac{1}{1 - 0.0047(H - 75)} \tag{3.11}$$

Where:
m_{CO_2} - CO_2 Mass Flow Rate (g/s);
$\dot{V}_{\text{ex}}$ - Exhaust Volumetric Flow Rate (corrected to standard conditions) (m^3/s);
ρ_{CO_2} - CO_2 density at the standard conditions (1.830 kg/m^3);
X_{CO_2} - CO_2 volume fraction measured by the iPEMS (%);
m_{NO_x} - NO_x Mass Flow Rate (g/s);

ρ_{NO_x} - NO_x density at the standard conditions (1.913 kg/m^3);
X_{NO_x} - NO_x volume fraction measured by the iPEMS (ppm);
H - Humidity (%).

As for the PM emission rates, the methodology that was used was slightly different than the one that was used for the remaining pollutants and it was based on the procedures suggested by the parSync company and it is explained in detail in the Appendix 1.1. The voltages that were provided by the Scattering, Ionization and Opacity sensors present in the parSYNC were converted to mass units and subsequently used to calculate the PM particle mass (in μg/m^3), using the Eq. (3.12). Afterwards, in order to obtain the PM value in (mg/s), the Eq. (3.13) was applied:

$$PM_{\mathrm{m}} = 0.39 \times IonizationPM_{\mathrm{m}} + 0.06 \times OpacityPM_{\mathrm{m}} + 0.55 \times ScatteringPM_{\mathrm{m}} \quad (3.12)$$

Where:
PM_m - PM particle mass (in μg/m^3);
Ionization PM_m - Ionization PM particle mass (in μg/m^3);
Opacity PM_m - Opacity PM particle mass (in μg/m^3);
Scattering PM_m - Scattering PM particle mass (in μg/m^3);

$$PM = 0.001 \times PM_{\mathrm{m}} \times EFR \quad (3.13)$$

Where:
PM_m - PM particle mass (in μg/m^3);
PM - PM (in mg/s);
EFR - Exhaust Flow Rate (in m^3/s).

3.6.6 Vehicle Specific Power (VSP)

The Vehicle Specific Power (VSP) is a mathematical expression that has began to be developed at the Massachusetts Institute of Technology [Jimenez-palacios 1999]. This parameter is very useful in the analysis of remote sensing data, chassis dynamometer data, and in emissions modeling for three major reasons: it can be calculated from on-road measurements, it acquires most of the dependence of light-duty vehicle emissions on driving conditions, and it is directly indicated in emission certification cycles. Basically, a general group of coefficients values estimating VSP for a certain light duty fleet is used as an important support for characterization and it is a very useful explanatory variable for emissions [Jimenez-palacios 1999, Frey *et al.* 2006]. It involves a mathematical representation of engine load against aerodynamic lag, rolling resistance of the tyres, acceleration, adding the kinetic and potential energies of the vehicle, being all of this divided by the mass of the car. Eq. (3.14) is used to estimate VSP for light duty vehicles and it can be described as [Jimenez-palacios 1999]:

$$VSP_{\mathrm{i}} = v_{\mathrm{i}} \times [1.1a_{\mathrm{i}} + 9.81 \times r + 0.132] + 0.000302 \times {v_{\mathrm{i}}}^3 \quad (3.14)$$

Where:
VSP_i - Vehicle specific power in the second of travel i (kW/ton);
v_i - Speed in the second of the travel i (m/s);
a_i - Acceleration in the second of travel i (m/s^2);

r - Road grade (%).

Each second-by-second measurement of VSP was stratified into 14 bins and for each bin the average CO_2, NO_x and PM emission rates were calculated. The obtained values for each one these bins and for both cars are listed in the Section 4.5 of the Chapter 4. Modes 1 and 2 represent deceleration or downhill driving, while the Mode 3 indicates vehicle idling and low speed situations. Increasing VSP from the Mode 4 until the Mode 14 represents cruising, acceleration or uphill driving. Higher speeds were attained on the highway routes (R2;R3) with the purpose of registering a higher frequency of VSP Modes 14. The power values which characterize each VSP bin are listed in the Table 3.7.

Table 3.7: VSP bins values [EPA 2002]

VSP Mode	**Definition (kW/ton)**
1	VSP $<$ -2
2	-2 $\leq VSP <$ 0
3	0 $\leq VSP <$ 1
4	1 $\leq VSP <$ 4
5	4 $\leq VSP <$ 7
6	7 $\leq VSP <$ 10
7	10 $\leq VSP <$ 13
8	13 $\leq VSP <$ 16
9	16 $\leq VSP <$ 19
10	19 $\leq VSP <$ 23
11	23 $\leq VSP <$ 28
12	28 $\leq VSP <$ 33
13	33 $\leq VSP <$ 39
14	VSP $\geq$ 39

From the total of performed trips, these were divided in two distinct sets. The first set consisted in gathering about 70% of the total trips, which were named as the "training trips" and that were the ones that were employed to develop the emission factors, becoming the remaining ones to be used as "testing trips" [Liu *et al.* 2017].

Chapter 4

Results and Discussion

This is the chapter where the main results obtained and consequent discussion will be performed. The results and discussion chapter can be split into 6 distinct sections. It is composed by the validation of all of the performed test trips (Section 4.1), the presentation of the main driving parameters obtained (Section 4.2), the on-road emissions data that were gathered during the data collection (Section 4.3), the analysis of the emissions hotspots that were present throughout the routes for each pollutant (Section 4.4), the VSP-based approach prediction model for vehicular emission rates (Section 4.5), and, the validation of the performed VSP prediction model (Section 4.6).

4.1 Validation of the test trips

As stated in Chapter 3, subsection 3.6.1, the validation of the trips was performed complying with the two conditions that are present in the Commission Regulation (EU) 2017/1151 regarding the maximum value of the $va_{pos\_}[95]$ and the minimum value of the RPA per route [European Parliament and Council of the European Union 2007]. A total of 25 trips were performed on the vehicle V1, as follows: a) 19 on R4, all valid; b) 2 on R1, one valid; c) 2 on R2, all valid; and d) 2 on R3, one valid. For the vehicle V2, 16 trips (all valid) were performed, as follows: 10 on R4 and 2 on R1, R2, and R3. The validation plots are displayed in Fig. 4.1 and Fig 4.2 for V1 and V2, respectively.

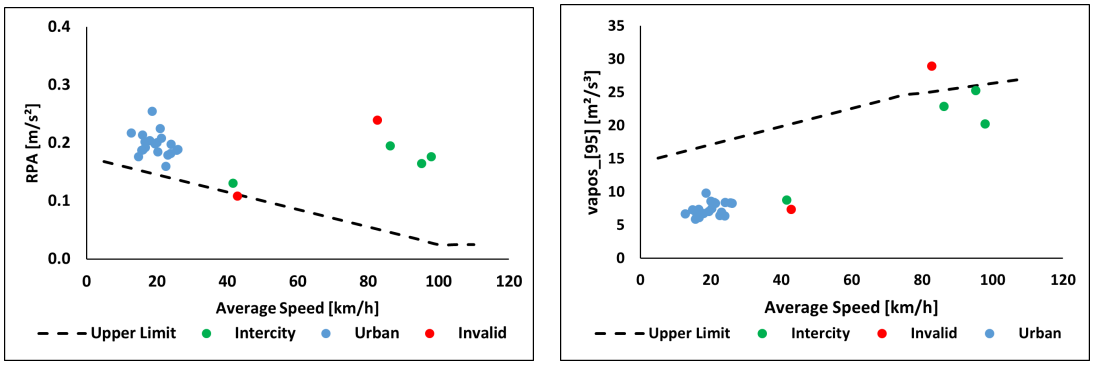

(a) (b)

Figure 4.1: Validation of V1 PEMS trips: a) RPA by speed; b) $va_{pos\_}[95]$ by speed

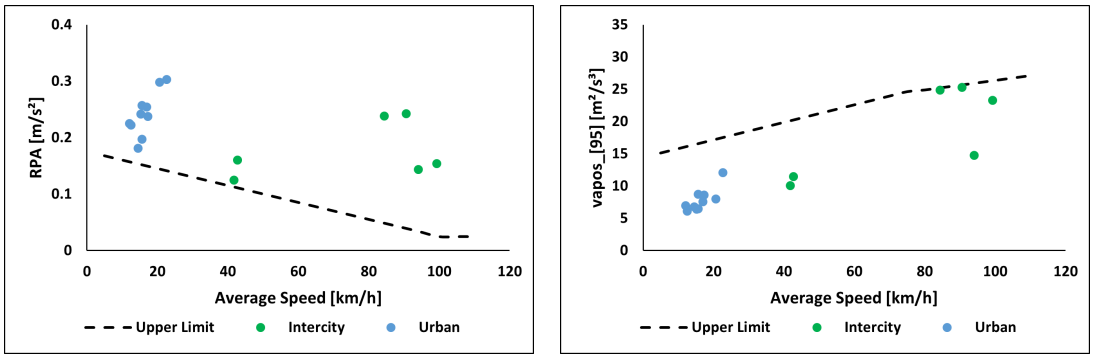

(a) (b)

Figure 4.2: Validation of V2 PEMS trips: a) RPA by speed; b) $va_{pos\_}[95]$ by speed

4.2 Driving style

In this section an analysis about the driving style related parameters, provided by the OBD that was connected to the vehicle, was performed. Histogram plots regarding speed, acceleration and vehicular jerk classes were made for both vehicles in order to check the main differences comparing the intercity routes (R1,R2,R3) with the urban one (R4). In the case of the vehicle V1, it is perfectly noticeable that the range of vehicle speed classes is significantly superior on the intercity routes (ranging from 0-160 km/h) compared to the urban one (which ranged from 0-50 km/h). This was obviously expected due to the fact that in intercity routes speed limits are way higher than in urban routes, being the driver able to achieve higher speeds. It can also be observed that the most frequent speed classes on intercity routes are the 40 km/h (15%), 50 km/h (17%) and the 120 km/h (10%), being the last two coincident with the most common speed limits for rural roads and for highways. On the contrary, in terms of acceleration and jerk classes ranges, these were very similar in all kind of routes. What stands out is that the most frequent class value to be reported in terms of acceleration is the "-1 m/s^2" and the "0 m/s^2", representing 24% and 66% for the intercity routes and 24% and 64% for the urban routes, respectively. In terms of jerk classes, the most frequent

ones in the intercity routes were the "-1 m/s^3" (35%) and the "0 m/s^3" (56%), as well for the urban routes, where they represented 30% and 58%, respectively. This means that most of the time the vehicle acceleration was constant, as stated in Fig. 4.3 and in Fig. 4.4.

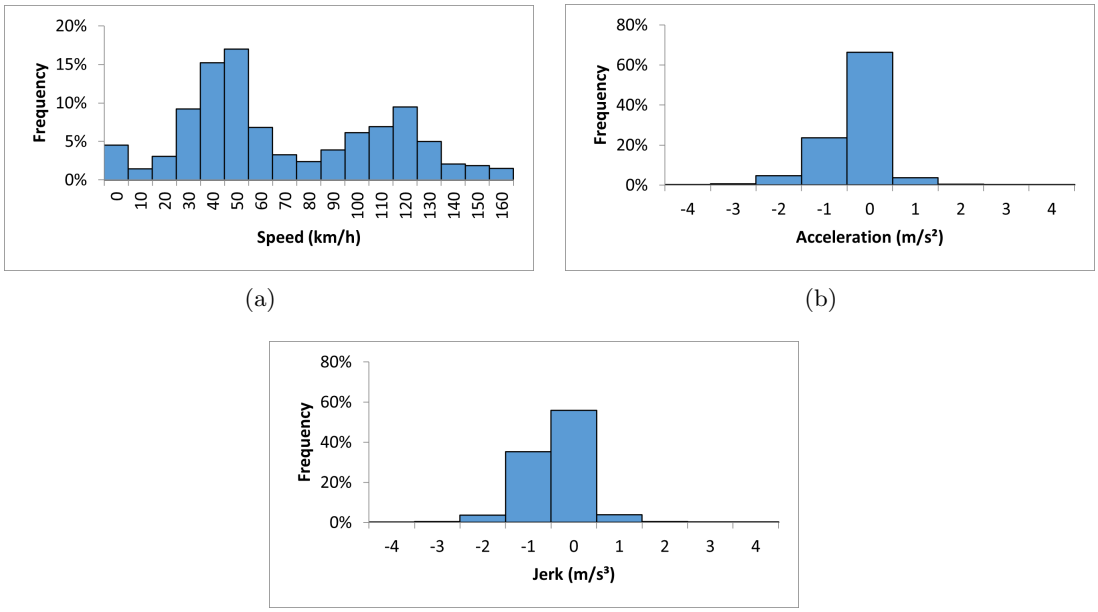

Figure 4.3: Histograms of Intercity V1 Routes: a) Speed classes frequency (km/h); b) Acceleration classes frequency (m/s^2); c) Jerk classes frequency (m/s^3)

In the case of vehicle V2, the acquired histograms are not much different from the ones acquired in the vehicle V1. The speed range in intercity routes (0-170 km/h) is still higher than in the urban route (0-50 km/h) as expected and due to the reasons that were mentioned above. Concerning the acceleration classes and as in the case of the vehicle V1 the most common values for the intercity routes were "-1 m/s^2" (17%) and "0 m/s^2" (71%), as well for the urban routes, where they corresponded to 14% and 71%, respectively. In terms of jerk classes and in the case of the intercity routes, the most frequent ones were "-1 m/s^3" and "-0 m/s^3", which corresponded to 30% and 51%, and, for the urban routes, to 24% and 51%, respectively. This means that during most of the time the acceleration or the speed of the vehicle were being constant. Despite of this, one fact that stood out was that the range of values of the acceleration classes [-5 to 5] and of the vehicular jerk classes in V2 was higher than in V1 (that varied only from [-5 to 3] in both classes), which could mean that more aggressive accelerations could have been made during the driving of the vehicle V2 compared to the one made in the vehicle V1. Also, for the intercity routes, it was stated that the V1 stayed above the 100 km/h speed for about 33% of the total time and the V2 only stayed above that speed approximately 28% of the time. The obtained histograms for this vehicle are represented in Fig. 4.5 and in Fig. 4.6.

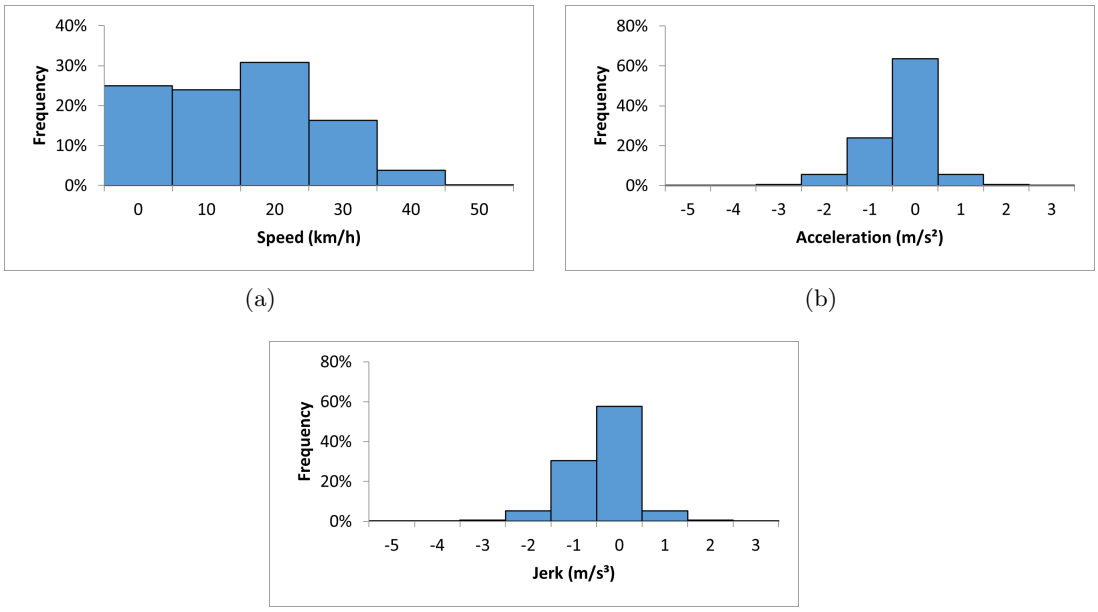

(a) (b)

(c)

Figure 4.4: Histograms of Urban V1 Route: a) Speed classes frequency (km/h); b) Acceleration classes frequency (m/s^2); c) Jerk classes frequency (m/s^3)

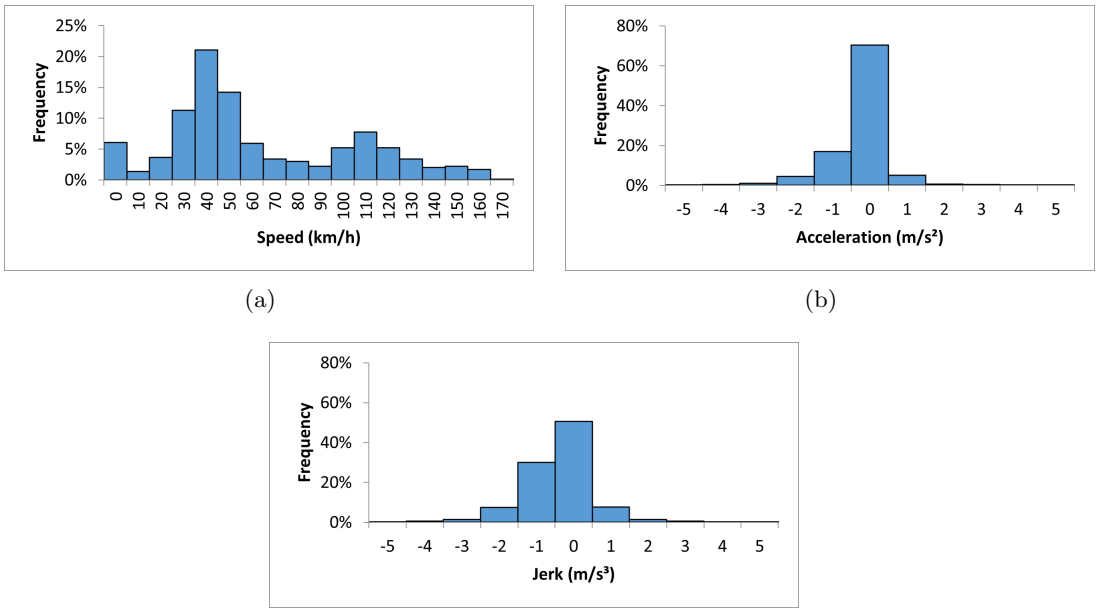

(a) (b)

(c)

Figure 4.5: Histograms of Intercity V2 Routes: a) Speed classes frequency (km/h); b) Acceleration classes frequency (m/s^2); c) Jerk classes frequency (m/s^3)

Afterwards, dispersion plots between the variance of "Acceleration versus Speed" and of the "Jerk versus Speed" were generated for both vehicles. The plots consisted in

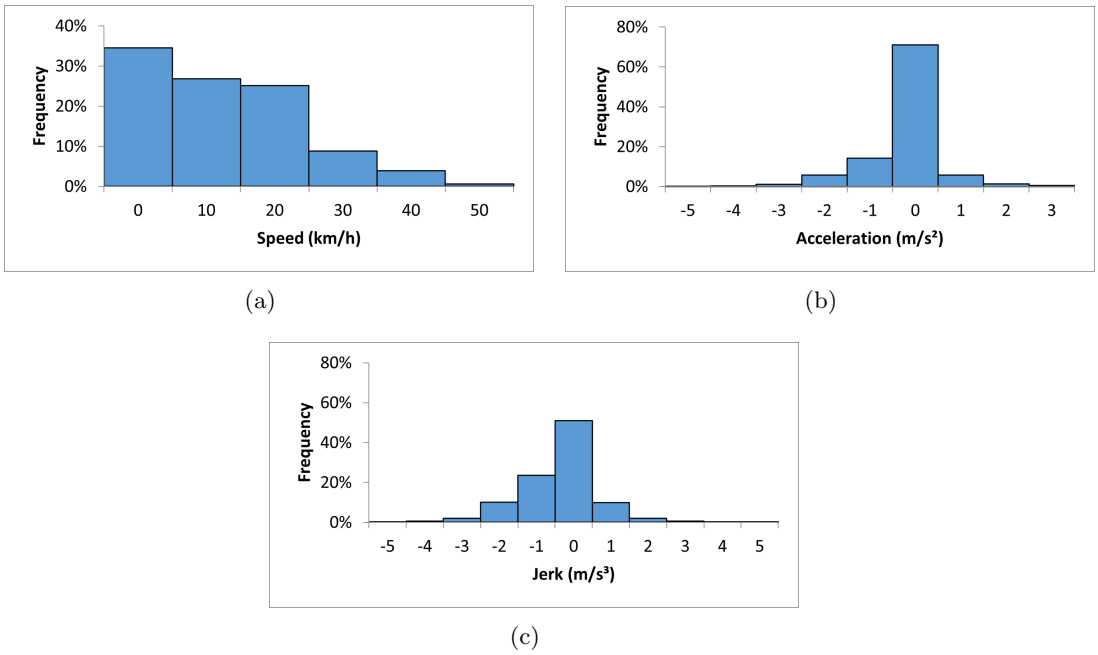

(a) (b)

(c)

Figure 4.6: Histograms of Urban V2 Routes: a) Speed classes frequency (km/h); b) Acceleration classes frequency (m/s^2); c) Jerk classes frequency (m/s^3)

approaching these parameters for the entire set of the intercity routes (R1,R2,R3) and for the urban route (R4) too.

For the vehicle V1, during the intercity routes, it can be observed that acceleration variance is significantly high on low and intermediate speeds, namely from 0 to 20 km/h and from 60 to 90 km/h, respectively. This means that accelerations were steeper during the increase of lower speeds they were also abrupt on intermediate speeds when the vehicle was accelerating in order to achieve the cruise speeds attained in the highways, as displayed in Fig. 4.7. Consequently and due to the reason that these two parameters are directly related, the vehicular jerk variance was also rather high during the first mentioned speed interval, meaning that an abrupter driving was being performed. Oppositely, the obtained variance for these two parameters was way more stable during the urban route. There was a slight spread of values in both parameters during the range of 0 to 15 km/h speeds but nothing significantly high compared to the spread that was observed in the intercity routes, being these parameters almost constant, which meant that a more harmonious driving was executed in this kind of routes, as displayed in Fig. 4.8.

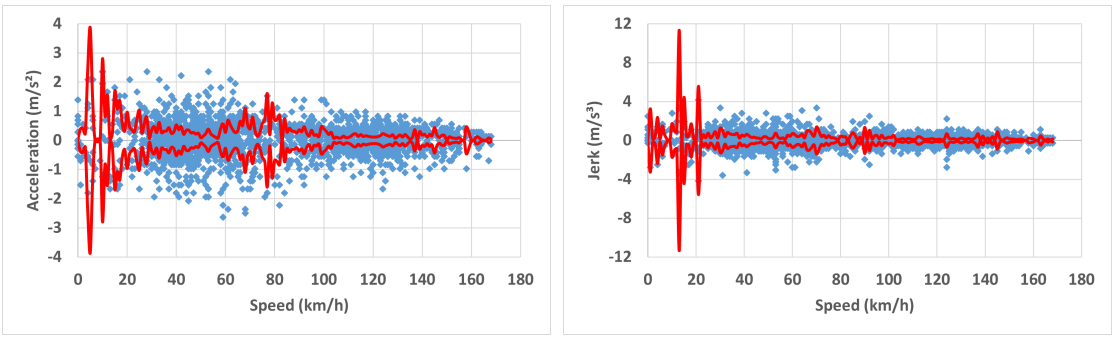

(a) (b)

Figure 4.7: Dispersion plots of the V1 Intercity Routes: a) Acceleration variance (m/s^2) versus Instant speed (km/h); b) Jerk variance (m/s^3) versus Instant speed (km/h)

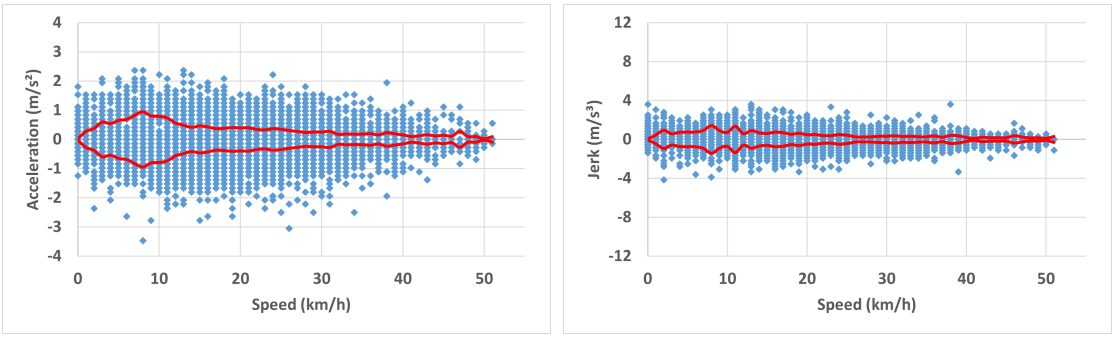

(a) (b)

Figure 4.8: Dispersion plots of the V1 Urban Route: a) Acceleration variance (m/s^2) versus Instant speed (km/h); b) Jerk variance (m/s^3) versus Instant speed (km/h)

In the case of the V2 plots, the observations that were made are roughly similar to what was observed in the created plots for the V1. Strictly speaking and in terms of the intercity routes, once again the values verified in the acceleration plot between the speeds of 0 to 20 km/h and the speeds of 60 to 90 km/h presented a higher value of associated variance, identical to what happened in the case of the vehicle V1, as depicted in Fig. 4.9. The reasons for the increase of variance values in this speed categories are the same as mentioned above in the V1 case analysis. Nevertheless, in terms of jerk variation there is a similarity in its increase as it happened in V1 for the first speed interval, however it can be observed that for the second speed interval the increase of jerk is 3 to 4 times superior than in the case of the V1. This means that probably during the moment that the driver was in the acceleration lane to enter the highway main lanes, he has accelerated in a slightly steeper way than he had done when driving the vehicle V1. As for the urban route, a similarly variation in the acceleration and jerk variance occurred in the V2 as in the V1. This means that there was a slight variance variation in both parameters in the speeds between 0 to 15 km/h, as displayed in Fig. 4.10, but nothing as significant as in the intercity routes situation, for instance.

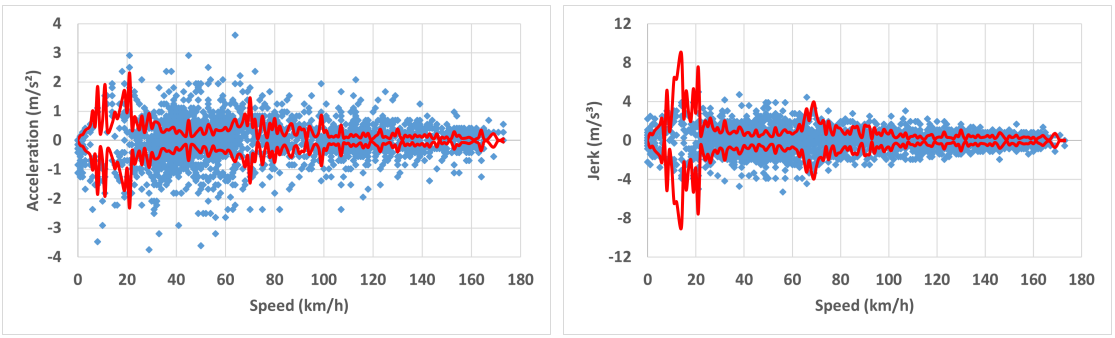

(a) (b)

Figure 4.9: Dispersion plots of the V2 Intercity Routes: a) Acceleration variance (m/s^2) versus Instant speed (km/h) ; b) Jerk variance (m/s^3) versus Instant speed (km/h)

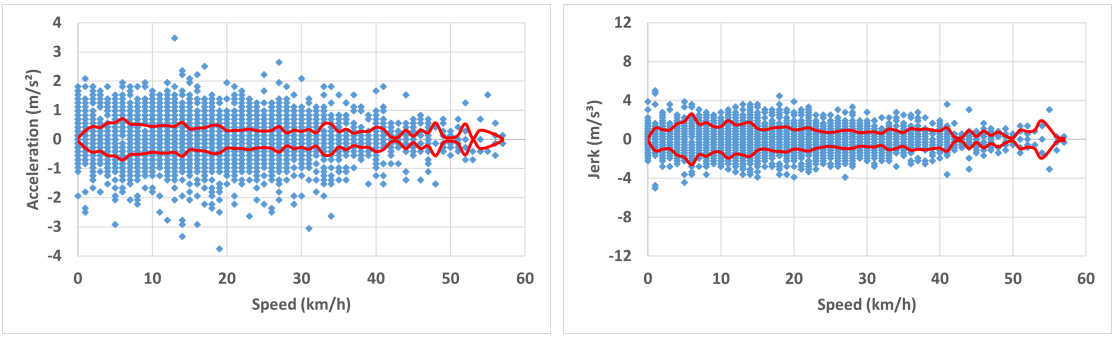

(a) (b)

Figure 4.10: Dispersion plots of the V2 Urban Route: a) Acceleration variance (m/s^2) versus Instant speed (km/h) ; b) Jerk variance (m/s^3) versus Instant speed (km/h)

Finally, an analysis regarding the acceleration, deceleration and jerk variations was performed for each route (with respect to time) and for both vehicles, as well as the rate of trips which were over the RPA thresholds stated by the WLTC for urban and rural areas, as stated in Table 4.1. In the case of the V1, it can be noticed that the route that has the minor values of acceleration and jerk is the R1. This is due to the fact that in rural routes a more constant driving is performed. Oppositely, the R2 and the R3 are the routes which have the highest acceleration values and in terms of jerk they only stay slightly below the values obtained in the R4. This was expected because of the fact that on highways it is where accelerations are more frequent due to the superior speed limits and to the almost constant possibility of performing overtaking manoeuvres. For the R4, what stands out is that it has the highest values of jerk between all routes. The reason for this fact is that more driving volatility exists in this kind of routes. In the case of the V2, once again the R1 was the route that had the lowest values in terms of acceleration and jerk, which proves what was mentioned above. For the remaining routes, the case was slightly different from what was noticed in the V1. This time, the acceleration and jerk values registered for the R2 only stayed slightly above the values that were noticed in the R1 and significantly below the ones of the R3 and R4. In the case of the

R3, it was once again the route which presented the highest values of acceleration and jerk due to the mentioned above reasons. However and for the jerk, it can be noticed that in comparison to the V1 the values that were obtained are approximately 3 times superior. This is due to the fact that a more abrupt type of driving was performed in this kind of route when driving the V2. Finally, in the case of the R4, it can be observed that it presents the lowest values in acceleration but high values in terms of jerk. In fact, comparatively to what was verified in this route in the V1, the obtained jerk is approximately 2 times higher. As for the R3, in the R4 a more aggressive driving was performed while driving the V2.

Table 4.1: Driving parameters classification per route

Vehicle ID	**Route ID**	**Acceleration (% time)**			**Jerk (% time)**	
		a**<3.4**	a**>**a_i^+	a**>2.16**	j**>0.9**	j**<-0.9**
V1	R1	0.00	17.10 (0.38)	0.39 (0.06)	3.24 (0.52)	2.84 (0.41)
	R2	0.09 (0.03)	21.13 (0.41)	0.72 (0.08)	4.80 (0.66)	5.07 (0.57)
	R3	0.00	21.91 (0.41)	0.86 (0.09)	5.71 (0.70)	5.29 (0.77)
	R4	0.02 (0.02)	17.14 (0.38)	0.60 (0.08)	5.95 (0.24)	6.03 (0.40)
V2	R1	0.00	18.93 (0.39)	0.40 (0.06)	7.07 (0.26)	6.82 (0.21)
	R2	0.18 (0.04)	19.34 (0.40)	0.90 (0.09)	7.16 (0.26)	7.97 (0.41)
	R3	0.36 (0.06)	21.85 (0.41)	2.79 (0.16)	15.33 (0.36)	15.11 (0.33)
	R4	0.02 (0.04)	17.47 (0.38)	1.74 (0.13)	12.59 (0.33)	12.72 (0.39)

Note: the values which are in parenthesis represent the standard deviation values when applicable.

4.3 On-road emissions

In this section, the average of CO_2, NO_x and PM emissions per kilometer for both vehicles will exhibited. The density values that were used for each pollutant were the following [Leland and Stanard 2018]: $\rho_{CO_2} = 1830$ g/m^3 and $\rho_{NO_x} = 1913$ g/m^3. Fig. 4.11 represents the obtained values of these emissions per unit distance, in g/km, for the vehicle V1. The height of the bar represents the mean of the specified parameter for each trip, the range bar indicates the standard deviation of each value. The vehicle-specific CO_2 approval stated by the vehicles manufacturers was of 119 g/km for V1 and 118 g/km for V2, while the Euro 6 imposed limit for the NO_x was of 0.08 g/km for V1 and 0.06 g/km for V2, being the PM emissions limit 0.0045 g/km for both vehicles.

For the V1 and in terms of CO_2 emissions, the most critical route is the R3, which has values that are 16% higher than the ones that R2 presents (due to a superior cumulative altitude gain and to a slightly more aggressive driving style), 24% higher than R4 and 49% superior than in R1. The only route that presents CO_2 emissions below the type-approval values was the R1 (by a margin of 25%). The average value of CO_2 emissions for all routes (137.6 g/km) is about 15% superior to the type-approval one. As mentioned before, the standard deviation was null for R1 and R3 due to the fact that only one trip per route was validated for these two routes. R4 was the route which presented the

highest variability coefficient.

For the NO_x pollutant it can be observed that the obtained values were considerably high. What immediately stands out is that all of the trips obtained emissions values significantly exceeded the Euro 6 standard limits. R3 exceeded it in about 83 times, R2 in 53 times, R4 in 23 times and the R1 in 16 times, being the average value 44 times superior to the limit value. The emissions of NO_x are higher on highways than on the remaining type of routes, accordingly to what was verified for the CO_2. The variability coefficient on this case was 80% higher in R2 compared to R4, which meant that on both performed trips for this route the car emitted different amounts of NO_x. These discrepancies are in agreement to previously published studies [Weiss *et al.* 2011, Fernandes *et al.* 2019a].

In the PM scenario, every route stayed below the Euro 6, being the urban one the route which registered the highest emission values (61%, 42% and 61% superior than R1, R2 and R3, respectively). This led to an average PM emission levels that stayed 78% below the Euro 6 limits. The variability coefficient was higher on R4 compared to R2 (20% superior), which meant that emission values substantially varied during the urban route, probably caused by the traffic variation that occurred throughout the different times that the urban routes were being performed (11 AM to 12:30PM and 4:45PM to 7:15PM), caused by the rush hour traffic jams.

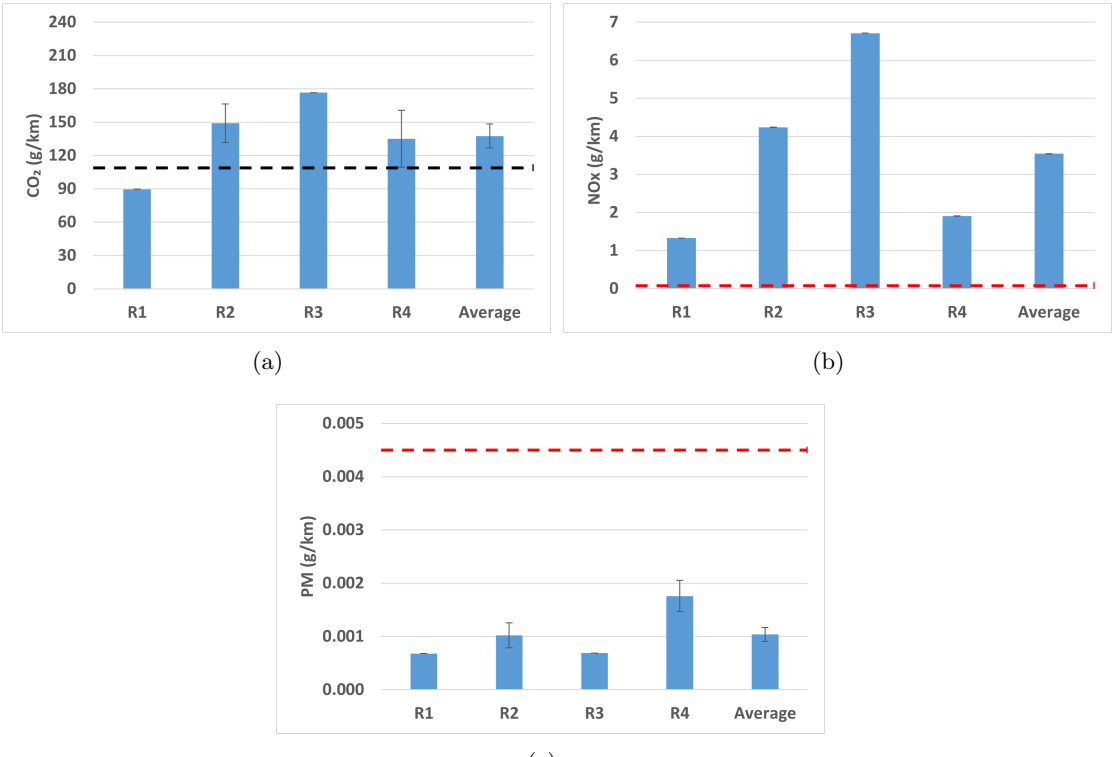

Figure 4.11: On-road emissions per route for V1 *(with standard deviation values)*: a) CO_2 (g/km); b) NO_x (g/km); c) PM (g/km). *Note: the black dashed line represents the CO_2 manufacturer type approval value and the red dashed lines represent the Euro 6c limit value for each pollutant.*

In the vehicle V2 emission scenario and what concerns to the CO_2 emissions, differently from what was observed in the V1, the route with the most emissions was the urban one, R4. Being 24% superior to the R3 values, 64% to the R2 and 86% superior to the ones registered in R1, as displayed in the Fig. 4.12. The highest variability coefficient value was the one from the R4. The average CO_2 emissions value was approximately 27% above the vehicle-specific approval value.

In terms of NO_x emissions, this time the most critical route was the R3, showing to have merely 5% higher values than the ones registered in R4, 56% than in R1 and 66% than in R2. The standard deviation value was larger in the R3, probably due to driving style variations or traffic increase during the two trips that were performed in this route which caused the values to vary. Half of the registered values for NO_x emissions for all routes stayed within the Euro 6 standards, namely on route R1 and R2, while the remaining routes surpassed it. So, this led to an average emission value of NO_x for all trips which surpassed by 66% the previously defined limits.

In the PM emissions, the route that presented the highest values for PM emissions was the R3, although every route stayed within the Euro 6 limits. The other routes presented very similar values in terms of this pollutant emission sums compared to the R3, being the R1 values 28% lower, the R2 33% and the R4 48% inferior than in R3. The V2 average PM emissions value stayed within the Euro 6 standards value by a difference of 51%, which indicates a compliance with the European Union regulations.

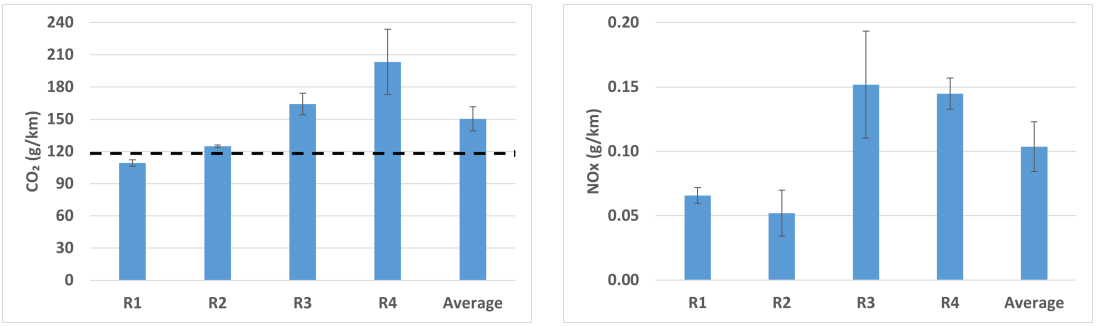

(a) (b)

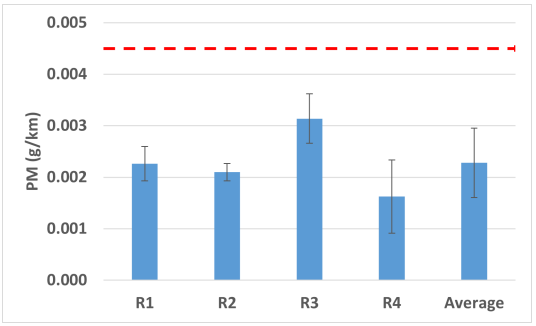

(c)

Figure 4.12: On-road emissions per route for V2 *(with standard deviation values)*: a) CO_2 (g/km); b) NO_x (g/km); c) PM (g/km). *Note: the black dashed line represents the CO_2 manufacturer type approval value and the red dashed line represent the Euro 6c limit value for the PM.*

4.4 Hotspot emission locations by route

This section consists in the representation of the CO_2, NO_x and PM emissions along each one of the test routes for both vehicles. An analysis of the hotspots was performed based on the emission peaks that were registered along the route. The black dashed line on each graph represents the turning point of the plotted route, which is the moment in that the trip that was being performed in the North direction ends and gives place to the trip that was performed in the South direction. The distances in which this turning point occurs are the following: 11700m for R1, 14600m for R2, 16800m for R3 and 2700m for R4.

For the R1 scenario and in the case of the V1, unfortunately and as mentioned before, the only trip that was validated was the one that was performed in the North-South direction. In terms of CO_2 and NO_x emissions along this trip, seven critical coincident points of emissions in both plots are noticeable at a distance of 600m, 1800m, 2700m, 3800m, 5200m, 9400m and 10800m, as displayed in Fig. 4.13 a and b. After checking the collected data and the GPS coordinates, it was inferred that the first peak in emission levels occurred due to the reason that an abrupt acceleration was performed in order to enter a double lane roundabout. In the case of the second and third peaks, a acceleration which increased the vehicle speed from 30 to 50 km/h along a road segment of 200m was the motive for them to happen. The fourth one also occurred due to an acceleration, but this time it was due to an increase in 15 km/h along 50m of road. It was concluded that the fifth peak occurred due to an increase of elevation (approximately 15m in a 300m segment) in this part of the route, which subjected the engine to a higher effort causing the increase on its emissions. In the scenario of the sixth noticeable peak, the reason for it to occur was the same as in the previous one, which was an increase in the level of altitude of about 19m in a 300m segment. The seventh peak occurred again because of an increase in the altitude gain (13m) along 100m of road segment. The summed up value of these 7 peaks contributed to 2.5% of the total CO_2 emissions, to 3.7% of the total NO_x emissions and to 2.7% of the PM emissions during this trip, as depicted in Fig. 4.13 c.

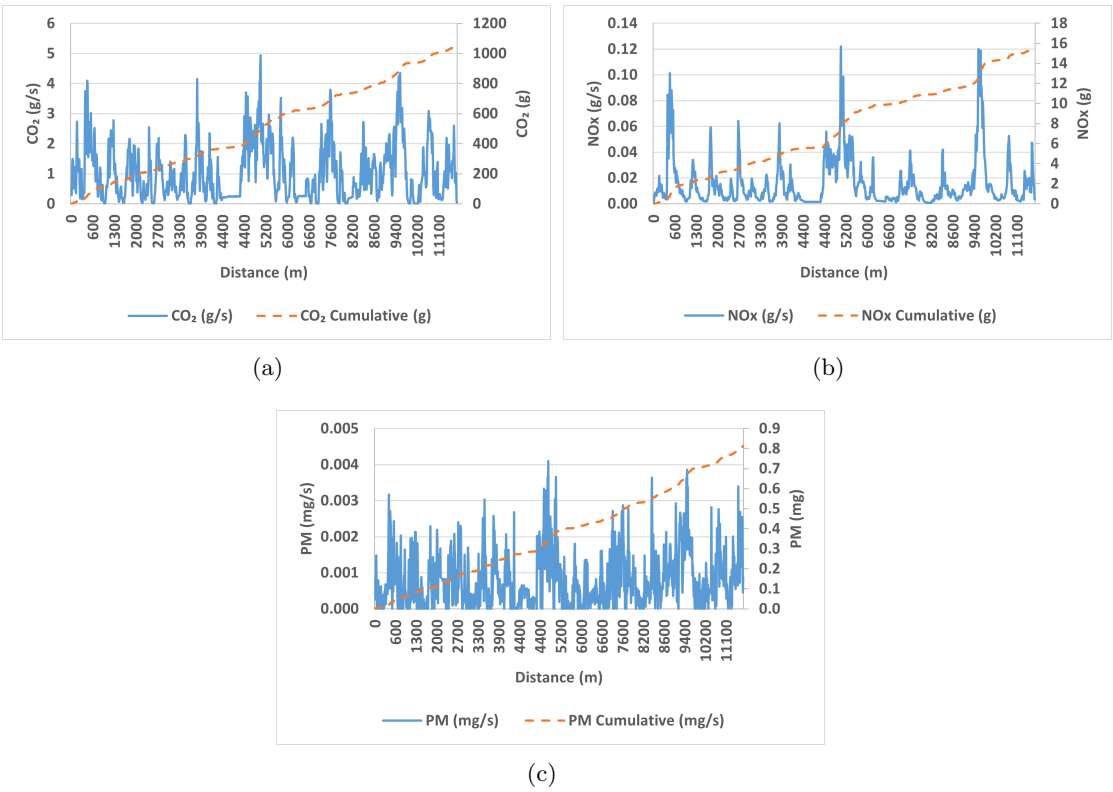

Figure 4.13: R1 (North-South direction) on-road emissions hotspots for V1: a) CO_2 (g/s); b) NO_x (g/s); c) PM (mg/s).

Also for the route R1, this time in both directions of travelling and for the V2, an analysis on each pollutant ratio was performed. In the case of the CO_2, it stands out that right on the start of the route the highest peak value occurs, as displayed in the Fig. 4.14 a. This can be explained by the increase of speed after the vehicle being stopped while setting everything up for the beginning of the data collection session. The same happens in the beginning of the returning trip, especially due to the fact that the turning point was located right next to a roundabout. For the NO_x, what immediately stands out is the peak that occurs at the distance of 8300m, which represents 1.3% of all of this pollutant emissions registered in this route, as observed in Fig. 4.14 b. After checking the collected data, it was concluded that this peak occurred due to an increase on elevation in about 8m along a 150m segment of road, which was located after a green traffic light. In the case of the PM emissions, it can be stated that several peaks were attained, being the three ones that stay above the value of 0.6 g/s, the ones which are more critical, as stated in Fig. 4.14 c. The first one occurred at an initial distance of 500m, in a slight section of increasing elevation (5m along 100m of distance) and during an increase in the acceleration values too. The second one and the highest, representing 1.4% of the total emissions along this route, occurred at the distance of 18900m, in the returning trip, during an ascent with an increase in the elevation of about 10m along 200m of road. The third one that happened at a distance of 21900m, after an attentive analysis of the data, was concluded to be derived from another variation in the parSYNC

sensors, so it can be classified as an outlier. However, eight other peak values which are located between 0.2 g/s and 0.6 g/s of PM are also relevant to analyse. The first one that led to an increase of about 4.5 times in emissions, was located at a distance of 1700m and it was caused by a slope which produced a 10m gain of altitude along 200m of road. The second, third, fourth and eight peaks, which occurred at a distance of 3500m and 6500m, 8900m and 21400m, respectively, were considered as outliers and represented about 1.7% of the total emissions along this route. The peak number five, at a distance of 11400m, occurred due to a 10m gain of altitude along 150m of road. The sixth peak, which took place at a distance of 17100m, also occurred due to a 5m altitude gain along 100m of road. For the case of the seventh one, noticed at a distance of 19900m and being 5.5 times higher than the average emission rates, it happened because of the increase of vehicle speed in about 25 km/h in a segment of 150m of road.

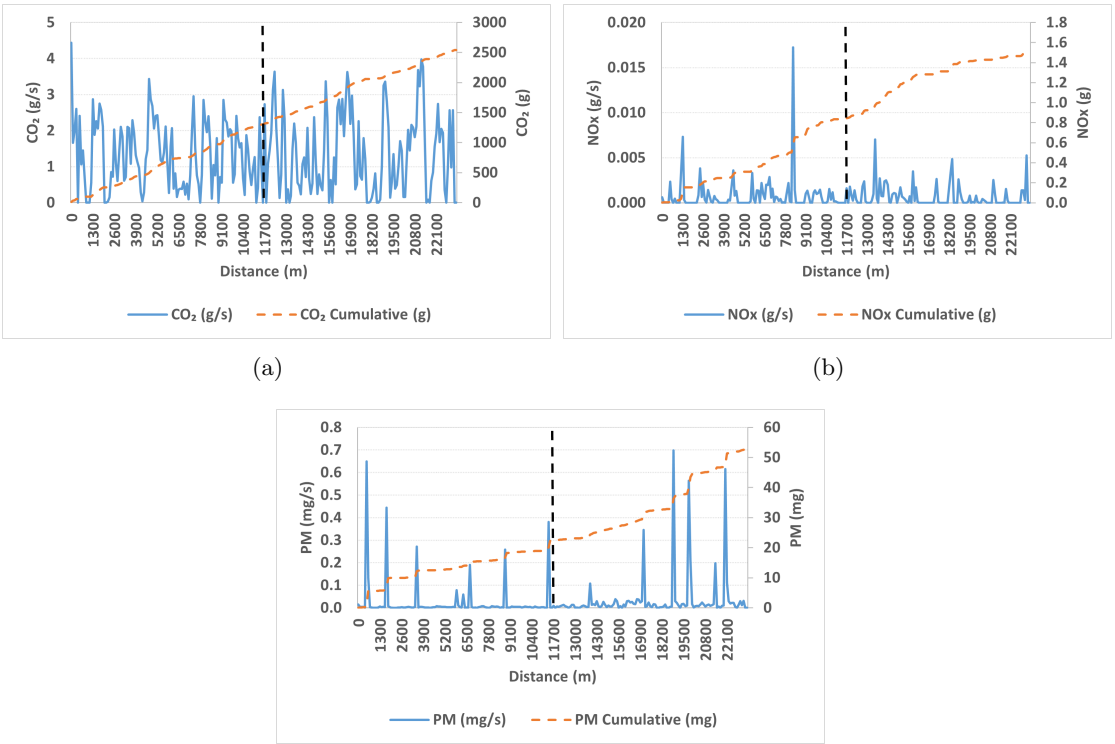

(a) (b)

(c)

Figure 4.14: R1 on-road emissions hotspots for V2: a) CO_2 (g/s); b) NO_x (g/s); c) PM (mg/s). *Note: the black dashed line represents the turning point in the direction of the route (11700m).*

In the route R2 and for the vehicle V1, it is possible to see that the places where each peak was attained by the 3 pollutants were more synchronised than in the R1, as displayed in Fig 4.15. There are two critical zones along with two major peaks standing out within all pollutants. The first interval where the emissions were higher was from 2600m to 12600m, which is a segment of the highway A29 where the speeds varied between 110 and 150 km/h. The first peak was registered at a distance of 9500m, when the vehicle registered an increase of speed from 140 km/h to 157 km/h in a distance of

1000m. The CO_2 peak value was approximately 0.3% of all of the pollutant quantity emitted during the entire route, the NO_x about 0.7% and the PM value of about 0.8%. The second interval where the emissions were clearly superior was between the 15900m and the 24500m, which is also a segment of the R2 route but on the opposite direction. This time the speeds varied between 90 and 140 km/h. The second peak occurred at a distance of 16700m, exactly at the moment in which the driver increased the vehicle speed from 120 to 143 km/h along a distance segment of 500m. About 0.3% of all of the CO_2 emitted during the entire route, 0.6% of the NO_x and 0.7% of the PM values were registered during this instant, as stated in Fig. 4.15.

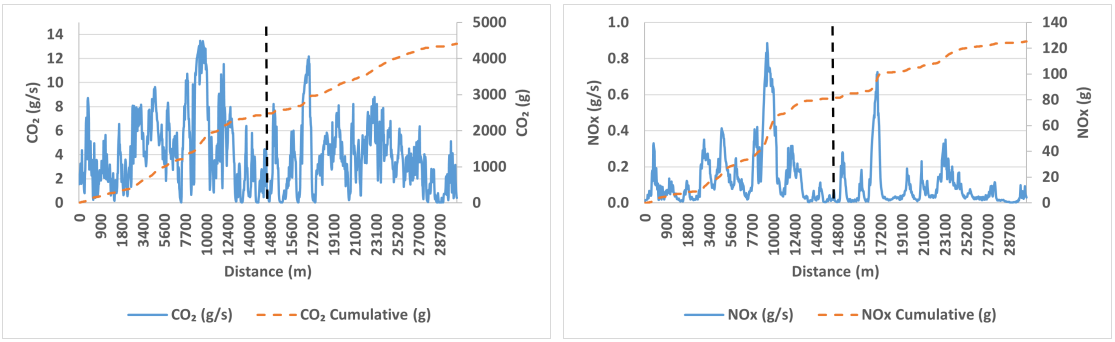

(a)

(b)

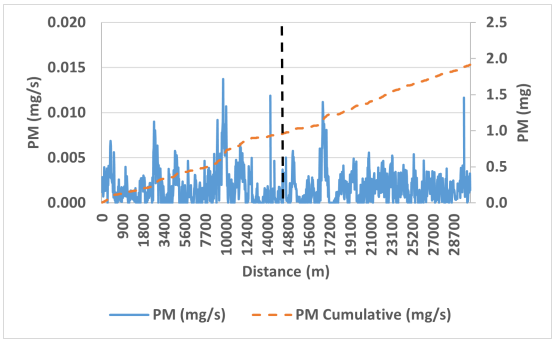

(c)

Figure 4.15: R2 on-road emissions hotspots for V1: a) CO_2 (g/s); b) NO_x (g/s); c) PM (mg/s). *Note: the black dashed line represents the turning point in the direction of the route (14600m).*

In the V2 scenario, the highest value of instant CO_2 emission was registered simultaneous with the third highest value of registered NO_x, at the distance of 3300m, due to an increase in speed from 95 to 115 km/h, jointly with an elevation increase of 15m in a segment of 300m of highway (A1), contributing to 0.3% and to 1.8% of the CO_2 and NO_x total emissions along this route, respectively, as displayed in Fig. 4.16 a and b. The highest value of NO_x emission was registered together with one of the highest ones of CO_2 values too, at the distance of 6200m, due to an elevation increase of 12m along a 300m distance along with a 10km/h increase. However, again a common point in what concerns peak of the emissions was noticed simultaneously for the 3 pollutants. This occurred at a distance of 13900m. After analysing the data and after checking the

GPS coordinates, it was detected that this peak occurred inside and on an exit of a interchange roundabout outside the highway. An increase in speed was performed from 30 to 78 km/h in a distance of 200m, which led to a peak in the emissions of all pollutants, constituting 0.2% of the CO_2 total emissions, 1.8% of NO_x and 2% of the PM ones, as depicted in Fig. 4.16 c.

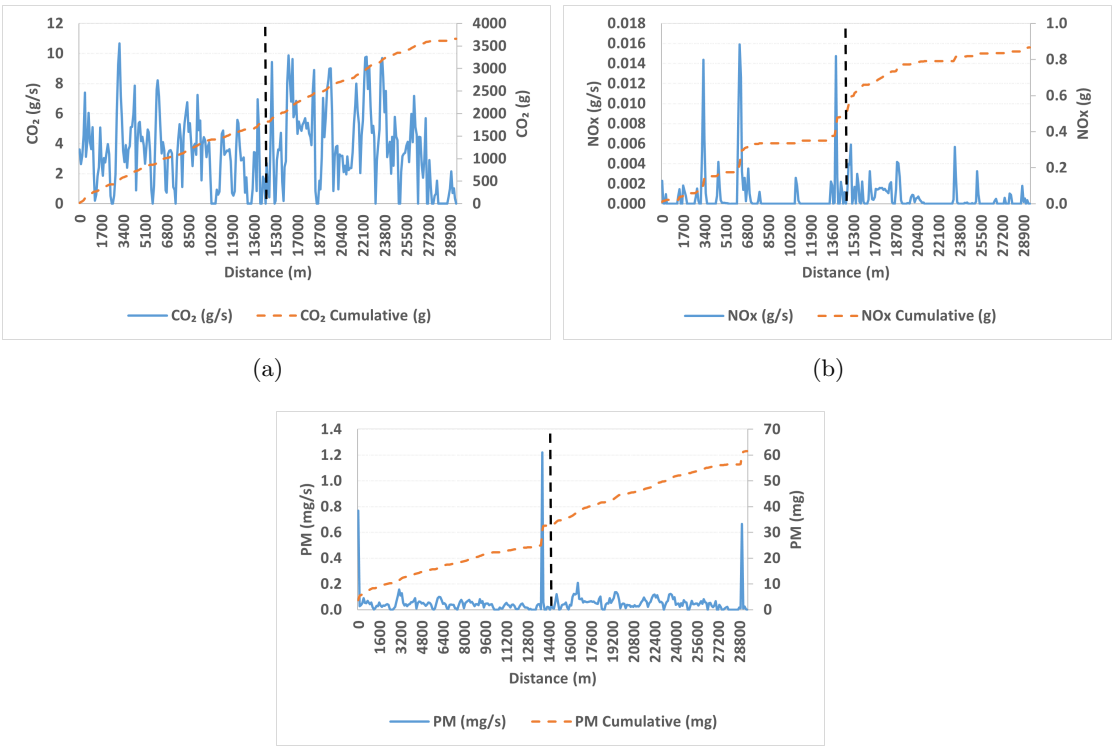

(a) (b)

(c)

Figure 4.16: R2 on-road emissions hotspots for V2: a) CO_2 (g/s); b) NO_x (g/s); c) PM (mg/s). *Note: the black dashed line represents the turning point in the direction of the route (14600m).*

In what concerns to the R3 scenario and to the V1, similarly from what happened in R1, only one trip was validated (the one in the South-North direction). From Fig. 4.17, two critical zones can be identified, among one major peak placed in the first one and among with four other significant peaks placed in the second zone, which affected all of the 3 pollutants. The first critical area can be placed between the 300m and the 2100m. This first segment of the trip was characterised by the entry in the secondary highway portion which led to the entry in the main highway designed for the majority of the R3 route (A1). The first peak, placed at the distance of 1600m, occurred due to an elevation increased of about 25m in a 400m segment of highway, being the speed of 120 km/h maintained, which caused the emissions rate to grow. The second critical area is placed between the 3800m and the 13300m. At the distance of 3800m, the driver led the car to a complete stop due to the fact that he reached the main highway and its respective toll plaza. From the 3800m until the 5400m the driver was entering the main highway through its access segments, increasing its speed from 0 to 135 km/h, leading to

another peak on emissions. The two highest obtained peaks were placed at the 7100 and 8600m, contributing for 0.5% of the CO_x total emissions for each one, 0.9% and 0.7% of NO_x total emissions and for 0.9% of the PM total emissions for each peak. These two peaks occurred due to a speed of 160 km/h and of 168 km/h attained by the driver, respectively. The last significant peak was registered at a distance of 10700m due to an increase in speed of 130 to 150 km/h in a segment of 300m. This peak represented 0.5% of the CO_2, 0.7% of the NO_x and 0.9% of the total PM emissions along the entire route, as stated in Fig. 4.17.

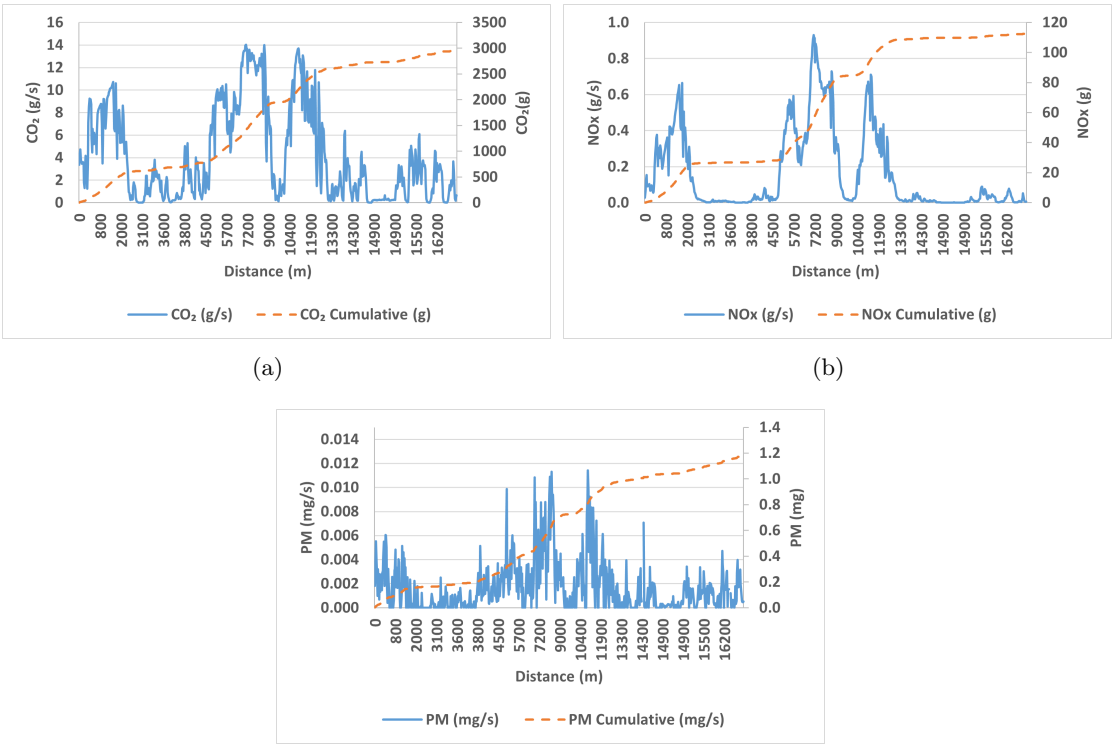

Figure 4.17: R3 on-road emissions hotspots for V1: a) CO_2 (g/s); b) NO_x (g/s); c) PM (mg/s).

In the R3 case for the V2, again the CO_2 peaks variation and frequency is superior to the other pollutants ones. One hotspot which affected the three pollutants was noticed along with 2 more that affected similarly the CO_2 and the NO_x emissions rates, at the distances of 7600m, 19100m and 19900m, respectively. The first one was caused by the fact that the driver reached a speed of 175 km/h, provoking an increase of emissions in all pollutants. An amount of 0.3% of the CO_2, 2% of the NO_x and 0.5% of the total PM emissions along the route were emitted during this moment. The second hotspot occurred due to the reason of the increase in speed from 100 to 130 km/h, along 300m in the access road to the highway. Along this peak 0.3% of the CO_2 and 2% of the NO_x total emissions along the route were emitted. The third peak had the same type of background, due to the motive that the driver increased the vehicle speed from 130 to 145 km/h in a segment of 200m, causing emissions that represented 0.2% and 1.8%

of the CO_2 and NO_x total ones along the route, respectively, as displayed in Fig. 4.18 a and b. In the case of the PM, 2 major peaks can be observed, namely at a distance of 7600m and 33000m. The first one occurred due to an increase of high speeds, namely from 155 km/h to 167 km/h, along 400m of highway segment. The second one occurred due to an acceleration that was performed to enter an interchange roundabout outside the highway, as depicted in Fig. 4.18 c.

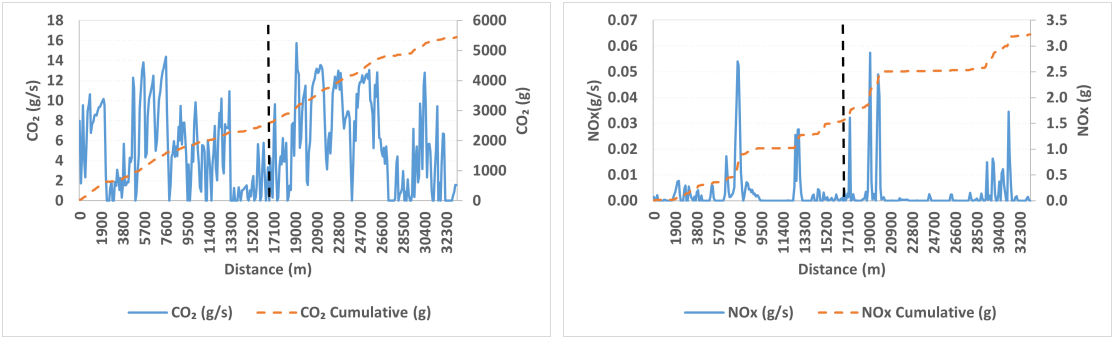

(a)

(b)

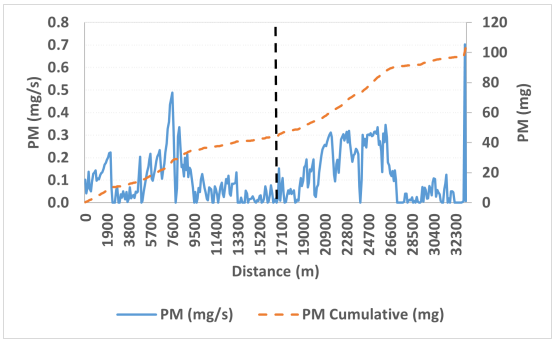

(c)

Figure 4.18: R3 on-road emissions hotspots for V2: a) CO_2 (g/s); b) NO_x (g/s); c) PM (mg/s). *Note: the black dashed line represents the turning point in the direction of the route (16800m).*

Concerning the urban route, R4, and for the vehicle V1, one peak in which the increase of CO_2 and NO_x occur and another one where the emission rate of the three pollutants increase are perfectly noticeable. Right in the first 100m there is a peak which corresponds to a variability in acceleration when entering a two lane roundabout that is located next to the University of Aveiro, that was the starting point. About 0.2% of the CO_2 and 2.8% of the NO_x emissions along all route correspond to this moment, as displayed in Fig. 4.19 a and b. The other peak is situated at the 4000m of distance, in the opposite direction of the first one, due to an increase in altitude of about 10m in a segment of 200m, forcing the engine to make an extra struggle and consequently to emit a high quantity of pollutants. This peak led to a 0.2% CO_2, to a 3.4% NO_x and to a 0.4% PM emission compared to the overall ones along the route. In terms of PM peaks, the two that are placed in the 2700 and 2900m distance are due to the fact that two distinct traffic lights were situated at these points, which obliged the driver to come to

a complete stop and to decelerate and to consequently accelerate. Finally, there is one smaller peak at the distance of 800m that might seem unnoticed but it was a critical point of the route due to the fact that a traffic light was placed right in the end of a slope (5m in a 50m segment), which impelled the vehicles to come to a complete stop and to start driving while going upwards, as depicted in Fig. 4.19 c.

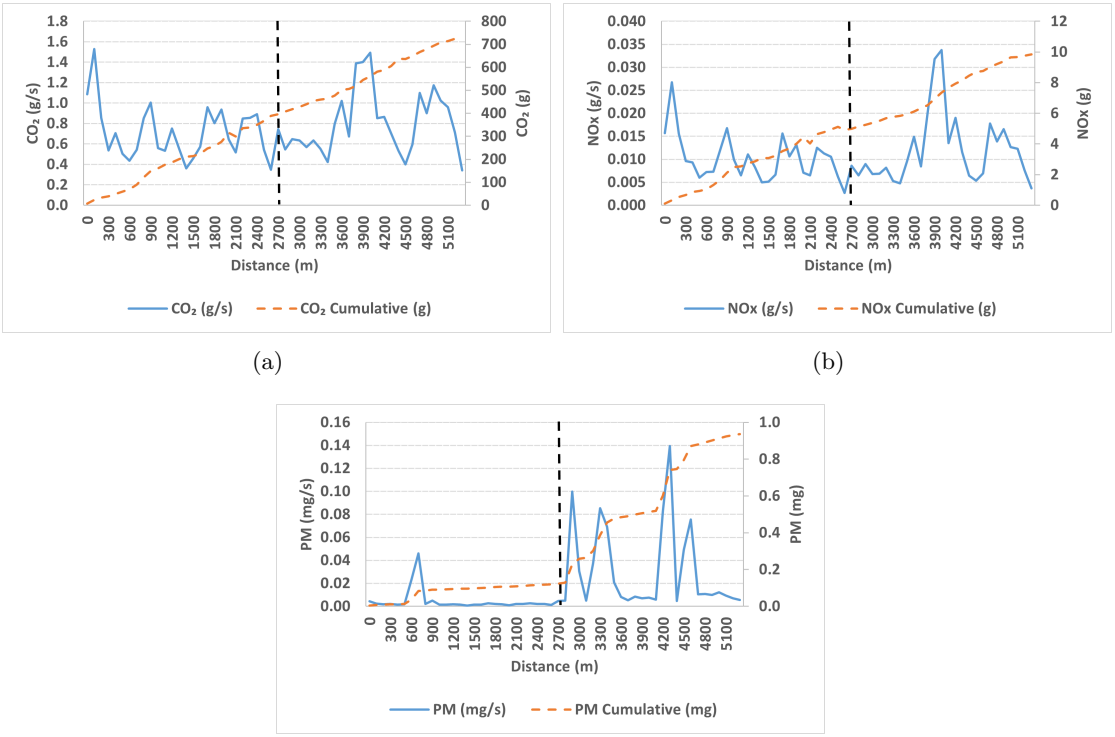

Figure 4.19: R4 on-road emissions hotspots for V1: a) CO_2 (g/s); b) NO_x (g/s); c) PM (mg/s). *Note: the black dashed line represents the turning point in the direction of the route (2700m).*

Finally, in the R4 case for the vehicle V2, one hotspot that affects all of the three pollutants emission rates can be identified at the distance of 4900m. After analysing the collected data and the GPS coordinates, it was concluded that this point is located next to a roundabout which has a pedestrian crosswalk that is located alongside of the exit of it. Due to the fact that it is located between the Aveiro Hospital and the University of Aveiro, this crosswalk has a high number of pedestrian which cross it, forcing the cars to come to a complete stop. This hotspot caused a 0.2% CO_2, a 0.2% NO_x and a 1.3% PM emission rate compared to the overall ones along the entire route, as stated in Fig. 4.20. Another one of the critical points of this route stands out right away by observing the PM emissions plot. As previously mentioned for V1 and for the case of this route, perhaps the most critical point in terms of causing emissions to increase occurs at the distance of 800m, in the opposite direction of the previous one. The slope of about 10% of road grade along with the traffic light placed on the top of it, caused a 2.3% PM emission rate only at this segment compared to the total one obtained during all route.

CO_2 and NO_x also increased on this segment, despite not as much as in the PM case.

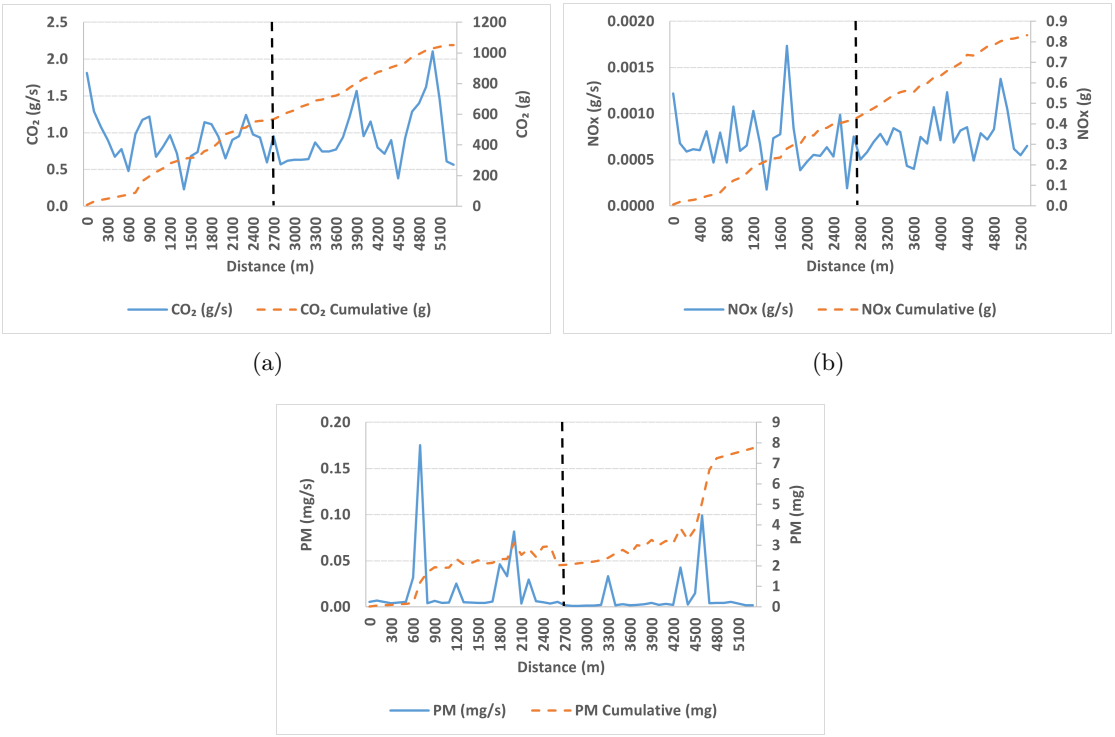

(a) (b)

(c)

Figure 4.20: R4 on-road emissions hotspots for V2: a) CO_2 (g/s); b) NO_x (g/s); c) PM (mg/s). *Note: the black dashed line represents the turning point in the direction of the route (2700m).*

4.5 VSP versus Emission Rates

In this section, the VSP-based approach was performed for each bin, as previously described in the methodology chapter, in order to predict the CO_2, NO_x and PM emission rates for both vehicles, obtaining a coefficient of determination (R^2) for each one of the predicted and the on-road measured pollutants emission rates.

For the V1, the obtained modal rates per VSP mode associated to each pollutant, using the training set of trips, was as expected in the case of the CO_2 and of the NO_x but it was not exactly how it was expected to be in the case of the PM. The higher the VSP mode in which a vehicle is operating, the higher its emission modal rate should be in that second of travel. VSP increases with the increase of the vehicle instant speed, acceleration and the grade of the road, so, due to the extra effort that the engine is subjected when the vehicle reaches superior VSP modes, the emission rate of the pollutants that it is emitting should increase too. As stated in the Fig. 4.21 and in the case of the CO_2 and of the NO_x, the tendency of the increase of the modal rates along with the increase of the VSP mode is perfectly noticeable, specially from the VSP mode 9 until the VSP mode 14. However, in the case of the PM, it can be observed that a raise

in the modal rates values occurs from the VSP mode 1 until the VSP mode 8, decreasing after from that same mode until the final VSP mode 14 which enters in disagreement with the explanation given before. The most likely reason for this decrease to happen is due to the fact that in the training set, from the total of 16 used trips, 13 of the were urban and only 3 of them belonged to the intercity trips, being 2 of them performed on highways. The largest VSP modes values, as natural, are way more frequent to occur on highways than on any other kind of routes. As indicated in the figures that are present in the Appendix 1.2, the distribution of VSP modes for this vehicle shows that the lower VSP modes, which are more common on urban routes, are the most frequent ones and this fact can explain the alterations verified in the plot that illustrates the relation between the PM modal rates and the VSP mode. The VSP Mode 3 was the most frequent (31%), followed by the Modes 1 and 4 (17% each), the Mode 2 (11%), Mode 5 (9%), Mode 6 (5%) and, the Modes 7 to 14, together, only occurred about 10% of the total VSP registered modes, which is an extremely low value. Furthermore, it can be stated in the Fig. 4.11 that the PM emissions, in g/km, along the urban route, R4, were approximately 2 times higher than in the remaining routes and it was stated that in this route about 98% of the registered VSP obtained modes ranged from 1 to 8, which led to an increase of the modal rates compared to the ones that were more frequent on highways, where the PM registered emissions were lower.

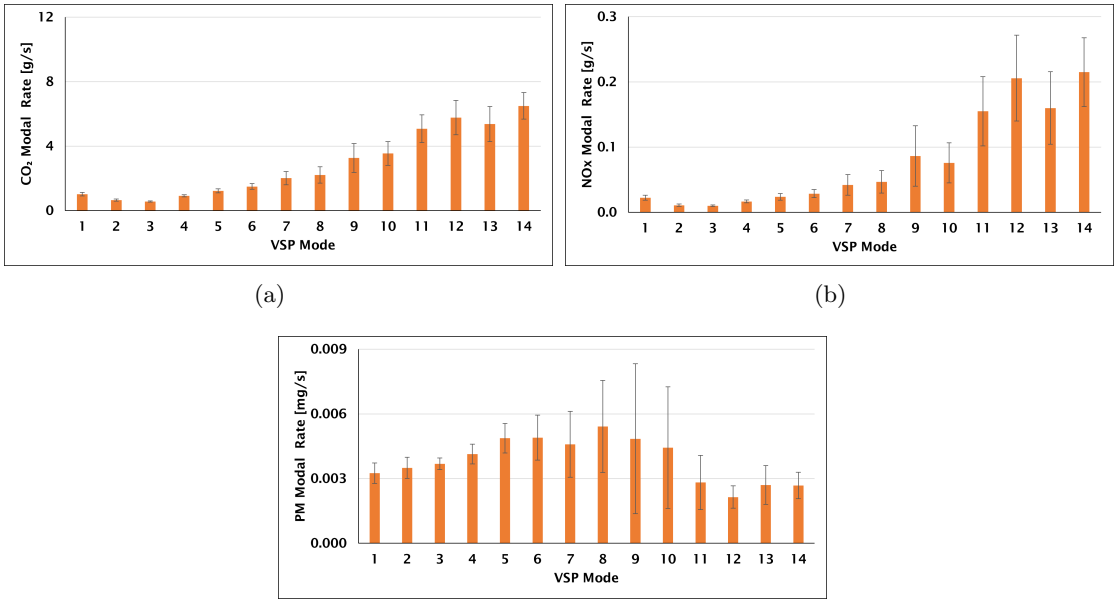

Figure 4.21: Relationship between the VSP modes and the emission rates for V1: a) CO_2 modal rates (g/s); b) NO_x modal rates (g/s); c) PM modal rates (mg/s).

In the V2 scenario, the acquired emission modal rates per VSP mode plots were according to what was expected. For the CO_2, for the NO_x and for the PM, an increasing tendency between the modal rates values and the VSP mode values is perfectly noticeable, as shown in Fig. 4.22. The difference from the V2 to the V1 is that in the case of the V2 and oppositely to what happened in the V1 situation in what concerns to the

distribution of the types of trips which compose the training set, is that from the overall of 11 employed trips, 7 of them were from the urban type and 4 of them were from the intercity type, being 3 of them performed on highways. This means that the frequency of each VSP mode was much better distributed in the case of this vehicle than in the case of the previous one, as verified in the plots present in the Appendix 1.3 and which reinforce what was referred before.

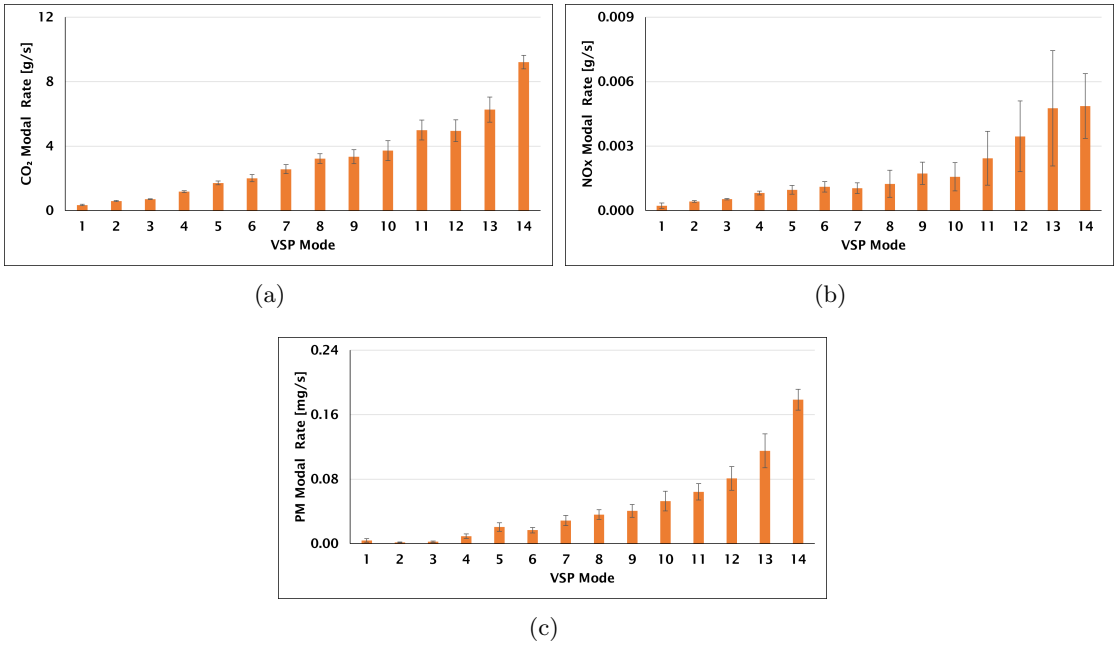

Figure 4.22: Relationship between the VSP modes and the emission rates for V2: a) CO_2 modal rates (g/s) per VSP mode; b) NO_x modal rates (g/s) per VSP mode; c) PM modal rates (mg/s) per VSP mode.

The difference between the above stated modal rates per VSP mode for each both vehicles is stated in the Fig. 4.23.

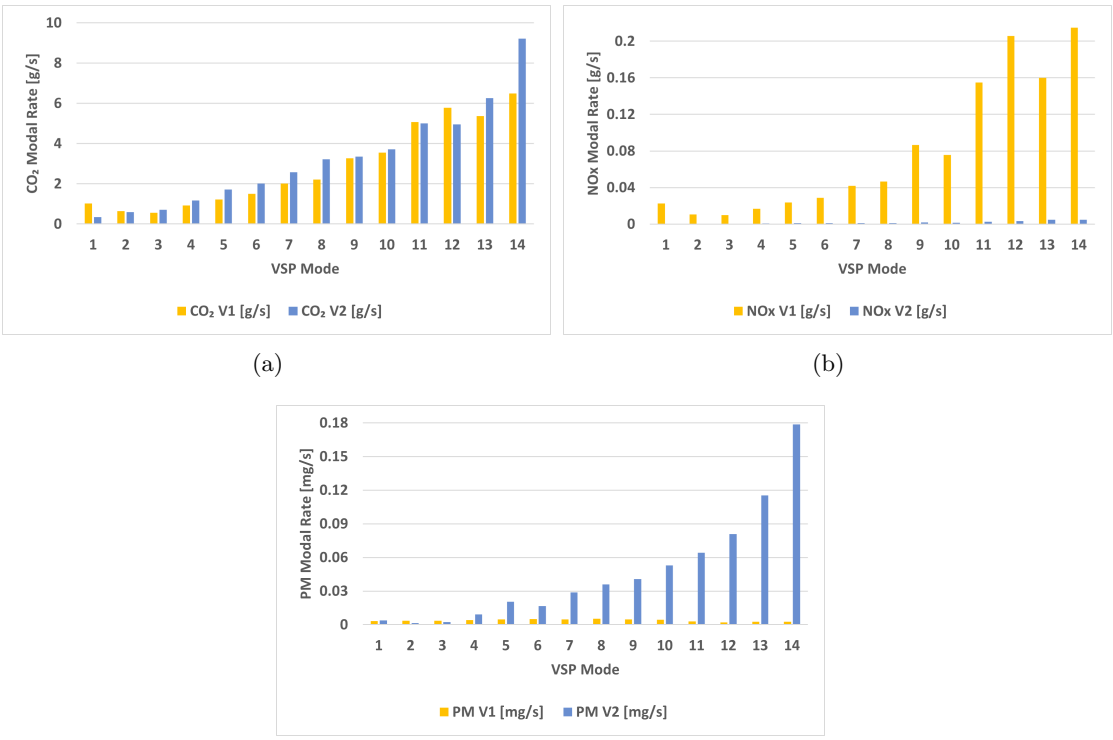

(a) (b)

(c)

Figure 4.23: VSP Modal Rates comparison for both vehicles: a) CO_2 modal rates (g/s) per VSP mode; b) NO_x modal rates (g/s) per VSP mode; c) PM modal rates (mg/s) per VSP mode.

The next step consisted in verifying the relationship between the training predictive model and the testing model, plotting the obtained results in terms of emission modal rates and VSP modes relationship obtained for each one of the models, verifying the capacity of prediction of the training model compared to the testing one by the use of a linear regression and by the analysis of the coefficient of determination that was given by it.

In the case of the V1, different results were obtained for each one of the three analysed pollutants, as displayed in Fig. 4.24. For the CO_2, the acquired regression between the predicted and the obtained emission rates was very good, being the $R^2 > 0.96$, which demonstrates a really high linear relationship between both data sets. With respect to the NO_x, the same can be noticed, being the $R^2 > 0.91$, proving that a high relationship between the predicted and the obtained emission rates exists. However, in the case the PM, the model did not perform so well as in the case of the previously analysed gases, as explained by the R^2 value of 0.61. The explanation for this fact can be based on what was mentioned before related to the short amount of data collected on intercity routes compared to the urban ones, affecting the VSP modes distribution and its consequent modal rates prediction. The p-value was below 5% for all linear regressions regarding each pollutant, which means that the generated regressions are trust worthy.

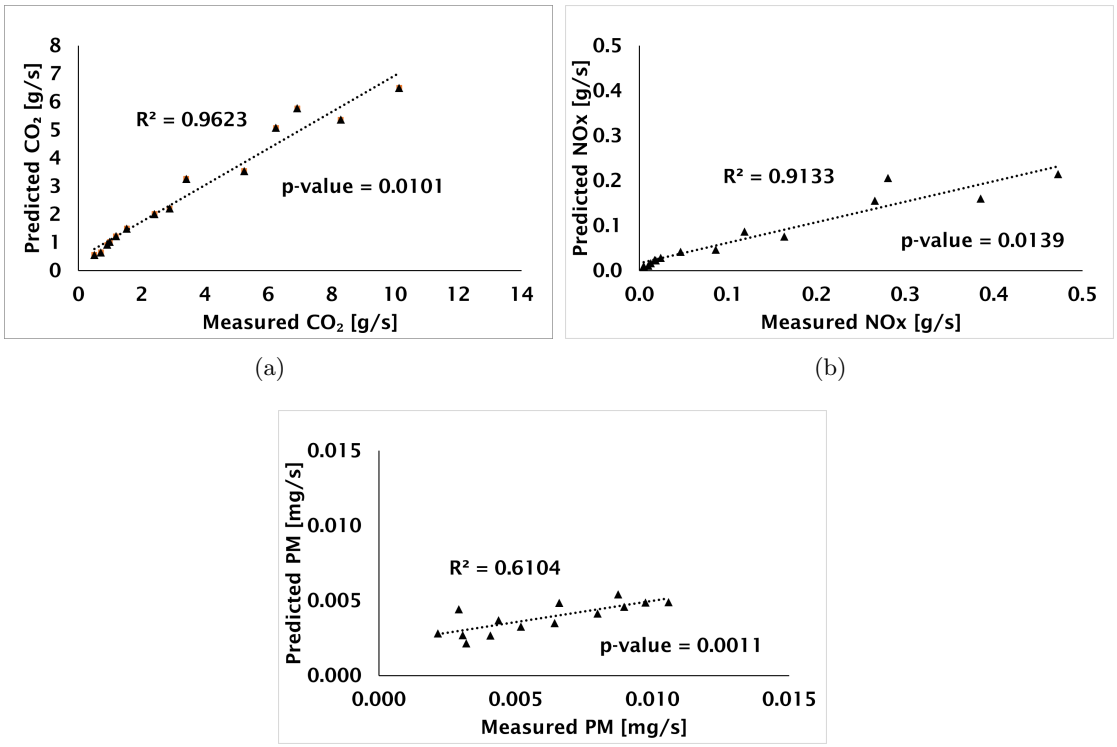

(a) (b)

(c)

Figure 4.24: Emission rates comparison between the predicted and the measured obtained values based on a VSP-modal approach for V1: a) CO_2 (g/s); b) NO_x (g/s); c) PM (mg/s) per route. *Note: Predicted CO_2;NO_x;PM are the emission rates from the training set; Measured CO_2;NO_x;PM are the emission rates from the testing set.*

In what concerns to the V2 predicted and measured emission rates for the three kinds of pollutants, the case was slightly different than for the V1. In terms of CO_2 emission rates prediction, the model worked very well and better for this pollutant than for the two others again, being the value of $R^2 > 0.96$. In the case of the NO_x, a $R^2 > 0.83$ value indicates that the relation between the predictive model and the obtained emission rates is rather strong. For the PM and after obtaining a value of $R^2 > 0.92$ it can be concluded that the predicted and obtained values show an almost perfect correlation, as stated in Fig. 4.25 and on the contrary of what happened for the V1, due to the above mentioned reasons. Once again the p-value was below 5% for all linear regressions regarding each pollutant, which indicates that the generated regressions are trust worthy.

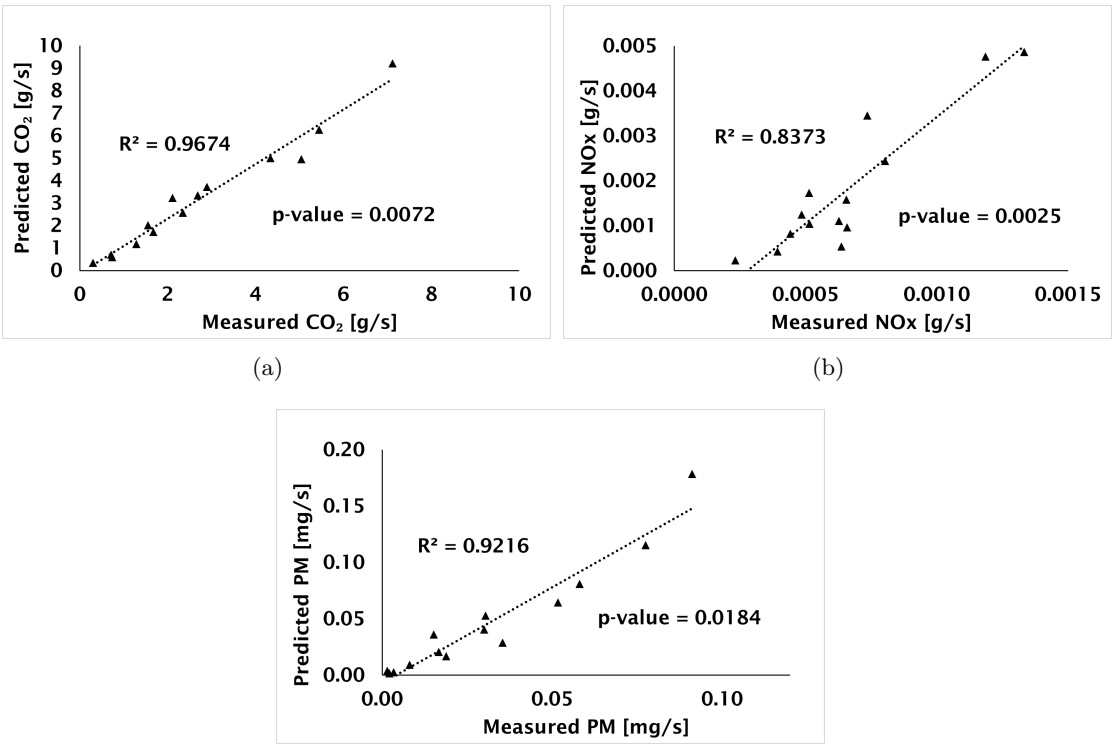

Figure 4.25: Emission rates comparison between the predicted and the measured obtained values based on a VSP-modal approach for V2: a) CO_2 (g/s); b) NO_x (g/s); c) PM (mg/s) per route. *Note: Predicted CO_2;NO_x;PM are the emission rates from the training set; Measured CO_2;NO_x;PM are the emission rates from the testing set.*

4.6 Validation of the VSP based predictive model

With the purpose of verifying the reliability of the VSP based predictive model on emission modal rates, a sum between the on-road obtained emission rates and the predicted ones by the model was performed for each one of the testing routes and for each one of the vehicles, encompassing the three analysed pollutants, as depicted in Table 4.2.

In the Table 4.2, for V1, it can be observed that the average VSP CO_2 and NO_x predicted values were about 8% and 28% higher than the ones measured on the field, respectively. The average VSP PM predicted values were 46% lower than the ones obtained on the road.

For the V2 scenario, the proximity between the predicted values and the on-road obtained ones was slightly better among all of the three analysed pollutants than on the case of the V1. CO_2 predicted emission rates were only about 7% superior to the field measured ones, the NO_x predicted values were approximately 20% higher than the on-road verified values and the PM foreseen emission rates were 33% above the ones that were registered throughout the test trips.

Table 4.2: On-road obtained emission rates versus the ones predicted by the predictive model for each test trip

Car ID	**Trip ID**	**Route ID**	**CO_2 [g/km]**		**NO_x [g/km]**		**PM [mg/km]**	
			On-road	**VSP**	**On-road**	**VSP**	**On-road**	**VSP**
V1	1	R3	176.7	116.5	6.7	3.3	0.1	0.1
	2	R4	149.5	183.3	1.5	3.2	0.6	0.9
	3	R4	180.5	223.5	2.3	3.8	3.0	1.1
	4	R4	120.8	142.2	1.6	2.6	2.8	0.6
	5	R4	153.4	193.1	2.1	3.3	0.4	0.9
	6	R4	122.5	164.6	1.8	3.0	0.6	0.7
	7	R4	205.7	163.8	1.5	3.0	1.6	0.7
Average			158.4	170.4	2.5	3.2	1.3	0.7
V2	1	R1	112.3	110.4	0.03	0.07	0.7	1.0
	2	R2	126.1	147.2	0.02	0.08	1.6	2.2
	3	R4	187.2	201.5	0.1	0.1	0.6	1.5
	4	R4	162.6	181.1	0.1	0.1	1.6	1.7
	5	R4	184.3	186.3	0.1	0.1	1.7	1.5
Average			154.5	165.3	0.08	0.1	1.2	1.6

Note: On-road measured and VSP predicted values for CO_2, for NO_x and for the PM were divided by the total distance of each trip

Intentionally blank page.

Chapter 5

Conclusions and Future Work

The main objective of this masters dissertation was to perform the experimental monitoring of pollutants emissions from different road vehicles that use different types of fuels on different kind of routes. An empirical method embracing vehicle data collection regarding its operating conditions and its consequent hot stabilised emissions was used. The two main purposes of the development of this method were to be able to, firstly, observe what are the impacts that different driving parameters, such as the acceleration, vehicular jerk or RPM, along with the VSP and the characteristics of the route, will have on the emission rates of the CO_2, NO_x and PM pollutants; and, secondly, to be able to analyse the relationship between the VSP and the obtained on-road emission rates by applying a predictive model based on this parameter. Several engine specifications data were gathered regarding two distinct vehicles, being one of them powered by diesel (V1) and the other one by gasoline (V2), along with the emissions that each one of them produced. Data were collected along four different type of routes (one partly urban/rural, two highways and one urban), which presented different sorts of features that varied from distinct altitude elevation gains values to diverse traffic conditions or that even presented a contrasting amount of roundabouts, intersections or traffic lights, which interfere with the collected data. An analysis regarding the acceleration-based parameters was carried out in order to characterize the driving style and to consequently validate or not the performed PEMS trips along all of the four routes. Afterwards, an extensive examination was consummated with the objective of comprehending the influence of the variation of these driving parameters on emission values, along with the influence of the different kinds of routes characteristics too. A comparison between the on-road obtained emission values and the European Union imposed limits was also carried out. At last, the development of the VSP-based approach model was developed in order to predict the on-road emissions.

In the intercity routes scenario, the speed range obtained in the case of the V2 (0 to 170km/h) was superior to the one obtained for the V1 (0 to 160km/h), as well as the obtained acceleration range for the V2 [-5 to 5m/s^2] compared to the V1 [-4 to 4m/s^2], as the obtained vehicular jerk for V2 [-5 to 5m/s^3] in comparison to the V1 jerk range [-4 to 4m/s^3]. For both vehicles the acceleration and jerk most frequent class to be noticed is between [-1;0] (approximately 80% for both vehicles), which means that most of the time the vehicle acceleration of the vehicle speed was maintained constant. The variance of the acceleration and of the vehicular jerk along different speeds was verified to be much wider at low speeds than at the higher ones, for the intercity routes and for

both vehicles. As for the urban one, the variance of these two parameters was practically null, meaning that a smoother driving was performed. The route with the highest values of acceleration and vehicular jerk was the R3, being the a>2.16m/s^2 about 2.79% of the travel time and the vehicular jerk > 0.9 about 15.33% of the trip time.

For both vehicles, the average CO_2 per unit distance was above the vehicle-specific approval values, being approximately 15% superior for the V1 and about 27% for the V2. In terms of the NO_x emissions, it was stated that the V1 surpassed the Euro 6 standards in about 44 times, instead of the V2 that only exceeded it in roughly 66%. In the PM, both vehicles complied with the Euro 6 limits, staying the V1 below them in about 78% and the V2 in 51%. It was figured out that the most common reason for emission rates to increase was the presence of slopes along the route, which boosted the CO_2 emissions up to 5 times more and the NO_x and PM emissions up to 10 times more, in the verified case of the V1 during the partly urban/rural route. Other one of the most common reasons were the abrupt increases of high speeds observed in the case of the V2 along one of the highway routes (R3), which led to a rise of about 14 times in the CO_2 emissions, 6 times in the NO_x emissions and 5 times in the PM emissions. The predictive VSP-based approach model was found to perform well in both vehicles. In the V1, high coefficients of determination were obtained in the case of the CO_2 and of the NO_x ($R^2 > 0.90$ for both), however, in the PM scenario, the determination coefficient was not so high ($R^2 > 0.61$). The most likely reason for this lack to happen is related to the short amount of collected data and the unbalance between the urban and the intercity performed trips, having registered a low frequency of the highest modes of VSP (a frequency of 90% was acquired for VSP Modes 1-6 and a frequency of only 10% was obtained for VSP Modes 7-14). In the case of the V2, the model performed better for the CO_2 and for the PM, obtaining determination coefficient values of $R^2 > 0.92$ for both, also performing well in the case of the NO_x ($R^2 > 0.83$). The balance between the urban and the intercity routes performed in the V2 and present in the training and testing set of trips might have been crucial to this improvement on the model reliability relatively to what was verified in the V1 case. Regarding the validation of the VSP models and for the V1, it was concluded that the average VSP CO_2 and NO_x predicted values were about 8% and 28% higher than the ones measured on the field, and, for the PM, the average VSP predicted values were 46% lower than the ones registered on the road, respectively. In the case of the V2, the average VSP CO_2, NO_x and PM predicted values were 7%, 20% and 33% superior to the field measured ones, respectively.

The need for an efficient regulation concerning to its emission standards urges. Since the laboratory emission testing cycles, such as the NEDC and the WLTC, lack on rigorousness regarding the registered values on vehicle emissions compared to their real ones, innovative methods such as the appliance of the RDE are needed. However, it might be complicated to perform this kind of procedure due to its considerable costs. The implementation of an effective method such as the VSP-based one is useful to estimate emissions in diesel or gasoline vehicles for all types of driving cycles and it even could be incorporated on national inventories in order to calculate traffic emissions, for instance.

Two main limitations have to be stood out throughout this entire work, being motivated by the emerge of the Covid-19 pandemic and consequently by the obligation of the quarantine and social distancing period. The first limitation was related to the short amount of trips performed for both vehicles, which directly affected the quality and the variety of the collected data. The second one consisted in the small sample size

of the test fleet, which only consisted in two vehicles instead of the four or five initially programmed to be submitted to testing.

Therefore, future research should encompass a larger sample size of the test fleet, embracing different emission standard ranges (from Euro 1 to Euro 5) and different kind of propulsion systems such as hybrid electric vehicles. A wider variety of routes and a larger amount of performed trips should be done for each one the vehicles in order to obtain well distributed data which are characteristic from each type of route, resulting in a balanced amount of data collected. The monitorization of pollutants such as HC or CO should also be implemented, as well as the use of parameters as the MAP, IAT or the exhaust temperature in order to obtain even more reliable values in terms of NO_x emission rates. The use of a higher number of drivers could also be implemented, with the purpose of obtaining different driving styles and to observe their impact on emissions and on fuel consumption. Also, an analysis regarding the effect of different slopes present in distinct routes on emission rates could be performed, as well as an analysis on the effects that the PEMS uncertainties and cold emissions may provoke on the obtained emission rates results. The development of different emission predictive models based on distinct engine parameters (such as the MAP or the RPM) or even based on driving volatility (jerk) could be performed, followed by a comparison with the previously developed VSP based model.

Intentionally blank page.

List of References

[3DATX 2020] 3DATX. Real Driving Emissions. pp. 1–2, 2020.

[Bagdadi 2013] Omar Bagdadi. Assessing safety critical braking events in naturalistic driving studies. *Transportation Research Part F: Psychology and Behaviour*, 16:117–126, 2013.

[Bagdadi and Várhelyi 2012] Omar Bagdadi and András Várhelyi. Development of a method for detecting jerks in safety critical events. *Accident Analysis and Prevention*, 50:83–91, 2012.

[Baldino *et al.* 2017] Chelsea Baldino, Uwe Tietge, Rachel Muncrief, Yoann Bernard and Peter Mock. ROAD TESTED: COMPARATIVE OVERVIEW OF REAL-WORLD VERSUS TYPE-APPROVAL NOx AND CO2 EMISSIONS FROM DIESEL CARS IN EUROPE. *International Council on Clean Transportation: White paper*, p. 38, 2017.

[Boriboonsomsin and Barth 2009] Kanok Boriboonsomsin and Matthew Barth. Impacts of Road Grade on Fuel Consumption and Carbon Dioxide Emissions Evidenced by Use of Advanced Navigation Systems. *Transportation Research Record Journal of the Transportation Research Board*, 2139:21–30, 12 2009.

[Boroujeni and Frey 2014] Behdad Yazdani Boroujeni and H Christopher Frey. Road grade quantification based on global positioning system data obtained from real-world vehicle fuel use and emissions measurements. *Atmospheric Environment*, 85:179–186, 03 2014.

[Brand 2016] Christian Brand. Beyond 'Dieselgate': Implications of unaccounted and future air pollutant emissions and energy use for cars in the United Kingdom. *Energy Policy*, 97(X):1–12, 2016.

[Choi and Frey 2009] Hyung Wook Choi and Frey. Light duty gasoline vehicle emission factors at high transient and constant speeds for short road segments. *Transportation Research Part D: Transport and Environment*, 14(8):610–614, 2009.

[Choi *et al.* 2017] Eunjin Choi, Eungcheol Kim, Korea Road and Traffic Authority. Critical aggressive acceleration values and models for fuel consumption when starting and driving a passenger car running on LPG. *International Journal of Sustainable Transportation*, 11(6):1–47, 2017.

[Cnr *et al.* 2018] Istituto Motori Cnr, Maria Vittoria Prati, Giovanni Meccariello, Livia Della Ragione and Maria Antonietta. Real Driving Emissions of a Light-Duty Vehicle in Naples . Influence of Road Grade. *12th International Conference*

on Engines and Vehicles: ICE 2015 ; September 13 - 17, 2015, Capri, Napoli (Italy), 09 2018.

[Coelho *et al.* 2009] Margarida C. Coelho, H. Christopher Frey, Nagui M. Rouphail, Haibo Zhai and Luc Pelkmans. Assessing methods for comparing emissions from gasoline and diesel light-duty vehicles based on microscale measurements. *Transportation Research Part D: Transport and Environment*, 14(2):91–99, 2009.

[Degraeuwe and Weiss 2016] Bart Degraeuwe and Martin Weiss. Does the New European Driving Cycle (NEDC) really fail to capture the NOx emissions of diesel cars in Europe? *Environmental Pollution*, 222:1–8, 2016.

[Delavarrafiee and Frey 2018] Maryam Delavarrafiee and H Christopher Frey. Real-world fuel use and gaseous emission rates for flex fuel vehicles operated on E85 versus gasoline E85 versus gasoline. *Journal of the Air & Waste Management Association*, 68(3):235–254, 2018.

[Deligianni *et al.* 2017] Stavroula Panagiota Deligianni, Mohammed Quddus, Andrew Morris, Aaron Anvuur and Steven Reed. Analyzing and Modeling Drivers' Deceleration Behavior from Normal Driving. *Transportation Research Record*, 2263:134–141, 2017.

[Driven 2020] The Driven. Electric Vehicle and Hybrid Sales Hit Record Share of 18 Percent in Europe. `https://thedriven.io/2020/08/31/electric-vehicle-and-hybrid-sales-hit-record-share-of-18-per-cent`, 2020. The Driven, Accessed 20 April 2020.

[EEA 2012] EEA. Title 40 - Protection of Environment. CHAPTER I - ENVIRONMENTAL PROTECTION AGENCY (CONTINUED). SUBCHAPTER C - AIR PROGRAMS (CONTINUED). PART 86 - CONTROL OF EMISSIONS FROM NEW AND IN-USE HIGHWAY VEHICLES AND ENGINES. Subpart B - Emission Regulations for 1977 and Later Model Year New Light-Duty Vehicles and New Light-Duty Trucks and New Otto-Cycle Complete Heavy-Duty Vehicles. 94, 2012.

[EEA 2016] EEA. Explaining road transport emissions. Luxembourg:Publications Office of the European Union, 2016, 2016.

[EPA 2002] EPA. Methodology for Developing Modal Emission Rates for EPA's Multi-Scale Motor Vehicle and Equipment. Technical report, 2002.

[EPA 2020] EPA. Particulate Matter Basics. `https://www.epa.gov/pm-pollution/particulate-matter-pm-basics`, 2020. EPA, Accessed 3 April 2020.

[EU 2016] EU. Paris Agreement. `https://ec.europa.eu/clima/policies/international/negotiations/paris_en#tab-0-1`, 2016. European Comission, Accessed 10 April 2020.

[EU 2020] EU. Reducing CO2 Emissions from Passenger Cars. `www.https://ec.europa.eu/clima/policies/transport/vehicles/cars_en`, 2020. European Comission, Accessed 18 April 2020.

[European Parliament 2017] EU European Parliament. Comission Regulation (EU) 2017/1151. *Official Journal of the European Union*, (692):1–643, 2017.

[European Parliament and Council of the European Union 2007] European Parliament and Council of the European Union. REGULATION (EC) No 715/2007 OF THE EUROPEAN PARLIAMENT AND OF THE COUNCIL of 20 June 2007 on type approval of motor vehicles with respect to emissions from light passenger and commercial vehicles (Euro 5 and Euro 6) and on access to vehicle repair and mai. *Official journal of the European Union*, L171(December 2006):1–16, 2007.

[Feng *et al.* 2017] Fred Feng, Shan Bao, James R Sayer, Carol Flannagan, Michael Manser and Robert Wunderlich. Can vehicle longitudinal jerk be used to identify aggressive drivers ? An examination using naturalistic driving data. *Accident Analysis and Prevention*, 104(February 2016):125–136, 2017.

[Fernandes *et al.* 2019a] P Fernandes, E Macedo, B Bahmankhah, R F Tomas, J M Bandeira and M C Coelho. Are internally observable vehicle data good predictors of vehicle emissions ? *Transportation Research Part D*, 77:252–270, 2019.

[Fernandes *et al.* 2019b] P. Fernandes, C. Sousa, J. Macedo and M. C. Coelho. How to evaluate the extent of mobility strategies in a university campus: An integrated analysis of impacts. *International Journal of Sustainable Transportation*, 14(2):120–136, 2019.

[Fernandes *et al.* 2019c] P. Fernandes, M. Vilaça, E. Macedo, C. Sampaio, B. Bahmankhah, J. M. Bandeira, C. Guarnaccia, S. Rafael, A. P. Fernandes, H. Relvas, C. Borrego and M. C. Coelho. Integrating road traffic externalities through a sustainability indicator. *Science of the Total Environment*, 691:483–498, 2019.

[Fernandes *et al.* 2020] P. Fernandes, R. Tomás, F. Acuto, A. Pascale, B. Bahmankhah, C. Guarnaccia, A. Granà and M.C. Coelho. Impacts of roundabouts in suburban areas on congestion-specific vehicle speed profiles, pollutant and noise emissions: An empirical analysis. *Sustainable Cities and Society*, 62:102386, 2020.

[Fiat 2019] Fiat. Fiat Tipo Catalogue. Fiat, 2019.

[Frey *et al.* 2006] H Christopher Frey, Nagui M Rouphail and Haibo Zhai. Estimates for On-Road Light-Duty Vehicles on the Basis of Real-World Speed Profiles. *Transportation Research Record Journal of the Transportation Research Board*, 6:128–137, 2006.

[Frey *et al.* 2008] H. Christopher Frey, Kaishan Zhang and Nagui M. Rouphail. Fuel use and emissions comparisons for alternative routes, time of day, road grade, and vehicles based on in-use measurements. *Environmental Science and Technology*, 42(7):2483–2489, 2008.

[Frey *et al.* 2017] Henry Christopher Frey, Tanzila Khan and H Christopher Frey. Comparison of real-world and certification emission rates for light duty gasoline vehicles Science of the Total Environment Comparison of real-world and certification emission rates for light duty gasoline vehicles. *The Science of the Total Environment*, 622-623:790–800, 12 2017.

[Gaines and Richa 2019] Linda Gaines and Kirti Richa. Review Key issues for Li-ion battery recycling. *MRS Energy Sustainability-A Review Journal 5*, pp. 1–14, 2019.

[Gallus *et al.* 2017] Jens Gallus, Ulf Kirchner, Rainer Vogt and Thorsten Benter. Impact of driving style and road grade on gaseous exhaust emissions of passenger vehicles measured by a Portable Emission Measurement System (PEMS). *Transportation Research Part D: Transport and Environment*, 52(2):215–226, 2017.

[German 2015] John German. Hybrid vehicles: Trends in technology development and cost reduction. *2015 International Council on Clean Transportation*, (1):1–18, 2015.

[Grimaldi and Millo 2015] Carlo N Grimaldi and Federico Millo. Internal Combustion Engine (ICE) Fundamentals. In Handbook of Clean Energy Systems. American Cancer Society, 2015.

[Hu and Frey 2017] Jiangchuan Hu and Henry Christopher Frey. Comparison of Real World Light-Duty Gasoline Vehicle Emissions for High Altitude Mountainous Versus Low Altitude Piedmont Study Areas. *Annual Conference and Exhibition, Air and Waste Management Association; June 2017, Pittsburgh, PA, USA*, (September 2018), 2017.

[Huang and Wang 2018] Quanan Huang and Huiyi Wang. Fundamental Study of Jerk : Evaluation of Shift Quality and Ride Comfort. *SAE Technical Papers*, (724), 2018.

[IMT 2020] IMT. Relatório de Tráfego na Rede Nacional de Autoestradas. Instituto da Mobilidade e dos Transportes, (IMT, I.P.), 2020.

[Inc 2020] Crain Communications Inc. Reign at crisis: Why the VW faces an incertain future. *Automotive News Europe*, 11(2):1–37, 2020.

[Jimenez-palacios 1999] Jose Luis Jimenez-palacios. Understanding and Quantifying Motor Vehicle Emissions with Vehicle Specific Power and TILDAS Remote Sensing. (1993), 1999.

[Kadijk 2012] Gerrit Kadijk. Supporting Analysis regarding Test Procedure Flexibilities and Technology Deployment for Review of the Light Duty Vehicle CO 2 Regulations Service request # 6 for Framework Contract on Vehicle Emissions. European Commission, Brussels, 2012.

[Khattak *et al.* 2019] Asad Khattak, Jackeline Rios-Torres and Jun Liu. Fuel consumption for various driving styles in conventional and hybrid electric vehicles: Integrating driving cycle predictions with fuel consumption optimization. *International Journal of Sustainable Transportation*, 13(2):123–137, 2019.

[Leach *et al.* 2020] Felix Leach, Gautam Kalghatgi, Richard Stone and Paul Miles. The scope for improving the efficiency and environmental impact of internal combustion engines. *Transportation Engineering*, 1:100005, 2020.

[Leland and Stanard 2018] Amber Leland and Alan Stanard. CRC Report No . E-122 LIGHT DUTY PEMS VALIDATIONS / CHASSIS DYNAMOMETER CORRELATION. Coordinating Research Council, 06 2018.

[Lindroos and Ekholm 2015] Tomi J Lindroos and Tommi Ekholm. Emission gap to 2 degree pathways – Framework to assess the ambition of Intended Nationally Determined Contributions , INDCs. *VTT Publications*, VTT-R-00140-15, 02 2015.

[Liu 2015] Jun Liu. Driving Volatility in Instantaneous Driving Behaviors: Studies Using Large-Scale Trajectory Data, PhD diss., University of Tennessee. 2015.

[Liu *et al.* 2017] Han Liu, Alexander Gegov and Ella Haig. Unified Framework for Control of Machine Learning Tasks Towards Effective and Efficient Processing of Big Data, pp. 123–140. 03 2017.

[Macfarlane and Croft 2003] Sonja Macfarlane and Elizabeth A Croft. Jerk-Bounded Manipulator Trajectory Planning : Design for Real-Time Applications. *IEEE Transactions on Robotics and Automation*, 19(1):42–52, 2003.

[Mock *et al.* 2014] Authors Peter Mock, Jörg Kühlwein, Uwe Tietge, Vicente Franco, Anup Bandivadekar and John German. The WLTP : How a new test procedure for cars will affect fuel consumption values in the EU. *2014 International Council on Clean Transportation*, (October 2014), 2014.

[Ntziachristos and Dilara 2012] Leonidas Ntziachristos and Panagiota Dilara. Sustainability Assessment of Road Transport Technologies. EUR 25341 EN – Joint Research Centre – Institute for Energy and Transport, 2012.

[Othman *et al.* 2008] Rizal Othman, Zhong Zhang, Takashi Imamura and Tetsuo Miyake. A Study of Analysis Method for Driver Features Extraction. *2008 IEEE International Conference on Systems, Man and Cybernetics*, pp. 1501–1505, 2008.

[Penkala *et al.* 2018] Magdalena Penkala, Pawel Ogrodnik and W. Rogula-Kozłowska. Particulate Matter from the Road Surface Abrasion as a Problem of Non-Exhaust Emission Control. *Environments*, 5, 01 2018.

[Qstarz 2020] Qstarz. Qstarz BT-Q1000XT Specifications. `http://www.qstarz.com/Products/GPS%20Products/BT-Q1000XT-S.htm`, 2020. Qstarz, Accessed 2 May 2020.

[Renault 2019] Renault. Renault CLIO. 2019.

[Roser 2016] Max Roser. Global Greenhouse Gas Emissions By Sector. `https://ourworldindata.org/emissions-by-sector`, 2016. Our World in Data, Accessed 05 May 2020.

[Sandhu *et al.* 2013] Gurdas S Sandhu, United States, Environmental Protection and Henry Christopher Frey. Effects of Errors on Vehicle Emission Rates from Portable Emissions Measurement Systems. *Transportation Research Record Journal of the Transportation Research Board*, 2340:10–19, 12 2013.

[Satlawa *et al.* 2020] Mateusz Satlawa, Piotr Pajdowski and Dariusz Pietras. The Impact of the Driver's Driving Style on the EXHAUST Emissions of a Passenger Car during a Real Road Cycle. In *SAE Technical Paper*. SAE International, 09 2020.

[The European Commission 2016] The European Commission. Commission Regulation (EU) 2016/646 of 20 April 2016 amending Regulation (EC) No 692/2008 as regards emissions from light passenger and commercial vehicles (Euro 6). *Official Journal of the European Union*, 109(1):1–22, 2016.

[Tietge *et al.* 2017] Uwe Tietge, Sonsoles Díaz, Zifei Yang and Peter Mock. FROM LABORATORY TO ROAD INTERNATIONAL A COMPARISON OF OFFICIAL AND REAL-WORLD FUEL CONSUMPTION AND CO2 VALUES FOR PASSENGER CARS. *2017 International Council on Clean Transportation*, 11 2017.

[ToolBox 2019] Engineering ToolBox. Density of fuel oils as function of the temperature. `https://www.engineeringtoolbox.com/fuel-oil-density-temperature-gravity-volume-correction-ASTM-D1250-d_1942.html`, 2019. The Engineering Toolbox, Accessed 27 April 2020.

[Transport and Environment 2015] Transport and Environment. Mind the Gap 2015 Closing the chasm between test and real-world car CO2 emissions. *2015 International Council on Clean Transportation*, 2015.

[Tutuianu *et al.* 2015] Monica Tutuianu, Pierre Bonnel, Biagio Ciuffo, Takahiro Haniu, Noriyuki Ichikawa, Alessandro Marotta, Jelica Pavlovic and Heinz Steven. Development of the World-wide harmonized Light duty Test Cycle (WLTC) and a possible pathway for its introduction in the European legislation. *Transportation Research Part D*, 40:61–75, 2015.

[Tzirakis *et al.* 2007] E Tzirakis, F Zannikos and S Stournas. Impact of driving style on fuel consumption and exhaust emissions: defensive and aggressive driving style. *Technology Kos island*, (May 2014):5–7, 2007.

[Viviani 1995] Paolo Viviani. Minimum-Jerk, Two-Thirds Power Law, and Isochrony: Converging Approaches to Movement Planning. *J Exp Psychol Hum Percept Perform*, 21(1):32–53, 1995.

[Wali *et al.* 2019] Behram Wali, Asad J. Khattak and Thomas Karnowski. Exploring microscopic driving volatility in naturalistic driving environment prior to involvement in safety critical events—Concept of event-based driving volatility. *Accident Analysis and Prevention*, 132(August):105277, 2019.

[Wang *et al.* 2018] Haohao Wang, Yunshan Ge, Lijun Hao, Xiaoliu Xu, Jianwei Tan, Jiachen Li, Legang Wu, Jia Yang, Dongxia Yang, Jian Peng, Jin Yang and Rong Yang. The real driving emission characteristics of light-duty diesel vehicle at various altitudes. *Atmospheric Environment*, 191:126 – 131, 2018.

[Weiss *et al.* 2011] Martin. Weiss, Pierre Bonnel and Rudolf Hummel. Analyzing on-road emissions of light-duty vehicles with portable emission measurement systems (PEMS). p. 54, 2011.

[Weiss *et al.* 2012] Martin Weiss, Pierre Bonnel, Jörg Kühlwein, Alessio Provenza, Udo Lambrecht, Stefano Alessandrini, Massimo Carriero, Rinaldo Colombo, Fausto Forni, Gaston Lanappe, Philippe Le, Urbano Manfredi, Francois Montigny and

Mirco Sculati. Will Euro 6 reduce the NO x emissions of new diesel cars ? e Insights from on-road tests with Portable Emissions Measurement Systems (PEMS). *Atmospheric Environment*, 62(2):657–665, 2012.

[Yang *et al.* 2019] Zhengjun Yang, Yunshan Ge, Daisy Thomas, Xin Wang, Sheng Su, Hu Li and Hongwen He. Real driving particle number (PN) emissions from China-6 compliant PFI and GDI hybrid electrical vehicles. *Atmospheric Environment*, 199(November 2018):70–79, 2019.

Intentionally blank page.

Appendices

.1 parSYNC: How to Compute Particle Mass and Particle Number from the Raw Voltages of the Scattering, Ionization, and Opacity Sensors

This process was computed in the software through columns that were created for each intermediate part of the output.

1. For all 3 sensors, the process started with an analysis of the first thirty seconds values of acquired voltages to determine a baseline.
2. For all 3 sensors, the average of the last ten records of the sensors' voltages from the first 30 was computed.
   (a) This gives the baseline voltages for each sensor.
   (b) Columns names
      i. Scattering (V)
      ii. Ionization (V)
      iii. Opacity (V)
   (c) Variables used to represent these baseline values
      i. Scattering_V0
      ii. Ionization_V0
      iii. Opacity_V0
   (d) Variables used to represent the record at any time
      i. Scattering_V
      ii. Ionization_V
      iii. Opacity_V
3. For each record starting with the time at 31 seconds, the voltage is computed by the use of the following formula:
   (a) Scattering
      i. Scattering_zeroed = Scattering_V – Scattering_V0
   (b) Ionization
      i. 3.2.1.1. Ionization_zeroed = Ionization_V0 – Ionization_V
   (c) Opacity
      i. Opacity_zeroed = Opacity_V0 – Opacity_V
4. The trends in the data were removed to compensate for the sensors being affected by the device temperature. These are Scattering_adj, Ionization_adj, and Opacity_adj.
5. For each record where a Scattering_adj, Ionization_adj, and Opacity_adj were determined, the particle mass, PM ($\mu g/m^3$), was determined as follows:

(a) Scattering_PM = 6534200*Scattering_adj^2 + 375640*Scattering_adj

(b) Ionization_PM = -948.97*Ionization_adj^2 + 6319.9*Ionization_adj

(c) Opacity_PM = 269670*Opacity_adj^2 + 28252*Opacity_adj

(d) PM = 0.39*Ionization_PM + 0.06*Opacity_PM + 0.55*Scattering_PM

.2 Frequency of the VSP modes per route for V1

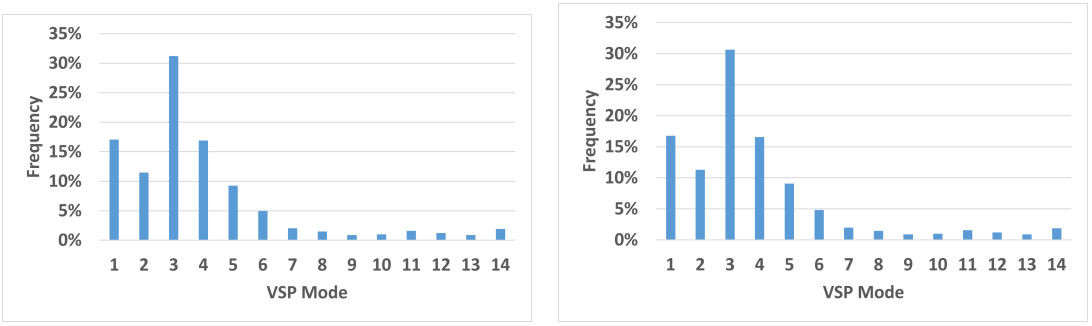

(a) (b)

Figure 1: Frequency of the VSP modes per route for V1: a) Training Set; b) Testing Set

.3 Frequency of the VSP modes per route for V2

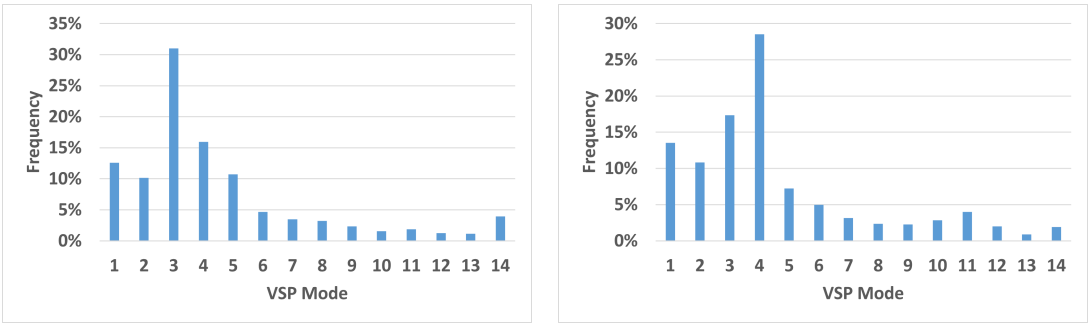

(a) (b)

Figure 2: Frequency of the VSP modes per route for V2: a) Training Set; b) Testing Set